The CXCL10/CXCR3 axis cross-talk between emerging T cell acute lymphoblastic leukemia and thymic epithelial cells

Inaugural-Dissertation

zur

Erlangung des Doktorgrades

Dr. rer. nat.

Der Fakultät für Biologie

an der

Universität Duisburg-Essen, Germany

vorgelegt von

Ashwini M. Patil

aus Nashik, Maharashtra,

Indien

Essen, Juni 2019

Die der vorliegenden Arbeit zugrundeliegenden Experimente wurden in der Klinikfür Hämatologie des Universitätsklinikums Essen durchgeführt.

1. Gutachter: PD. Dr. Joachim R. Göthert
2. Gutachter: Prof. Dr. Matthias Gunzer

Vorsitzender des Prüfungsausschusses: Prof. Dr. Astrid Westendorf

Tag der mündlichen Prüfung: 09.10.2019

DOI: 10.17185/duepublico/70693
URN: urn:nbn:de:hbz:464-20210107-063037-3

Dedication

This thesis is dedicated to my parents

To the memory of my father,

Madhukar D. Patil

Who inspired and supported me

and

To my mother

Ranjana M. Patil

Who inspires me every day with

Determination and affection

Table of Contents

List of Abbreviations

7-AAD	7-amino-actinomycin D
AIRE	Autoimmun Regulator
APC	Adenomatous polyposis coli
β-5t	Thymoproteasome subunit-β5T
B-Cell	Bone marrow derived lymphocyte
Ccl25	Chemokine (C-C motif) ligand 24
CCR7	C-C chemokine receptor type 7
CCR9	C-C chemokine receptor type 9
CCL2	Chemokine (C-C motif) ligand 2
CCL25	Chemokine (C-C motif) ligand 25
CD62L	L-selectin
CD8ISP	CD8+ immature single-positive
CDKN1B	Cyclin-dependent kinase inhibitor 1B
cDNA	Copy deoxyribonucleic acid
Ct	Threshold-Cycle
cTEC	cortical thymic epitheila cell
CXCL10	C-X-C motif chemokine ligand 10(IP10)
CXCL11	C-X-C motif chemokine ligand 11
CXCL12	C-X-C motif chemokine ligand 12
CXCL9	C-X-C motif chemokine ligand 9
DAPI	4′,6-diamidino-2-phenylindole
DC	Dendritic cell
Ddit4	DNA-damage-induced transcript 4
ddNTP	Didesoxyribonucleoside triphosphate
DEPC	Diethylpyrocarbonat
DLL1	Delta-like ligand 1
DLL4	Delta-like ligand 4
DMEM	Dulbecco's Modified Eagle Medium
DMSO	Dimethyl sulfoxide
DN	Double negative
DNA	Deoxyribonucleic acid
dNTP	Deoxyribonucleoside triphosphate
DP	Double positive
D-PBS	Dulbecco´s Phosphate Buffered Saline
GLI1	Zinc finger protein GLI1
EDTA	Ethylenediaminetetraacetic acid
EMT	Epithelial–mesenchymal transition
EpCAM	Epithelial cell adhesion molecule
EthBr	Ethidiumbromid
Ex	Exon
FACS	Fluorescence activated cell sorting

FAM	6-Carboxyfluorescein
FBXW7	F-Box And WD Repeat Domain Containing 7
FCS	Forward scatter
FGFR2	Fibroblast growth factor receptor 2
FITC	Fluorescein isothiocyanate
FKS	Fetales Kälberserum
FSC	Forward scatter
gDNA	Genomische Desoxyribonukleinsäure
HE	Hamatoxylin-Eosin
HOXA	Homeobox protein Hox-A
HOX11	Homeobox protein 11
Hprt	Hypoxanthin-Guanin-Phosphoribosyltransferase
Ig	Immunglobulin
IGF1	Insulin-like growth factor 1
IL-18	Interkleukin 18
IL-22	Interkleukin 22
IL-7	Interkleukin 7
IMDM	Iscove's Modified Dulbecco's Medium
K14	Keratin 14
K8	Keratin 8
kDa	Kilodalton
KGF	Keratinocyte growth factor
LMO1	Rhombotin-1
LYL1	Protein lyl-1
Ly51	6C3/BP-1
M	Molar
mg	Milligram
$MgCl_2$	Magnesiumchlorid
MHC	Major histocompatibility complex
Min.	Minutes
ml	Milliliter
mM	Milimolar
mRNA	Messenger ribonucleic acid
mTEC	Medullary thymic epithelial cell
NaCl	Sodium chloride
NaOH	Sodium hydroxide
NF-κB	Nuclear factor 'kappa-light-chain-enhancer' of activated B-cells
ng	Nanogram
NK	Natural killer cell
NOTCH	Notch homolog , translocation-associated
NOTCH1	Notch homolog 1, translocation-associated
NTC	Non template control
OPF	Upper Percoll fraction

Pan-Ck	Pan-Cytokeratin
PBS	Phosphate buffer saline
PCR	Polymerase chain reaction
PE	Phycoerythrin
PerCP	Peridinin Chlorophyll
PI	Propidiumiodid
qPCR	Quantitative polymerase chain reaction
Rn	Normalized reporter signal
RNA	Ribonucleic acid
RPM	Rounds per minute
RT	Room temperature
RT	Reverse transcriptase
RT-PCR	Real-time polymerase chain reaction
SCF	Stem cell factor
SD	Standard error
SEM	Standard error of the mean
SP	Single positive
SSC	Side scatter
Tab.	Tabel
TAE	Tris-Acetat-EDTA
T-ALL	T-cell acute lymphoblastic leukemia
Taq	Thermus aquaticus
TCR	T cell receptor
TEC	Thymic epithelial cell
TGFβ	Transforming growth factor beta
T-LBL	T lymphoblastic lymphoma
Treg	Regulatory T cell
T-cell	Thymus derived lymphocyte
UEA	Ulex europaeus agglutinin
UTR	Untranslated region
UV	Ultraviolett
V	Volt
VEGF	Vascular endothelial growth factor
w/v	Weight per volume
WT	Wildtype
µg	Micrograms

List of Figures

List of Tables

CHAPTER-1

INTRODUCTION

1 INTRODUCTION

1.1 Thymus

T-cell maturation takes place under the influence of various molecular signals on the cellular level. The thymus is a primary lymphatic, two-lobed organ located in the mediastinum below the sternum, caudally of the thyroid gland and cranial of the pericardium.[1] A connective tissue capsule surrounds each lobe, which is comprised of numerous lobules, formed by invagination of connective tissue derived from the capsule. Analysis of the thymic structure at the histological level allows the distinction of three separate areas: The thin subcapsular region, the lymphocyte-rich cortex and the epithelial cell-dense medulla. In conventional light microscopy, the cortex is separated from the medulla by a visible cortico-medullary junction (CMJ) **(Fig. 1).** During embryonic development, endoderm of the third pharyngeal pouch differentiates into cortical (cTECs) and medullary thymic epithelial cells (mTECs). Later developmental stages are controlled by the interaction of TECs with developing T cells.[2] Developing T cells are called thymocytes and differentiate in direct physical contact with various types of stromal cells, which together form different microenvironments consisting of thymic epithelial cells and non-epithelial cells such as fibroblasts, macrophages, and dendritic cells. The autochthonous TECs are the most common population of stromal cells, and their specific function distinguishes them from the hematopoietic stromal cells of the bone marrow (BM). Together, the TECs form an integrated cellular matrix that provides significant developmental niches for cells of the T lymphoid lineage.

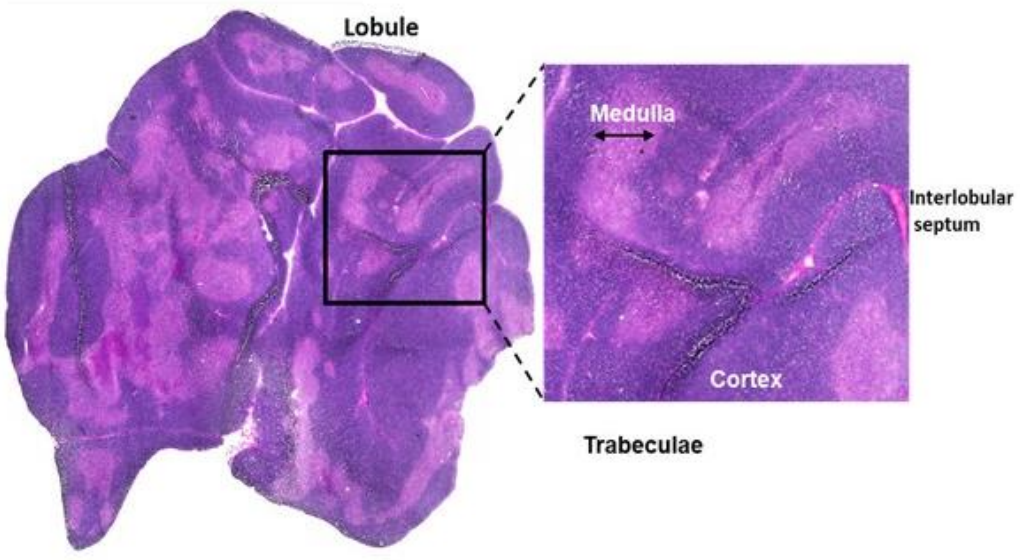

Figure 1. The thymic architecture.
Hematoxylin and eosin-stained representative section of an adult murine thymus. The thymus is composed of an outer cortex and an inner medulla. The thymus forms an interconnected lobules and

is surrounded by a mesenchymal capsule. Thymus cortex; a darker peripheral zone, thymus medulla; a lighter central zone.

1.1.1 The development and maturation of T cells in the thymus

Different types of hematopoietic progenitor cells pass from the BM into the blood. Only a particular progenitor subpopulation is capable of entering the thymus. These progenitors adhere to specialized thymic endothelial cells of small venous capillaries located in the CMJ and transmigrate into the thymic tissue.[3] For this process, the surface receptor CD44 is required.[4] After entering the CMJ, the thymic progenitors are referred to as double negative thymocytes (DN thymocytes). The term "double negative" refers to the lack of the expression of surface markers (co-receptors) CD4 and CD8. These co-receptors assign the mature T-cells to either the T-helper (CD4) or the cytotoxic T-cell lineage (CD8). These surface receptors are only expressed towards the final stages of T-cell development. The maturity and development status of DN thymocytes is defined by the expression of the surface molecules CD25 and CD44.[5, 6] These molecules are up- or down-regulated by the DN cells depending on the stage of development. These progenitors pass through several defined developmental stages before eventually developing into mature single positive (SP) CD4+ or CD8+ T cells. During their differentiation process, the developing thymocytes migrate through different thymic microenvironments where they receive specific differentiation signals from the local stromal cells, in particular from the TECs.

1.1.1.1 Development of double-negative thymocytes

The T cell progenitors initially entering the CMJ of the thymus via bloodstream are characterized phenotypically by the expression of CD25-CD44+CD117+CD4-CD8- and are referred to as DN1. The signal cascade through the transmembrane receptor tyrosine kinase (c-kit) and its ligand stem cell factor (SCF) is indispensable for the differentiation of DN1 to the DN2 stage.[7] Furthermore, signaling via the transmembrane NOTCH1 receptor and its ligand delta-like-1 (DLL4) becomes indispensable for T cell development during these early thymocyte developmental stages as it suppresses the B cell lineage fate decision. In addition, signals via Notch enhance c-kit expression.[8] Another important mediator inducing early thymocyte proliferation and survival is interleukin-7 (IL-7).[9]

After the first differentiation process, the thymocytes are called DN2 because they upregulate CD25 resulting in the phenotype CD25+CD44+CD117+CD4-CD8-. During this

differentiation process from DN1 to DN2 stage (DN1-2 transition), the progenitors strongly express the chemokine receptors CCR7 and CXCR4. The chemokine ligands for these receptors are expressed and secreted by the cortical TECs (cTECs). The thymocytes in DN1-2 transition and the DN2 thymocytes migrate into the cortical area.[10] CCL25 expressed by TECs directs the DN3 cells towards the outer cortical area.[11] For the proliferation and differentiation of DN3 cells signals conferred by NOTCH ligands are required.[12, 13] The DN3 downregulate CD44 and are thus characterized by the phenotype CD44-CD25+CD4-CD8-. At this stage, they also start to express the pre-TCR molecule by rearrangement of the first chain of the TCR, the β-chain. TCR rearrangement generates diversity, which allows the recognition of various specific peptide antigens that will later be offered to the TCR of mature T cells by antigen-presenting cells in combination with an MHC complex. Again, indispensable induction and differentiation signals are provided via NOTCH signaling.[12] T-cells completing a fully functional TCRβ rearrangement can express the β chain protein of the TCR, which then dimerizes with the invariant pre-TCRα chain (pTα) and appears on the cell surface as a precursor TCR (pre-TCR) complex.[14] After reaching the subcapsular zone, the DN3 thymocytes continue to express CXCR4 and CCR9.[15] After reaching the subcapsular zone, the DN3 thymocytes continue to express CXCR4 and CCR9.[15] DN3 thymocytes incapable of expressing the pre-TCR complex because they failed to rearrange their TCRβ locus die by apoptosis successfully. In contrast, pre-TCR thymocytes passing this called β-selection checkpoint, start to proliferate and finally downregulate CD25 to become DN4 thymocytes (CD44-CD25-CD4-CD8-).

1.1.1.2 Double-negative to double-positive transition and the development of mature T cells

As DN4 cells successfully passed the beta-selection checkpoint, they keep proliferating primarily driven by a combined preTCR and NOTCH1 signal. In mice, DN4 cells initiate upregulation of CD8 first, and as they do not express high levels of the mature TCRαβ complex yet they are called CD8, immature single-positive cells (CD8ISPs). After establishing CD8 on the surface CD4 is upregulated, the CD8ISPs differentiate into CD4, and CD8 double positive (DP) thymocytes and proliferation are terminated. Next, recombination of the TCRα locus is initiated and a complete TCRαβ complex is expressed on the cell surface. Finally, positive selection commences. This is the first process by which it is determined whether the developing T cell with its mature TCR is capable of recognizing

the body's own peptides in the context of MHC molecules. (Self)-antigens are presented by two different types of MHC molecules; MHCI and MHCII. During the random α chain rearrangement, many different receptor segments are randomly synthesized so that the T cell, with its matching TCR/CD3 complex, recognizes and binds multiple different MHC/peptide complexes. According to two classical theories, either the strength of the binding to MHC-I or MHC-II molecules and the associated signal cascades decide the further differentiation of the DP-T cell into the CD4+ or CD8+ SP-T cells.[16, 17]

After contact with the MHC complexes on the cortical TECs, which were used for positive selection the migration, polarity of the developing thymocytes is changed, and the path is again taken towards the middle of the thymus, the medulla. For this purpose CXCR4 is downregulated, CCR7 re-induced and CCR4 and CCR9 up-regulated.[15]

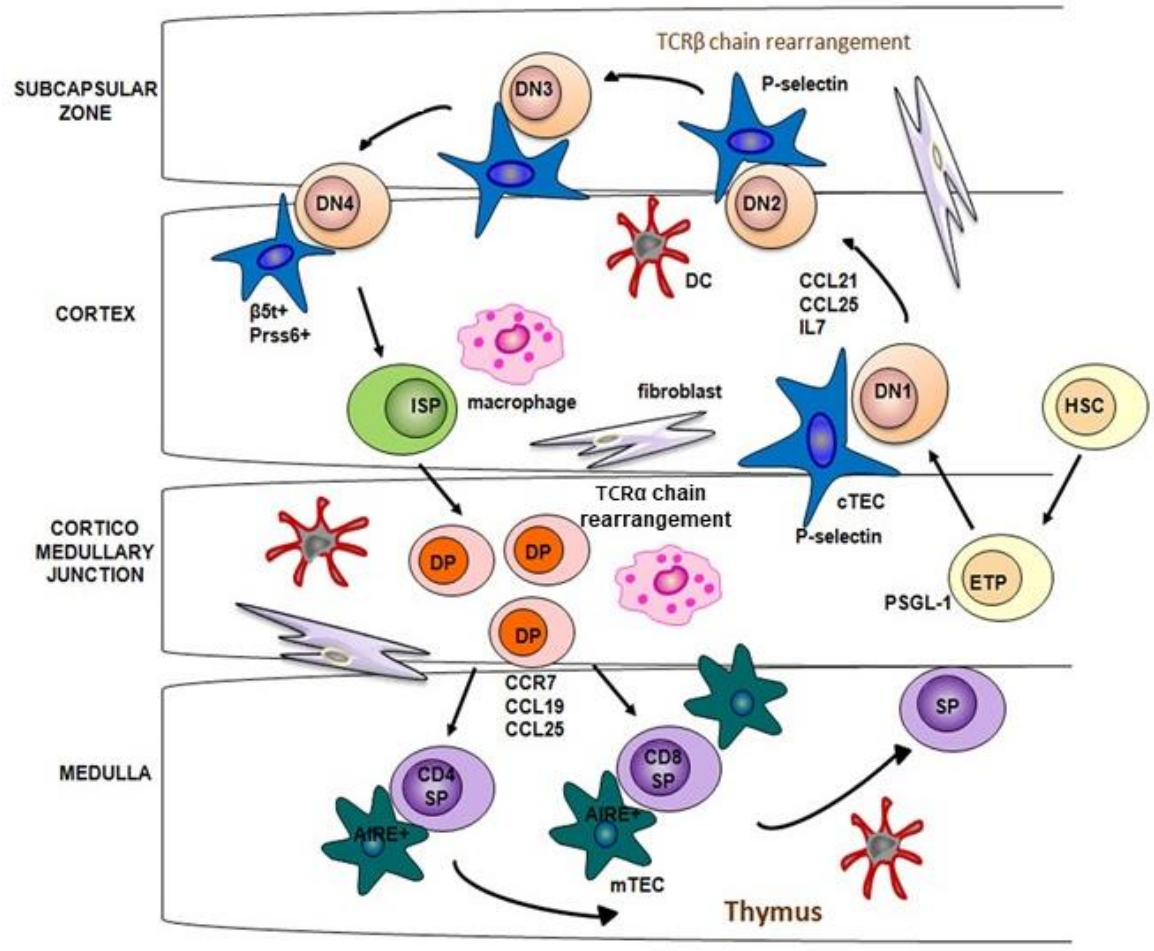

Figure 2. The thymic epithelial cells involvement in T cell development.

Bone marrow HSCs enter the thymus through the cortico-medullary junction (CMJ), a process mediated by CCL21 and CCL25 in the thymus and by the interaction between P-selectin and its cognate ligand PSGL-1 in adult thymus. Stimulation by IL-7 allows the re-location of DN thymocytes from the central cortex to the subcapsular region. DP thymocytes which display a mature

TCR and are capable of binding to self-MHC ligands are positively selected. Pssr6 and b5t modulate proteins expressed by cTECs in this process. Developing thymocytes are relocated from the cortex to the medulla by the chemotactic attraction between CCR7 and the ligands CCL19/CCL21 expressed by mTECs. In the medulla, self-reactive thymocytes are deleted through negative selection, a process mediated by dendritic cells and AIRE-expressing mTECs. AIRE, autoimmune regulator, a transcription factor; cTEC, cortical thymic epithelial cell; DC, dendritic cell; DN, CD4 and CD8 double-negative thymocyte; DP, CD4 and CD8 double-positive thymocyte; ETP, early thymic progenitor; HSC, hematopoietic stem cell; ISP, immature CD8 single-positive cell; mTEC, medullary thymic epithelial cell; SP, single-positive thymocyte. Adapted from ref.[18].

With the help of chemokine polarities successfully reaching the medulla, the SP cells are presented with a wide variety of antigens by dendritic cells, macrophages, and medullary epithelial cells again bound to MHC complexes. This is used to test whether the CD4+ and CD8+ single positive (SP) cells with their mature TCR are able to differentiate between endogenous and exogenous antigens and whether only exogenous antigens are able to bind to MHC complexes, which will later be required for pathogen elimination. If the binding between the TCR and the self-antigens is too strong, apoptosis is induced in these T cells. After successful attainment of the so-called central tolerance, the mature CD4+ and CD8+ SP cells leave the thymus by binding of spingosin-1-phosphate (S1P) molecules to the S1P receptor 1.

1.1.2 Thymic epithelial cells

In adult vertebrates, two anatomically distinct thymic compartments are distinguishable.[19] The cortex is dominated by a dense network of cortical TECs (cTECs) which in contrast to stratified epithelial cells on body surfaces have a three-dimensional organization.[20] In this network, other cell types such as fibroblasts, macrophages, and many immature thymocytes are integrated. The medulla consists of a network of medullary TECs (mTECs) and also macrophages and dendritic cells. Both the cortical and medullary compartments are also controlled by the extracellular matrix (ECM) consisting of collagen, glycosaminoglycans, and glycoprotein. These molecules are secreted by TECs and fibroblasts[21] cTECs, and mTECs populations cannot only be identified by their anatomical location but also by their by specific marker expression.[20-23] cTECs express antigens which bind specific monoclonal antibodies such as Ly51, CDR1, and ER-TR4. mTECs can be identified by the monoclonal antibodies G8.8, ER-TR5 and a lectin, the haemagglutinin I of the European broom Ulex europaeus (UEA). Binding of the lectin UEA to L-fucosyl residues on the cell surface identifies mTECs.[24] Not fully lineage-determined T cell precursors reach the

thymus via the bloodstream and migrate at the boundary between cortex and medulla into the thymus. Here, as mentioned above, they undergo two selection processes within about three weeks.[25]

1.1.2.1 Cortical thymic epithelial cells (cTECs)

cTECs are also characterized by the expression of the specific markers cytokeratin-8, CD205, and Ly51.[26-28] cTECs perform several indispensable functions to promote the development of T cells. They are the primary source of the chemokine CCL25 and the cytokines IL-7 and SCF.[29-31] They express MHC class I and II molecules on their cell surface in conjunction with the Notch ligand Delta-like 4 (DLL4, **Fig. 3**).[32-34] CCL25 is crucial for the proper homing of lymphocyte progenitors migrating from the BM.[35] CCL25 expression is initiated approximately at the time when the thymic system begins to develop at E12 and terminates in adult animals.[36, 37] CCL25 signals via the CCR9 receptor expressed on T-progenitors to allow specific migration into the thymus.[38] Thus, the expression of CCL25 by cTECs is the crucial factor in the colonization of the thymus by CD45+ lymphocyte progenitors.[35] cTECs are also an essential source for IL-7 and SCF.[30] IL-7 is an essential cytokine that supports the proliferation and differentiation of progenitor cells into functional αβ and γδ T cells.[39] Predominantly, signaling via the IL-7 receptor in progenitor cells is necessary to promote T cell development through the DN2 stage (CD44+CD25+) and to improve transcriptional access to the TCR locus.[40] The positive selection of immature T cells helps to enforce either a CD8+CD4- or CD8-CD4+ lineage decision, respectively.[41] Both CD4 and CD8 are required along with the TCR for proper signaling as the CD4 and CD8 molecules are associated with Src family protein kinases, Lck and Fyn.[42] Upon engagement of MHC-I by CD8 or MHC-II by CD4, the activated Lck kinase phosphorylates the intracellular domain of the TCR initiating various survival and proliferative programs.[41, 42] Therefore, the expression of MHC molecules by cTECs is a key process that promotes the continued development of the immature cell. Additionally, according to the kinetic signaling model for T-cell development, a positive signal provided by successful MHC engagement stops CD8 gene expression.[41] If the signal continues by engagement of the CD4 co-receptor with an MHC-II molecule, development continues as a CD4+CD8- cell. If the signal is aborted by the CD4 co-receptor engaging an MHC-I molecule, the immature cells stop CD4 expression and restore CD8 expression yielding a CD4-CD8+ T-cell. This entire process is termed positive selection and allows the generation of T-cells which are capable of recognizing self-peptide: MHC

complexes.[43] The necessity of proper peptide processing for presentation on MHC I and MHC-II molecules on cTECs was also demonstrated.[32, 43] While detailed knowledge of the molecular requirements and machinery for peptide processing and presentation on MHC-II within the thymus remains to be fully elucidated, recent studies have provided important insight into the mechanisms by which peptides are generated for CD8+ T-cell selection. The process of peptide generation begins with the proteasome, an intracellular catalytic structure of four stacked rings of subunits.[44] The inner β subunits compose the catalytic core while the outer subunits perform a regulatory function.[44] During inflammation, the inner β subunits are replaced with specialized "i" or "immuno" variants that generate peptides best suited for loading onto the MHC-I groove.[44] cTECs however, exclusively contain a unique β subunit, the β5t subunit.[32] First described in 2007 β5t is found within the proteasome of the vast majority of cTECs instead of the classical β5i variant.[32] The presence of β5t alters the catalytic activity of the cTEC proteasome to reduce chymotrypsin-like activity seen with the immunoproteasome.[32] β5t -/- mice display a marked defect in the ability to produce mature CD8+ T-cells indicating that the unique peptides generated by a β5t containing cTEC proteasome are critical in positive CD8+ T cell selection.[32] Finally, cTECs express the Notch ligand Delta-like 4 (DLL4). The engagement of DLL4 with Notch-1 receptor on progenitors represents the crucial step to enforce the T cell fate *vs.* other lineage choices and to promote proliferation **(Fig. 3)**.[33, 34]

1.1.2.2 Medullary thymic epithelial cells (mTEC)

mTECs are defined by the expression of CD80 and the transcription factor autoimmune regulator (AIRE) and by binding of the lectin Ulex Europaeus Agglutinin 1 (UEA-1).[27, 45, 46] The function of mTECs in the thymus is also key and non-redundant to that of cTECs.[47] Newly developed CD8+ and CD4+ single-positive (SP) T-cells express the chemokine receptor CCR7[48] and are attracted to the medullary region of the thymus via the mTEC secreted chemokine CCL19.[49] In the medulla, the SP T-cells interact with various cell types, including mTECs, DCs, and macrophages.[43, 47] These interactions are involved in negative selection, a developmental mechanism that removes SP T-cells, which have a high affinity for self-peptides in the context of self MHC molecules. mTECs play an essential role in negative selection. The cornerstone of this process requires developing SP T-cells to sample antigens expressed in tissues external to the thymus. Some of these are restricted to specific tissues. AIRE is a PHD zinc-finger type transcription factor which is

responsible for the promiscuous expression of tissue-specific antigens in mTECs.[46, 50] Mutations of the *AIRE* gene have been associated with a severe autoimmune disease in humans, and *Aire*-/- mice also display characteristics of autoimmune inflammation indicated by lymphocytic infiltration of multiple organs as well as the presence of autoantibodies.[50] In addition to the pivotal role in the expression of restrictive antigens by mTECs, AIRE also suggests to play a central role in the development of mTECs. A comparison of the physical ultrastructure of mTECs in *Aire*-deficient mice indicated that the medullary epithelium of knockout animals was poorly organized and had a markedly different phenotype than wildtype controls.[51] *Aire* knockout epithelial cells had nuclei with more chromatin, and the cytoplasm displayed an increased number of vacuoles.[51]

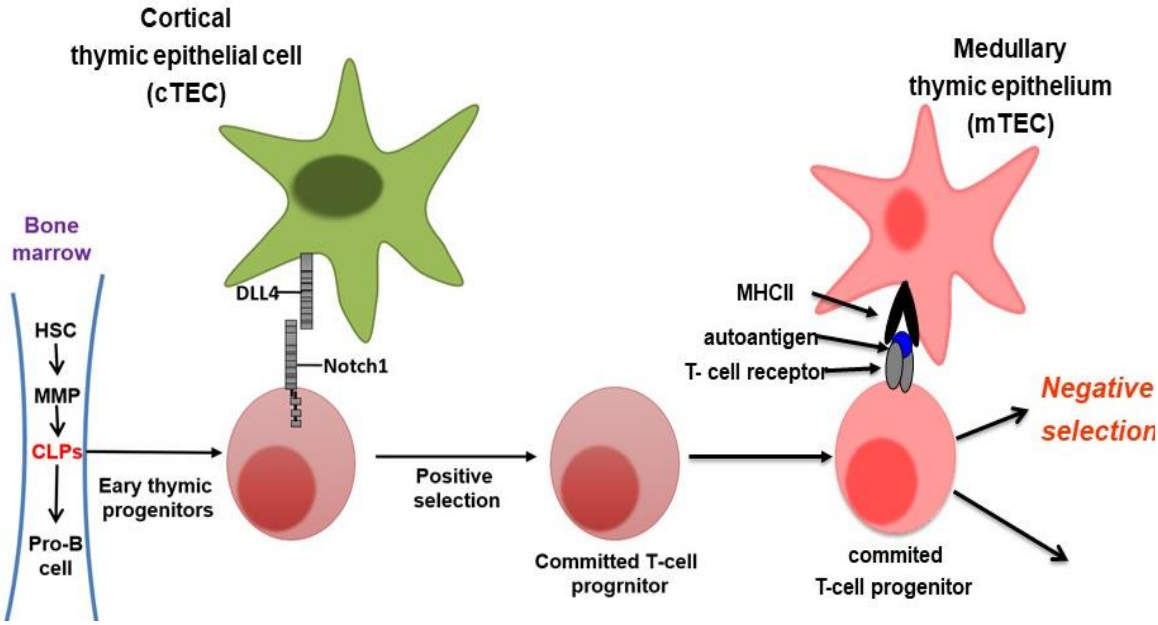

Figure 3. Cortical and medullary thymic epithelial cells control T cell development.

The ligation of the NOTCH1 receptor initiates NOTCH signaling on lymphoid progenitors with its transmembrane ligands including DLL4 on cTECs. DLL4 expression in the thymus is detectable primarily within cTECs. cTEC act as a key regulator of early stage T cell development and positive section. Thymocytes surviving after positive selection migrate towards the boundary of the cortex and medulla in the thymus. While in the medulla, they are presented with a self-antigen presented on the MHC complex of mTECs. Here, negative selection removes thymocytes that are capable of strongly binding with self-MHC peptides. CLP, common lymphocyte progenitor; HSC, hematopoietic stem cell; MMP, Multipotent Progenitor.

1.2 Leukemia

Cancer includes several different diseases, which are characterized by an abnormal overproduction of a specific cell type. These cancer cells acquired several alterations in their genome, resulting in proliferation at an unusually accelerated rate and their resistance to apoptosis. Leukemia is a cancer type of the hematopoietic system and is characterized by abnormal hyperproliferating cells within the BM or circulating blood. Frequently, the first genomic alteration in leukemia is acquired in immature progenitor cells leading to a block of normal differentiation. A second genetic hit often provides the signal for enhanced proliferation. Over time, the now malignant leukemic cells infiltrate the BM and prevent the production and function of other normal blood cells. By perturbing the production of erythrocytes, mature leukocytes and platelets, the most common clinical manifestations of leukemia are a weakness, bleeding complications, and susceptibility to infections.[52] Multiple different types of leukemia were defined but overall leukemias can be grouped according to the precursor cell from which they originate: lymphoblastic vs. myelogenous leukemia. In both groups, leukemias can be classified according to the progression rate of the diseases. Chronic leukemia is characterized by a slow progression rate leading to patients not showing any clinical signs of disease for several months or years. In acute leukemia, dramatic clinical complications occur instantly within days and weeks of disease onset requiring rapid initiation of treatment.

1.2.1 T- cell acute lymphoblastic leukemia (T-ALL)

Acute lymphocytic leukemia (ALL) has three significant subclasses: B-cell precursor (BCP) ALL, mature B-cell leukemia and T-ALL.[53] Acute T cell malignancies involve T-ALL and T cell lymphoma (T-LBL), both of which are classified as T lymphoblastic leukemia/lymphoma in the current WHO classification. T-ALL and T-LBL are usually regarded as different appearances of the same disease defined by the extent of BM involvement being the main feature to distinguish T-ALL (>25% BM blasts) from T-LBL (minimal BM involvement).[53] Although the entities have overlapping clinical, morphological, and immunophenotypic characteristics, some investigators revealed various gene expression profiles, indicating a potentially more significant biological variability than previously assumed. T-ALL is a malignancy originating from an immature thymocyte in the

thymus. The malignant clone proliferates and spreads across the body, particularly in BM, peripheral blood, lymph nodes, and the central nervous system (CNS).

T-ALL arises in the thymus and disseminates via the blood to other hematopoietic tissues and organs. Due to its infiltrative nature T-ALL blasts accumulate rapidly so that the BM is unable to generate sufficient blood cells, and if left untreated, patients will clinically deteriorate rapidly.[54, 55]

The clinical picture of a T-ALL is frequently characterized by the formation of a mediastinal mass emanating from the thymus. In children and adolescents, the proportion of T-ALL in all ALL cases is 10-15%. In adults, the proportion is higher (25% of ALL cases). The overall incidence of T-ALL decreases with age but also occurs in patients over 60 years of age.[56] Intensified polychemotherapy approaches have resulted in a 5-year event-free survival rate of 75% for children and 40% for adults. However, the 5-year event-free survival rate of over 60-year-olds is only 10%.[57] Accordingly, there is an unsatisfied medical requirement for the treatment of elderly T-ALL patients.

Recent innovations in profiling genomes revealed several genetic aberrations associated with T-ALL. These molecular aberrations can be subdivided into chromosomal aberrations and gene mutations.

1.2.1.1 TCR translocations

The activation of the TCR generates signals that are not only decisive for the T cell-mediated immune response but are also crucial for the survival and proliferation of T cells. Chromosomal translocations with TCR loci represent the oncogenic hallmark of T-ALL. Approximately 50% of T-ALL cases carry chromosomal aberrations that can be detected cytogenetically. T-cell receptor gene translocations represent a unique feature of T-ALLs. Most of these aberrations consist of active transcription regulatory components of the T-cell receptor (TCR) genes joint with genes encoding transcription factors. As a result, translocations with TCR loci most likely represent the initiating event of T-ALL development.[58] In about 20-30% of pediatric T-ALL cases, structural aberrations affecting the TCRα locus at 14q11, TCRβ locus [7q34] or TCRγ [7p14] are detected by G banding (Table 1).[59] In this group, the most common TCR translocations are observed with the genes HOX11, HOX11L2, Cyclin D2, LMO1, LMO2, NOTCH1, TAL1, TAL2, LYL1, BHLHB1 and LCK (**Tab. 1**).[60-62] However, several chromosomal translocations do not involve the TCR loci, such as TAL1 (SIL-TAL1), HOXA (PICALM-MLLT10), ABL1

(EML1-ABL1) and ETV6 (ETV6-JAK2).[61, 62]However, the frequency of chromosomal aberrations is relatively limited. All of these genes are essential for healthy T cell development.

1.2.1.2 Genetic mutations in T-ALL

Numerous different gene mutations were described in T-ALL.[63] Multiple different genes including NOTCH1, FBXW7, PTEN, CDKN2A/B, CDKN1B, 6q15-16.1, PHF6, WT1, LEF1, JAK1, IL7R, FLT3, NRAS, BCL11B, and PTPN2 are mutated in T-ALL (**Tab. 2**).[64] However, activating mutations within the NOTCH1 gene occur in more than 50% of T-ALLs and are thus recognized as the key event in T-ALL leukemogenesis.[65] Furthermore, loss-of-function FBW7 (F-box and WD repeat domain containing) mutations occurring in 15-30% of T-ALL cases also lead to NOTCH1 pathway activation as FBW7 is normally mediating proteasomal NOTCH1 degradation.[66] Deletions of CDKN2A and CDKN2B are significant secondary anomalies in pediatric T-ALL. Loss of the CDKN2A/B tumor suppressor expression was reported in 30-70% of T-ALL cases and is caused by chromosomal translocation, promoter hypermethylation, somatic mutation or gene deletions.[67] Activation of the X-linked plant homeodomain (PHD) finger 6 (PHF6) gene was reported in 16% of pediatric and 38% of primary adult T-ALL cases.[68] Several other genes including FLT3, IL7R, IRS4, JAK1, and NRAS, were found to be mutated in T-ALL.[69]

Recurring translocations in T-ALL					
TCR Rearrangements			**Non-TCR Rerrangements**		
Gene	**Rearrangement**	**Frequency**	**Gene**	**Rearrangement**	**Frequency**
TAL1	t(1;14)(p32;q11) t(1;7)(p32;q34)	~3 of T-ALL	TAL1	STIL-TAL1 (1p32 deletion)	12-25% T-ALL
TAL2	t(7;9)(q34;q32)	rare	HOXA	PICALM-MLLT10 (t(10;11)(p13;q14)) MLL-MLLT1 (t(11;19)(q23;p13)) SET-NUP214 9q34 deletions	
LMO1	t(11;14)(p15;q11) t(7;11)(q34;p15)	6-8% of T-ALL	ABL1	EML1-ABL1 (t(9:14)(q34;q32)) BCR-ABL1 (t(9;22)(q34;q11))	8% T-ALL for ABL1 6% T-ALL

				ETV6-ABl1 (t(9;12)(q34;p13)) NUP214-ABL1	for NUP214
LMO2	t(11;14)(p13;q11) t(7;11)(q34;p13) 11p13 deletions		ETV6	ETV6-JAK2 (t(9;12)(p24;p13) ETV6-ARNT (t(1;12)(q21;p13)	Rare
HOX11	t(10;14)(q24;q11) t(7;10)(q34;q24)	30% of T-ALL			
HOX11L2	t(5;14)(q35;q32)	20% Childhood T-ALL 4% Adult T-ALL			
HOXA	Inv(7)(p15q34) t(7;7)(p15;q34)				
LYL1	t(7;19)(q34;p13)	rare			

Table 1. Table of recurring translocations involved in T-ALL

The rearrangements are differentiated into those involving TCR and non-TCR loci. Adapted from (Michael Litt *et al.*, 2012, DOI: 10.5772/55144)

Recurring genetic alterations in T-ALL		
Gene	**Alteration**	**Frequency**
NOTCH1	Sequence mutations	~50% of T-ALL
FBW7	Sequence mutations	~20% of T-ALL
PTEN	Deletions/Sequence mutations	6-8% of T-ALL
CDKN2A/B	Deletions	30-70% of T-ALL
CDKN1B	Deletions/Sequence mutations	12% of T-ALL
6q15-16.1	Deletions	12% of T-ALL
PHF6	Deletions/Sequence mutations	16% of childhood T-ALL 38% of adult T-ALL

WT1	Frameshift mutations	13% childhood T-ALL 12% of adult T-ALL
LEF1	Focal deletions/sequence mutations	15% of childhood T-ALL
JAK1	Sequence mutations	18% of adult T-ALL
IL7R	Gain of function mutation	9% of T-ALL
FLT3	Internal tandem duplication	4% of adult T-ALL 3% of childhood T-ALL
NRAS	Sequence mutations	10% childhood T-ALL
BCL11	Deletions/Sequence mutations	9% to 16% of T-ALL cases with HOX11 overexpression
PTPN2	Deletion	6% of T-ALL

Table 2. Recurring genetic alterations in T-ALL

The type of alteration occurrence in T-ALL cases is indicated. Adapted from (Michael Litt *et al*., 2012 DOI: 10.5772/55144)

1.2.1.3 NOTCH1 signaling pathway in T-ALL

NOTCH1 is crucial for the T-cell fate decision and T-cell development in the thymus.[70] The first evidence that NOTCH1 might be of pathogenic significance for T-ALL was described in 1991 when the translocation t(7;9) (q34;q34) was cloned.[71] The translocation, present in <1% of T-ALL cases, leads to a truncated and thus constitutionally activated version of NOTCH1. When NOTCH1 mutations were found to occur in more than 50% of T-ALLs, the central role of this gene was revealed.[65] The oncogenic potential of activating NOTCH1 mutations was confirmed in experimental mouse modelsNOTCH1 is a transmembrane heterodimer receptor composed of an extracellular and a transmembrane/intracellular subunit which is interacting via the heterodimerization domain (HD). The extracellular complex binds to ligand molecules [the transmembrane proteins Delta-like ligand (DLL1, 3 and 4); and Jagged ligand (1 and 2)] which induce conformational rearrangements and downstream cleavage of NOTCH1, which leads to the intracellular domain (ICN1) being released into the cytosol. Two classes of mutations are commonly found in human T-ALL: extracellular domain mutations which increase ICN1 production

and C-terminal mutations promoting ICN1 activity by decreasing its degradation.[72, 73] The ICN1 translocates into the nucleus where it associates with DNA-binding proteins and cofactors, resulting in a complex that acts as a transcriptional activator. NOTCH1 thereby regulates the expression of several genes, including MYC, HES1 (which affect the PI3KAKT mTOR pathway) and CCND3, which are particularly involved in proliferation, metabolism, and cell cycle.[62] The transcriptional activation of NOTCH1 is terminated by proteasomal degradation of the intracellular ICN1, which is induced by proline, glutamic acid, serine, threonine-rich (PEST) domain detection of the FBXW7-SCF ubiquitin ligase complex.[74, 75] Taken together, the pathogenesis of T-cell leukemogenesis is directly connected to the abnormal stabilization or activation of the intracellular form of NOTCH1. Overexpression of DLL4 ligand is capable of inducing T-cell leukemia in mice via NOTCH1 signaling.[76]

1.2.1.4 Transcription factors in T-ALL

T-ALL results from a multi-stage transformation process in which different genetic mutations accumulate. This process usually starts with a defective T cell receptor rearrangement, which can lead to translocations and deletions. Here the RAG complex wrongly recombines at cryptic recognition sequences within the genome and not within the T cell receptor loci. As already mentioned, some of the most frequent recurrent chromosomal aberrations in abnormal T cell, chromosomal translocations of the TCR gene into the basic helix loop helix genes such as MYC, TAL1, TAL2, LYL1, bHLHB1, and the cysteine-rich LIM domain genes (LMO1, LMO2) as well as the homeodomain genes HOX11/TLX1, HOX11L2/TLX3.[77] The most common genetic aberration induced in T-ALL is SIL/SCL deletion, which leads to aberrant expression of the helix-loop-helix transcription factor SCL (also called TAL1) within T cell progenitors.[78] TAL1 expression is crucial for hematopoiesis. TAL1 modulates positively and negatively the target gene transcription as a significant complex composed of an E protein, the pure LIM proteins LMO1/2, GATA1/2, GATA/2, Ldb1, and other related co-regulators.[79, 80] It has been demonstrated recently that TAL1, GATA-3, LMO1, and RUNX1 combined form a pivotal transcription regulated T-ALL cell to amplify and maintain the TAL1-led leukemogenic program.[81]

1.2.1.5 T-ALL mouse models

In the present study, a double transgenic mouse model was used which consistently developed T-ALL by the aberrant thymic overexpression of the transcription factors TAL1/SCL and LMO1. This was used to investigate changes in the TEC compartment associated with T-ALL. To generate the leukemia model lck-ERT2-SCL and lck-LMO1 transgenic mice were intercrossed. Since the single transgenic lines were maintained heterozygous, only 25% of the offspring were of the double *SCL/LMO1* transgenic genotype.

1.2.1.5.1 Lck-ERT2-SCL

The most common genetic aberration in T-ALL is the SIL/SCL deletion, which leads to aberrant expression of the helix-loop-helix transcription factor *SCL/TAL1* within T cell progenitors. In order to study *SCL*-driven T-ALL we developed a transgenic mouse model allowing tamoxifen-inducible aberrant expression of *SCL* during T cell development (*lck-ERT2-SCL*). Tamoxifen-induced translocation of the *ERT2-SCL* fusion protein led to a T cell developmental block within the thymus. *SCL* induced an abnormal CD8+ T progenitor population, which was incapable of expressing a complete T cell receptor complex on the cell surface, and at the same time showed activation of the NOTCH1 signaling pathway. The observed CD8+ T progenitor pre-leukemic phenotype was strictly dependent on the presence of tamoxifen. However, the latency period of full-blown T-ALL development in *lck-ERT2-SCL* mice proved very long with more than one year, and the penetrance was not very high.[82] However, a background leakiness of *ERT2-SCL* from the cytoplasm into the nucleus could not be ruled out.

1.2.1.5.2 Lck-LMO1

Aberrant LMO1 and LMO2 proteins expression was described in up to 45% of T-ALL cases and overlapped with cases abnormally expressing *SCL*.[83] *LMO1* and *LMO2* were shown to interact with several other transcription factors aberrantly activated in T-ALL. LMO1 is a transcription factor that directly interacts and cooperates with aberrantly expressed *SCL* in T-ALL.[84, 85] Double-transgenic mice aberrantly expressing *SCL* and *LMO1* showed a strikingly accelerated leukemogenesis compared to the single transgenes with 100% penetrance. The median time to the development of T-ALL in *SCL/LMO1* double transgenic mice was 4 months.[86]

1.3 CXCR3 and its ligand CXCL10

CXC chemokines are of central importance for the recruitment and activation of different leukocyte subpopulations. These chemokines are all ligands of the CXCR3 receptor, which are preferentially expressed on activated T helper 1 (TH1) cells primarily regulating in the cellular immune response.[87] CXCR3 is also expressed by endothelial cells,[88] NK cells, monocytes, dendritic cells, and microglia.[89] Endothelial cells uniquely express the CXCR3B mRNA splice variant. Both CXCR3A and CXCR3B mRNAs are expressed in heart, kidney, liver, and skeletal muscles, whereas only the splice variant CXCR3A is found in the placenta.[90] In humans, the CXCR3 splice variants confer different effects depending on the cellular context. While CXCR3A mediates classical CXCR3 functions including chemotaxis and cell proliferation CXCR3B induces cell apoptosis and inhibits cell migration. In contrast, in mice only one CXCR3 isoform exists.[90]

The following ligands bind to CXCR3: CXCL9 or Mig (monokine induced by gamma-interferon), CXCL10 or IP-10 (interferon-inducible protein of 10 kDa) and CXCL11 or I-TAC (interferon-inducible T-cell alpha chemoattractant).[91] CXCR3 reacts to the binding of CXCL9, CXCL10 or CXCL11 by G protein activation. CXCL10 is capable of recruiting TH1+ T cells and is upregulated in inflamed intestinal tissue.[92] CXCL10 is also expressed by human intestinal epithelial cells.[93]

CXCR3 expression is present on subsets of CD4+ T helper cells and CD8+ cytotoxic T cells. Furthermore, CXCR3 is expressed on innate lymphocytes such as natural killer cells and NKT cells and plasmacytoid dendritic cells. By binding its ligands, the CXCR3 receptor is rapidly upregulated on naïve T cells, resulting in their activation. This CXCR3 expression persists preferentially and to a high degree in TH1 CD4+ T cells, CD8+ T effector cells and NK as well as NKT cells. In addition to the differences in the expression patterns of CXC chemokines, there is also a hierarchy with which they bind to CXCR3. CXCL11 has the highest binding affinity to CXCR3, followed by CXCL10 with a medium affinity and CXCL9 with the lowest affinity to the receptor.[91]

1.3.1 CXCR3/CXCL10 involvement in cancer

Chemokine and chemokine receptor interactions have recently become indispensable for the development and progression of cancer. CXCL10 is highly expressed in a large variety of

human diseases. CXCL10 is involved in the abnormal processes of primary diseases, cancer, and infectious diseases, inflammatory and autoimmune diseases.[94]

In contrast to potential tumor limiting measures, CXCL10 also mediates tumor-promoting effects. The CXCL-10/CXCR3 axis promotes the anti-tumor cytotoxic T lymphocyte (CTL) response by mediating immune cell migration, differentiation, and activation. On the other hand, CXCL10 induces tumor growth and metastasis via an autocrine axis by autochthonous CXCR3 cancer cell expression.[95] For example, in mammary cancer cell lines MDA-MB-435 and MCF-7 Ras trigger overexpression of CXCL10 via RAF and PI3 kinase signaling pathways. When overexpressed, CXCL10 binds to CXCR3 and promotes breast cancer growth.[96] CXCL10 has previously been shown to be an autocrine invasion factor in natural nasal killer/T cell lymphoma.[97] Furthermore, the CXCL-10/CXCR3 axis mediates colorectal cancer metastasis and tumorigenesis in basal cell carcinoma and human glioma.[98, 99]

1.4 Aim of the thesis

The heterogeneous thymic epithelial cell network provides the microenvironment required for intrathymic T cell development and repertoire selection. The NOTCH receptor ligand DLL4, which is indispensable for T cell development, is expressed exclusively by thymic epithelial cells (TECs) within the thymus. The NOTCH1 signaling pathway plays a central role not only in normal T cell development but also in T cell lymphoblastic leukemia (T-ALL). The activity of most T-ALL NOTCH1 receptor mutations is ligand-dependent. Accordingly, we postulate that DLL4-expressing TECs play a crucial role in the development and maintenance of T-ALL. Also, thymic epithelial cells express several essential cytokines and chemokines, which may foster the emergence of T-cell acute lymphoblastic leukemia (T-ALL).

The principal hypothesis of the project is that TECs play a critical role in the development and maintenance of T-ALL.

The specific objectives of this project are:

(1) Characterization of the TEC compartment in preleukemic and leukemic T-ALL mice.
(2) Examination of the supporting influence of TEC cell lines on growth and survival of T-ALL cells.
(3) Investigation of the principal role of TEC secreted cytokines in supporting T-ALL development and maintenance.

CHAPTER-2

MATERIALS AND METHODS

2 MATERIAL AND METHODS

2.1 Material

2.1.1 Chemicals and reagents

Chemical/Reagents	Suppliers
10X PBS	Ambion, Life technologies, Darmstadt, Germany
Aceton	Sigma-Aldrich, Taufkirchen, Germany
Agarose Nusieve	Lonza, Basel, Switzerland
Agarose Ultrapure	Invitrogen, Darmstadt, Germany
Ampuwa	Braun, Ecotainer, Melsungen, Germany
Collagenase	Roche Diagnostics, Mannheim, Germany
DAPI	Sigma-Aldrich, Taufkirchen, Germany
Diastase (α-Amylase)	Sigma-Aldrich, Taufkirchen, Germany
Dispase	Gibco, Life technologies, Darmstadt, Germany
DMSO	Sigma-Aldrich, Taufkirchen, Germany
Dnase	Roche Diagnostics, Mannheim, Germany
dNTPs	Promega, Mannheim, Germany
D-PBS (w/o Ca_{2+}, w/o Mg_{2+})	Invitrogen, Darmstadt, Germany
D-PBS CTS™	Invitrogen, Darmstadt, Germany
EDTA	Sigma-Aldrich, Taufkirchen, Germany
Ethanol absolute	Sigma-Aldrich, Taufkirchen, Germany
FACS Clean	BD Biosciences, Heidelberg, Germany
FACS Flow	BD Biosciences, Heidelberg, Germany
FACS Rinse	BD Biosciences, Heidelberg, Germany
Fetal calf serum (FCS)	PAN Biotech, Aidenbach, Germany
Gel Loading Solution	Sigma-Aldrich, Taufkirchen, Germany
GoTaq®Hot Start Polymerase	Promega, Mannheim, Germany
Isopropanol	Sigma-Aldrich, Taufkirchen, Germany
Magnesium chloride	Promega, Mannheim, Germany
Mercapthoethanol	BioRad, Munich, Germany
Mounting medium Vectashield®HardSet® with DAPI	Vector Laboratories, Germany

PCR-Buffer	Promega, Mannheim, Germany
Penicillin/Streptomycin	Sigma-Aldrich, Taufkirchen, Germany
Percoll™ Propidium iodide (PI)	GE Healthcare, Sigma-Aldrich, Taufkirchen, Germany
Proteinase K	Sigma-Aldrich, Taufkirchen, Germany
Taq Polymerase	Promega, Mannheim, Germany
Tissue-Tek®O.C.T.™ Compound, Sakura®	Finetek, Alphen aan de Rijn, Netherland
Tris Ultra-Pure	Invitrogen, Darmstadt, Germany
Trypanblue	Sigma-Aldrich, Taufkirchen, Germany
TrypLE™Express	Gibco, Life technologies, Darmstadt, Germany
Xylol	Roth, Karlsruhe, Germany

Table 3. Suppliers of reagents utilized in this study

2.1.2 Medium

Medium	**Company**
DMEM, high glucose, GlutMAX™supplement, pyruvate	Gibco, Life technologies, Darmstadt, Germany
Iscove's Modified Dubelcco's Medium IMDM Medium	Gibco, Life technologies, Darmstadt, Germany
RPMI 1640 Medium	Gibco, Life technologies, Darmstadt, Germany

Table 4. List of the medium used in cell culture

2.1.3 Kits

Reagent	**Company**
APC BrdU Flow-kit der	BD Biosciences, Heidelberg, Germany
cDNA Eco Dry 20 Random	Thermofisher, Darmstadt, Germany
Fast frozen stain kit	Polysciences, warrington, PA,USA
QlAamp DNA Blood kit	Qiagen, Hilden, Germany
QlAamp DNA Micro kit	Qiagen, Hilden, Germany

QlAquick Gel Extraction kit	Qiagen, Hilden, Germany
Mouse CXCL10/IP-10/CRG-2 DuoSet ELIS	R&D Biosystems, Wiesbaden, Germany
RNase-free DNase set	Qiagen, Hilden, Germany
RNeasy Micro kit	Qiagen, Hilden, Germany
RNeasy mini kit	Qiagen, Hilden, Germany
RT^{2}Profiler PCR Array mouse Notch signaling pathway	Qiagen, Hilden, Germany
RT^{2}Profiler PCR Array mouse Epithelial to Mesenchymal Transition	Qiagen, Hilden, Germany
RT^{2}Profiler PCR Array mouse mouse cytokines & chemokines	Qiagen, Hilden, Germany
RT^2 SYBR® Green qPCR Mastermixes	Qiagen, Hilden, Germany
TaqMan Assays	Thermofisher, Darmstadt, Germany

Table 5. List of Kits used in this study

2.1.4 Antibodies

Mouse antibodies			
Name	**Conjugation**	**Clone**	**Company**
Armenian Hamster IgG	PE	eBio299Arm	eBioscience
BP-1	PE	BP-1	BD Pharmingen
CD19	PerCP-Cy5.5	6D5	BD Pharmingen
CD25	DAPI	eBio3C7	eBioscience
CD3e	PerCP-Cy5.5	145-2C11	eBioscience
CD31	PE	MEC13.3	BD Pharmingen
CD326 (EpCAM)	APC	G8.8	eBioscience
CD4	PerCP-Cy5.5	RM4-5	BD Pharmingen
CD4	PE-Cy7	RM4-5	BD Pharmingen
CD44	APC	IM7	BD Pharmingen
CD45	PE-Cy7	30-F11	BD Pharmingen

CD45R (B220)	PerCP-Cy5.5	RA3-6B2	BioLegend
CD8a	AlexaFluor 700	56-6.7	BD Horizon
CD8a	APC-Cy7	53-6.7	eBioscience
C-kit (CD117)	APC-Cy7	2B8	BioLegend
CXCR3	PE	CXCR3-173	Biolegend
Gr1 (Ly-6G and Ly6C)	PerCP-Cy5.5	RB6-8C5	BioLegend
Mac1 (CD11b)	PerCP-Cy5.5	M1/70	BioLegend
MHCII	APC-Cy7	M5114.15.2	eBioscience
Nk1.1	PerCP-Cy5.5	PK136	eBioscience
Notch1	PE	HMN1-12	BioLegend
TCRb	PE	H57-597	BD Pharmingen
TCRb	FITC	H57-597	BD Pharmingen
Ter119	PerCP-Cy5.5	TER119	eBioscience
UEA	FITC	Protein	Vector Laboratories
Mouse IgG1, κ	PE	-	Biolegend
Human antibodies			
Name	**Conjugation**	**Clone**	**Company**
CD183 (CXCR3)	PE	G025H7	Biolegend

Table 6. List of antibodies used for flow cytometric analysis

2.1.5 Primers and Taqman probes

Name	Sequence (5' > 3')
hLMO1_fwd	AAG TGT GCG TGC TGT GAC TG
hLMO1_rev	GCG AAG CAG TCG AGG TGA TA
SCL_hGH_fwd	GGA AGT CCC AAC TGA CCC TA
SCL_hGH_rev	ATT TTA GGG GCG CTT ACC TG
wt_SCL _fwd	AGC ATG CTC TTT TCC AGC AT
wt_SCL _rev	CTC AGG CTG GCC TAA AAC TG

Table 7. List of used genotyping and expression primers

Symbol	Gene	Exon	Assay ID
CCL25	Chemokine (C-C motif) ligand 25	4-5	Mm00436443_m1
CXCL10	Chemokine (C-X-C motif) ligand 10	1-2	Mm00445235_m1
CXCL12	Chemokine (C-X-C motif) ligand 12	2-3	Mm00445553
DLL4	Delta-like 4 (Drosophila)	6-7	Mm01338018_m1
DHH	Desert hedgehog	1-2	Mm01310203_m1
DTX1	Deltex 1 homolog	9-10	Mm00492297_m1
FBXO6	F-box protein 6	4-5	Mm01257500_m1
GLI1	GLI-Kruppel familiy member GLI1	2-3	Mm00494645_m1
HES1	Hairy and enhancer of split 1,	3-4	Mm00468601_m1
HPRT1	Hypoxanthine guanine phosphoribosyl transferase 1	6-7	Mm00446968_m1
IHH	Indian hedgehog	2-3	Mm00439613_m1
IL-7	Interleukin 7	2-3	Mm01295803_m1
IL-18	Interleukin 18	5-6	Mm00434226_m1
NOTCH1	Notch gene homolog 1	2-3	Mm00435245_m1
PTCH2	Patched homolog 2	19-20	Mm00436047_m1
VEGFA	vascular endothelial growth factor A	2-3	Mm01281447_m1
SHH	sonic hedgehog	2-3	Mm00436528_m1
TGFB1	transforming growth factor, beta 1	5-6	Mm01178820_m1

Table 8. List of used mouse-specific real-time PCR TaqMan assays

2.1.6 RT² profiler™ PCR array

RT² Profiler™ Mouse Cytokines & Chemokines PCR Array, QIAGEN, Hilden, Germany
Chemokines
CCL1 (I-309), CCL11 (EOTAXIN), CCL12 (MCP-5, SCYA12), CCL17 (TARC), CCL19, CCL2 (MCP-1), CCL20 (MIP-3A), CCL22 (MDC), CCL24 (MPIF-2 , EOTAXIN-2, MPIF-2, EOTAXIN-2), CCL3 (MIP-1A), CCL4 (MIP-1B), CCL5 (RANTES), CCL7 (MCP3), CX3CL1, CXCL1 (GRO1), CXCL10 (INP10), CXCL11 (ITAC, IP9), CXCL12 (SDF1), CXCL13, CXCL16, CXCL3, CXCL5 (ENA-78, LIX), CXCL9 (MIG), PF4, PPBP, XCL1.
Interleukins
IL10, IL11, IL12A, IL12B, IL13, IL15, IL16, IL17A, IL17F, IL18, IL1A, IL1B, IL1RN, IL2, IL21, IL22, IL23A, IL24, IL27, IL3, IL4, IL5, IL6, IL7, IL9.
Interferons
IFNA2, IFNG.
Growth Factors
BMP2, BMP4, BMP6, BMP7, CNTF, CSF1 (MCSF), CSF2 (GMCSF), CSF3 (GCSF), GPI1, LIF, MSTN (GDF8), NODAL, OSM, THPO, VEGFA.
TNF Receptor Superfamily Members
CD40LG (TNFSF5), CD70 (TNFSF7), FASL (TNFSF6), LTA (TNFB), LTB, TNF, TNFRSF11B (OPG), TNFSF10 (TRAIL), TNFSF11 (RANKL), TNFSF13B.
Other Cytokines
ADIPOQ (ACRP30), CTF1, HC, MIF, SPP1, TGFB2.
Anti-Inflammatory Cytokines
CCL19, IL10, IL11, IL12A, IL12B, IL13, IL18, IL2, IL22, IL23A, IL24, IL4, IL6, TGFB2.

Table 9. List of genes in Cytokine and chemokine involved in RT² Profiler™ array

RT² Profiler™ Mouse Notch Signaling Pathway PCR, QIAGEN, Hilden, Germany
Notch Signaling
Notch Ligands: NOTCH1, NOTCH2, NOTCH3, NOTCH4. Notch Binding: DLL1 (DELTA1), DLL3, DLL4, DTX1, JAG1, JAG2, LFNG, MFNG, NUMB, RFNG. Notch Receptor Processing: ADAM10, ADAM17 (CD156B), NCSTN, PSEN1, PSEN2, PSENEN. Transcription Factors & Cofactors: EP300, MAML1, MAML2, NCOR2, RBPJL, SNW1 (SKIIP).
Notch Target Genes
Apoptosis: CFLAR (CASPER), ID1, IFNG, NFKB1, PTCRA. Cell Cycle: CCND1, CDKN1A (P21CIP1, WAF1). Cell Adhesion Molecules: CD44, ERBB2 (HER-2, NEU). Cell Differentiation & Development: DTX1, HES1, HES5, HEY1, HEY2, HEYL, JAG1, KRT1, LFNG, LOR, NOTCH1, NR4A2 (NURR1), PPARG. Neurogenesis: ERBB2 (HER-2, NEU), FOS, HES1, HEY1, NR4A2 (NURR1). Immune Response: CHUK (IKBKA), IFNG, IL17B, IL2RA (CD25), NFKB1, NFKB2, STAT6. Transcription Factors & Cofactors: FOS, FOSL1 (FRA-1), HES1, HES5, HEY1, HEY2, HEYL, ID1, NFKB1, NFKB2, NR4A2 (NURR1), PPARG, STAT6.
Other Notch Signaling Genes
Cell Cycle: AXIN1, CCNE1, FIGF (VEGFD), GSK3B. Cell Growth & Migration: LRP5, SHH, WISP1. Cell Proliferation & Differentiation: CTNNB1 (CATNB), FIGF (VEGFD), GSK3B, IL6ST (GP130), LMO2, MMP7, PAX5, RUNX1 (AML1), SHH, STIL. Neurogenesis: NEURL1A (NEU1), PAX5, POFUT1, ZIC2 (HPE5). Transcription Factors & Cofactors: AES (TLE5, GROUCHO), CBL, CTNNB1 (CATNB), GLI1, HOXB4, HR, PAX5, RUNX1 (AML1), TLE1. Other Notch Signaling Genes: SEL1L, SUPT6.
Pathways Crosstalking with Notch Signaling
Hedgehog Signaling: GLI1, GSK3B, SHH, SMO, SUFU. WNT Signaling: AES (TLE5, GROUCHO), AXIN1, CTNNB1 (CATNB), FZD2, FZD3, FZD4, FZD5, FZD7, GSK3B, LRP5, TLE1, WISP1, WNT11.

Table 10. List of genes in Notch Signaling pathways covered by RT² Profiler™

2.1.7 Equipment

Equipment	Company
Analytical balance ALJ 220-4NM	Kern, Balingen, Germany
Autoclave D-65	Systec, Wettenberg, Germany
Cellsorter FACSAria II	BD Biosciences, Heidelberg, Germany
Centrifuge 5417C	Eppendorf, Hamburg, Germany
Centrifuge Allegra 6KR	Beckman Coulter, Krefeld, Germany
Centrifuge Allegra X-15R	Beckman Coulter, Krefeld, Germany
Cryomicrotome Leica CM1850 UV	Leica Biosystems, Wetzlar, Germany
Flow cytometer BD LSRII	BD Biosciences, Heidelberg, Germany
Gel Documentation System	Biometra, Göttingen, Germany
Gel electrophoresis chamber Sub-Cell®GT	BioRAD, München, Germany
Genetic sequencer 3130XL	Thermofisher, Darmstadt, Germany
Inkubator	Thermo Scientific, Braunschweig, Germany
Microscope BZ-9000	Leica Biosystems, Wetzlar, Germany
Microscope CK2	Keyence, Osaka, Japan
Microscope DM1000LED	Leica Biosystems, Wetzlar, Germany
Photometer plus	Eppendorf, Hamburg, Germany
Precision balance EW 4200-2NM	Kern, Balingen, Germany
QuantStudio™ Real-Time PCR	Applied Biosystems, Darmstadt, Germany
StepOne Plus Real-Time PCR System	Applied Biosystems, Darmstadt, Germany
Sterilbank Laminar Flow	BSH AG, Dettingen, Germany
Thermocycler Flex Cycler	Analytik Jena, Jena, Germany
Thermomixer comfort	Eppendorf, Hamburg, Germany
Table centrifuge Sprout	Heathrow Scientific, Illinois, USA

Vortexer Genius 3	STARLAB, Hamburg, Germany
Z2 Coulter Particle Count and Size Analyzer	Beckman Coulter, Krefeld, Germany

Table 11. List of Equipments

2.1.8 Plastic wares

Items	Company
Cell coun tainer with lid	Ratiolab, Dreieich, Germany
Cell culture bottles, 75cm2 with filter cap	Greiner Bio-One, Solingen, Germany
Cell sieve 40µm, 100µm (nylon)	BD Biosciences, Heidelberg, Germany
Centrifuge tube Falcon, 15 ml, sterile	Greiner Bio-One, Solingen, Germany
Centrifuge tube Falcon, 50 ml, sterile	Greiner Bio-One, Solingen, Germany
Cover glasses 24 x 40mm	Menzel, Braunschweig, Germany
Cover glasses, ground flat (24x24mm)	Menzel, Braunschweig, Germany
Freezing vessels Cryo.s ™	Greiner Bio-One, Solingen, Germany
Freezer container Nalgene® Mr. Frosty	Sigma-Aldrich, Taufkirchen, Germany
FACS tube 5ml	BD Biosciences, Heidelberg, Germany
ImmEdge-Pen	Vector Laboratories, Burlingame, California
Microtest™ U-Bottom, 96 well	BD Biosciences, Heidelberg, Germany
Microtome Blades Feather® Type S35	pfm medical, Cologne, Germany
Microcentrifuge tubes 1.5ml	StarLab, Hamburg, Germany
Mullkompressen	Beese Medical, Barsbüttel, Germany
Multiwell ™ 12 well, tissue culture treated	BD Biosciences, Heidelberg, Germany
Multiwell ™ 24 well, tissue culture treated	BD Biosciences, Heidelberg, Germany
Multiwell ™ 6 well, tissue culture treated	BD Biosciences, Heidelberg, Germany

Neubauer Kammer 0,1mm	Assistent, Sondheim, Germany
PCR strips, 0.2ml tubes and lids	Greiner Bio-One, Solingen, Germany
Pipette tips 10, 20, 100, 200, 1000µl	StarLab, Ahrensburg, Germany
Pipetting	Hirschmann® Laborgeräte, Eberstadt, Germany
Slides	Engelbrecht, Edermünde, Germany
Slide Superfrost® Plus	Menzel, Braunschweig, Germany
Slide holder Rotilabo®	Roth, Karlsruhe, Germany
Staining cuvettes Rotilabo®	Roth, Karlsruhe, Germany

Table 12. List of Plastic wares

2.1.9 Cell lines

Name	Origin	Reference
ANV41.2 (ANV)	Murine thymic epithelium of k14 E6 / E7 hyperplastic thymi; cortical properties	Andrew G. Farr University of Washington, Seattle, USA (Nelson *et al*., 1998) [100]
TE-71	Enzymatically dissociated murine Thymus stroma; medullary properties	Andrew G. Farr University of Washington, Seattle, USA (Farr *et al*., 1989) [101]
OP9- GFP	The OP9 cell line was established from newborn op/op mouse calvaria.(bone marrow/stroma)	Nakano T, *et al*. [102]
Jurkat	Peripheral blood of a 14 year old boy by Schneider et al.,	Weiss A, *et al*. [103]

	and was originally designated JM.	
DND-41	Peripheral blood of 13-years old boy with T- acute lymphoblastic leukemia(T-ALL;type III cortical)	Drexler, H.G., *et al*. [104]
ALL-SIL	Peripheral blood of a 17-year-old man with T-ALL (T cell acute lymphoblastic leukemia) at relapse	Drexler, H.G., *et al*. [104]
HPB-ALL	Established from the peripheral blood of a 14-year-old Japanese boy with ALL and thymoma at diagnosis	Morikawa, S. *et al*. [105]

Table 13. List of Cell lines

2.1.9.1 Composition of the media for cell culture

Medium for ANV cells: DMEM with GlutMAX™, 10% FCS, 1% Penicillin-Streptomycin

Medium for TE-71 cells: IMDM, 15% FCS, 1% Penicillin-Streptomycin

Medium for Jurkat cells: RPMI1640, 15% FCS, 1% Penicillin-Streptomycin

Medium for DND-41 cells: RPMI1640, 10% FCS, 1% Penicillin-Streptomycin

Medium for ALL-SIL and HPB-ALL cells: RPMI1640, 20% FCS, 1% Penicillin-Streptomycin

Freezing medium: 90% FKS, 10% DMSO

2.1.10 Solutions and buffers

FACS-Buffer:

- PBS
- 1 % NaN3
- + 2% FKS

Ear punch lysis buffer:

- 20ml 5M NaCl
- + 5ml 0.5M EDTA (pH8.5)
- + 50ml 0.1M Tris-HCl-Buffer (pH 8.5)
- + 12.5ml 20% SDS
- + 0.5mg/ml Proteinase K
- fill up to 500ml distilled water

TAE-Buffer (50X):

- 242gms Tris Base
- + 57.1ml Glacial acetic acid
- + 100ml 0.5M EDTA (pH 8)
- fill up to 1000ml distilled water

Tris-HCl-Buffer (1M):

- 121.14gms Tris Base
- fill up with 1000ml distilled water
- Adjust to pH 8.5 with HCl

Percoll solutions:

- 1.124g/ml
- 1 volume 10X PBS
- + 9 volume Percoll 1.13g/ml

- 1.115g/ml
- 0.726ml 1X PBS
- + 9.274ml 1.124gms per ml Percoll

- 1.065g/ml
- 4.76ml 1X PBS
- + 5.24ml 1.124g/ml Percoll

2.1.11 Software used

Evaluation of flow cytometry data was performed using FACSDiva (BD Biosciences) software and FlowJo 9.5.6 (Miltenyi Biotec) software. 384-well (Applied Biosystems) was used to evaluate the data from the RT-qPCR StepOnePlus (Applied Biosystems) and QuantStudio™ 5 Real-Time PCR System. All statistical data were obtained using Microsoft Excel 2010 and GraphPad Prism 5 (GraphPad Software). The BZ Analyzer software (Keyence) was used for the microscopic images. Primers were designed using primer 3. (http://frodo.wi.mit.edu/primer3/).

2.2 Methods

2.2.1 Mice

To investigate changes in the TEC compartment associated with T-ALL, we used previously described (Section, 1.2.1.5 mouse model) transgenic mouse lines lck-ERT2-SCL (*SCL*)[82] and Lck-LMO1 (*LMO1*)[84] (lck-ERT2-SCL;lck-LMO1, abbreviated *SCL/LMO1* mice) were intercrossed. Since the single transgenic lines were maintained heterozygous, only 25% of the offspring were of the double *SCL/LMO1* transgenic genotype. All investigations were approved by the governmental office for animal care (Landesamt für Natur, Umwelt und Verbraucherschutz North Rhine-Westphalia (LANUV NRW), Recklinghausen, Germany (reference number 84-02.04.2015.A146))

2.2.1.1 Keeping and breeding the mice, organ removal

The mice were bred in the central facility (ZTL) at University Hospital Essen and kept in cages under controlled environmental conditions (22 +/- 2 ° C temperature, 55 +/- 5% humidity, 12-hour day-night cycle). Pups were genotyped at 2 weeks of age by PCR analysis of the ear punch DNA and labeled with an individual ear piercing. At the age of 21 days, the animals were weaned and separated by gender. For analysis, mice were sacrificed by cervical dislocation or with carbon dioxide. Thorax and abdomen were opened, thymus were removed and placed in PBS / 2% FCS for experimental purposes, a piece of the kidney was stored at -20 ° C for confirmation of the genotype. Mice which could potentially developing T-ALL were monitored daily, and animals displaying any sign of illness (lethargy, weight lols hunched posture, ruffled fur, dyspnea or pallor) were euthanized, and the thymus, spleen and BM were harvested for analysis.

2.2.2 Genotyping

Young animals were separated from their parent by gender at the age of 21 days. At the same time, these animals were punched to get ear hole marks that represented their identification number. In order to genotype individual animals, the ear punch was removed, and the DNA was isolated. PCR detected the respective genetic transgene constellation.

2.2.2.1 DNA isolation from tissue and single cell suspensions

2.2.2.1.1 DNA extraction from the tissue (ear punch)

The DNA extraction was performed by an established protocol consists of three steps. First, the tissue was lysed burst cells to release the DNA by incubating the tissue with 20% sodium dodecyl sulfate (SDS). Proteinase K was added at a concentration of 0.5 mg per ml, leading to degradation of proteins. Further components of the ear punch lysis buffer are 0.2 M NaCl, 5 mM ethylenediaminetetraacetate (EDTA), 0.1 M Tris-HCl buffer and distilled water. The chelate compound EDTA promotes the disruption of cells by causing instability of the cell membrane and cell-to-cell adhesion caused by the binding of Ca_{2+}. Furthermore, EDTA inhibits the activity of nucleases.

The ear punch of the animals was incubated overnight at 55 ° C, shaking at 1200 RPM in one thermomixer digested in 500 ul each of the buffers. It followed the centrifugation step at 14000 rpm and room temperature (RT) for 10 min. In the second step, DNA precipitation followed. Nucleic acids are due to their negative charge hydrophilic, due to the phosphate groups (PO_3^-) along the sugar-phosphate backbone. The positive Na + ions, which contained in the buffer system used to neutralize the negative charge the phosphate groups and reduce the solubility of the DNA. In addition, 500 µl of 100% isopropanol additionally promotes the attraction of the ions, and the DNA fails. The precipitated molecule was prepared by gently inverting as a cloudy white structure. This was followed by another centrifugation in which the entire chromosomal DNA was pelletized, and the supernatant was discarded. DNA was eluted by washing the pellet with 70% ethanol. The supernatant was discarded for centrifugation, and the DNA pellet was dried. After the ethanol had evaporated, the DNA 200 µl H2O was dissolved at 1200 rpm and a temperature of 55 ° C within one hour.

2.2.2.1.2 DNA extraction from a single cell suspension

DNA isolation from a single cell suspension, e.g., thymocytes, was performed according to the protocol provided with Qiagen QIAamp® DNA Blood Kit. This protocol of nucleic acid extraction is based on the ability of DNA to bind to silica particles in the presence of certain salts. The DNA gets absorbed during the centrifugation of the cell lysate through the spinning columns. Impurities are removed in washing steps, and the DNA is then eluted in nuclease free distilled water. To purify the genomic DNA, 5×10^6 cells were used. After

isolation, the concentration of nucleic acids was determined by measuring the optical density (OD) at a wavelength of 260 nm photometrically.

Nucleic acids are measured at 260 nm because at this wavelength, the aromatic rings of the bases have their absorption maximum. The absorbance of double-stranded DNA is due to the so-called base stacking effect, which is lower than that of single-stranded nucleic acid so that different multipliers are used for the calculation of DNA and RNA. This corresponds to 1 OD 260 at a concentration of 40 µg / ml for RNA, while for DNA 1 OD 260 = 50 µg / ml certain amino acid residues (tryptophan, tyrosine) absorb strongly at a wavelength of 280 nm. The DNA obtained was then used for polymerase chain reactions to identify the genotype.

2.2.3 Polymerase chain reaction (PCR)

The polymerase chain reaction (PCR) becomes the exponential amplification of the DNA sequences used. Taq polymerase is one of the essential components of this amplification method. This polymerase catalysis is based on denatured double-stranded regions and specially annealed oligonucleotides and enables DNA replication with the help of the deoxyribonucleoside-5'-triphosphates (dNTPs) offered. PCR analysis can be divided into three main steps, each of which requires a different temperature optimum.

The first step is to denature the present DNA double helix at 95 °C. After separating the strands, primers are aligned in the second steps at a temperature of 50-60 °C called annealing. The hybridization of the primers with the DNA determines the starting point of the synthesis for the DNA and thus for the area to be amplified. The subsequent elongation, the extension of the primer at 72 ° C, leads to the synthesis of a double strand. The Taq polymerase uses the DNA present as a template to produce a complementary strand. Denaturation, annealing, and elongation are repeated cyclically. The repetition after the second cycle leads to a doubling of the part of the original DNA, limited by choice of oligonucleotides. Another important component of the PCR is magnesium (Mg) ions, which act as cofactors of the polymerase. The primer pairs used for genotyping are shown in **Table 7**.

2.2.4 Electrophoretic separation of the DNA

Agarose gel electrophoresis was performed for the analysis of the PCR products. Charged particles migrate in an electric field to the pole of the opposite charge. The DNA backbone

carries negative charges and migrates accordingly to the anode (+ charge). In a medium such as an agarose gel, DNA can be separated according to its length (in base pairs, bp). The molecular structure of an agarose gel acts as a matrix, making it harder for larger molecules to exist for smaller ones. As a result, smaller fragments migrate faster and further through the agarose. The migration speed of DNA molecules in an agarose gel is proportional to their size. The density of the matrix and thus the resolution can be varied by selecting the agarose concentration. To analyze the genotyping PCR detection, gels with an agarose concentration of 1.5% or 2% (w/v) were used in a TAE buffer system. The agarose was boiled in a TAE buffer and later add 2µl roti gel stain then poured into a casting device. The PCR products were provided with a charged buffer and separated at a voltage of 90 to 100 volts. The gel electrophoresis was carried out in a particular device and with an appropriate power supply. A size standard (φ X174 RF DNA / Hae III fragments) made it possible to estimate the length of the separated DNA fragments. The gel electrophoresis was analyzed using the BioDocAnalyze system.

2.2.5 Cell biology methods

2.2.5.1 Methods of cell culture

2.2.5.1.1 Freezing / thawing of cells

For the cryopreservation of the thymic epithelial cell lines ANV [100], TE-71 ([101], stromal cell line (OP-9) and the human T-ALL cell lines (Jurkat, DND-4, HPB-SIL, and ALL-SIL) were centrifuged (5 minutes, 1800 rpm) and re-suspended in a concentration up to 2×10^6 cells per ml freezing medium (90% FCS, 10% DMSO). Isopropanol-filled freezing aids (Nalgene® Mr. Frosty) were used for constant but gentle cooling of the ampoules (1°C/minute) to -80 °C. For long-term storage, the cells were stored in liquid nitrogen the next day. The thawing of the cells from the cryo tubes took place under constant movement in hot water bath until ice became visible. The cell suspension was then immediately placed in a cold medium, and the cells were removed from the DMSO by centrifugation (5 minutes 1800 rpm).

2.2.5.1.2 Subculturing of cells

The adherent growing cortical and medullary thymic epithelial cell lines (ANV and TE-71), OP-9 stroma cell line, and the human T-ALL cell lines (Jurkat, DND-4, HPB-SIL and ALL-SIL) used in this work were maintained in culture flasks with 75 cm culture areas and incubated at 37 °C and 5% CO_2. Subcultures were performed twice a week during the logarithmic growth phase at 80 to 90% confluence. The cells were washed with PBS, dissociated with 2 ml trypsin solution (GIBCO TripLETM) and incubated for 5 to 10 mins. until they were exposed to a single cell suspension. The cells released from the monolayer were then resuspended with fresh growth medium (DMEM with GlutaMax™, 10% FCS, 1% penicillin-streptomycin for ANV cells; IMDM, 15% FCS, 1% penicillin-streptomycin for TE-71 cells; and RPMI-1640 15% FCS, 1% penicillin-streptomycin for Jurkat cells) and diluted 1:10 in a new cell culture flask.

2.2.5.1.3 Living cell count using trypan blue

The membrane of dead cells is permeable to the trypan blue dye, which binds to cell proteins and thus makes the cell blue. On the other hand, the membrane of the living cell is intact, and the dye cannot pass due to its size. Therefore, these cells appear bright under the microscope. The cell suspension to be analyzed was mixed with trypan blue and then filled into a Neubauer chamber. The viable cell count was determined by counting the unstained cells under a light microscope at 10X magnification. With a vial volume of 0.1 µl, the total number of viable cells per ml was calculated by $Y \times Z \times 10^4$ (Y = mean value of cells counted from four large squares, Z = dilution factor).

2.2.5.1.4 Co-culture of *SCL/LMO1* leukemia cells with cell line

The thymic epithelial cell lines ANV and TE-71 and stromal cell line OP-9 were seeded to get confluent monolayer (2×10^5 cells per well in 6 well plates). Proliferated cell lines were mitotically inactivated by treatment of 10 µg/mL mitomycin-C (MMC) for 2 to 3 hours in the dark. Then, the cells were washed with DPBS (3X times), later cells were treated with complete fresh medium and feeder cell layers were used to co-culture *SCL/LMO1* leukemic cells derived from the thymus. Co-culture was allowed incubating for 72 hours. At the end of the experiment, the leukemic cells were harvested to check survival of leukemia cells **(Fig. 4).**

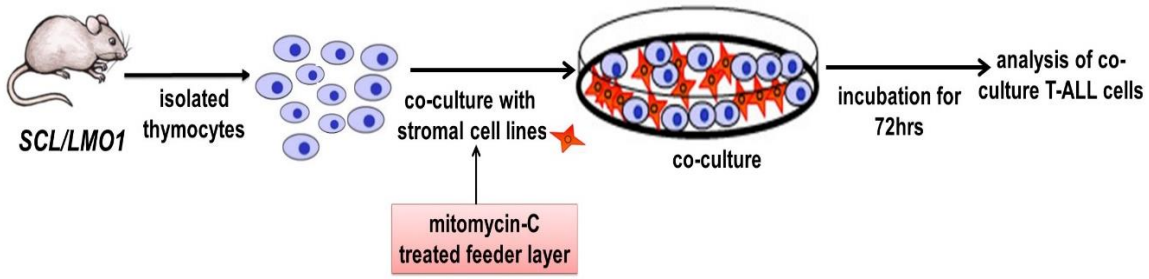

Figure 4. Experimental setup for co-culturing of thymic epithelial cell lines ANV and TE-71 with *SCL/LMO1* leukemic cells.

Schematic representation of the experimental design. Leukemic cells derived from the *SCL/LMO1* thymus co-culture on a mitomycin-C treated feeder layer of thymic epithelial cell lines ANV and TE-71 and stromal cell line OP-9 for 72hrs. and analysis co-cultured *SCL/LMO1* leukemic cells by cell count and FACS.

2.2.5.1.5 Direct and indirect co-culture

The TEC cell lines were added to the confluent 1×10^5 cells (target cells). Two different co-culture systems were investigated in parallel: Direct contact system with TEC cell lines as single-layer co-culture with *WT/WT* and *SCL/LMO1* thymocytes and indirect contact system, in which TEC cell lines are isolated from *SCL/LMO1* leukemia cells through a semipermeable membrane in a transwell system (0.4µm pore size; Falcon®), which only allowed the transit of soluble factors, the cells were cultured for 24 hours **(Fig. 5).** At the termination of the experiments, the target cells and the corresponding culture supernatant was harvested to measure cytokines level and analysis of gene expression.

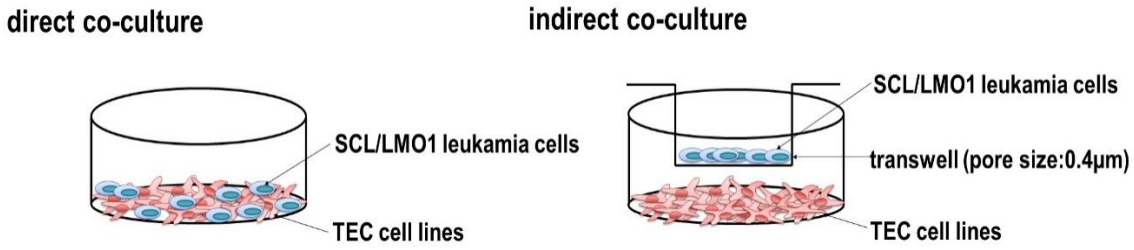

Figure 5. *In vitro* setup for direct co-culture and indirect co-culture system.

Schematic representation of two *in vitro* culture systems. Direct contact system with TEC cell lines as a monolayer with *WT/WT* and *SCL/LMO1* thymocytes and Indirect contact system, where TEC cell lines (ANV and TE-71) are separated from *SCL/LMO1* Leukemia cells by a semipermeable membrane in a transwell system incubated for 24h.

2.2.5.1.6 *In vitro*, Recombinant CXCL10 culture

To investigated the effect of recombinant CXCL10 in leukemia *SCL/LMO1* cells and controlled *WT/WT* cells 1×10^5 cells were seeded per well in a 12 well plate, and the medium was provided with recombinant CXCL10 (0.5µg, 0.1µg, and 0.05µg) for 8 h for survival assay and 24 hours for Real-Time analysis (**Fig. 6**). Cells were removed at the end of the experiment to check survival by annexin-V and gene expression analysis by real-time PCR. Similar culture condition was followed for human T-ALL cells with recombinant CXCL10 (0.5µg, 0.1µg, and 0.05µg) for 48 hrs for gene expression analysis by Real-Time PCR.

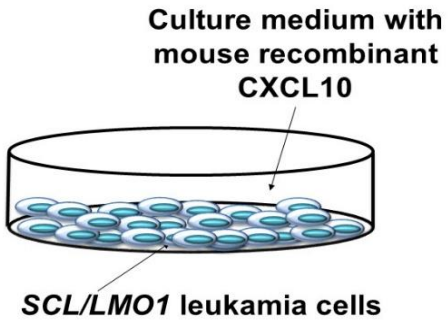

Figure 6. *In vitro*, recombinant CXCL10 culture with cell.
Schematic representation shows the culture system. *SCL/LMO1* leukemia cells, *WT/WT* cell and human T-ALL cell lines culture with recombinant CXCL10 with different concentration 0.05µg, 0.01µg, and 0.5µg.

2.2.5.1.7 AnnexinV apoptosis assay

The cells to be analyzed were first washed with DPBS and collected in 50 µl AnnexinV binding buffer. Subsequently, 400 µl of the AnnexinV binding buffer with 5 µl AnnexinV-FITC per stain was added. After 10-15 minutes incubation at room temperature (RT) in the dark, immediate flow cytometry analysis was performed.

2.2.5.2 Preparation of single cell suspensions of thymus

After organ removal, the thymus was placed in tissue culture dishes with 4 ml ice-cold DPBS / 2% FCS. The organs were dissociated into a single cell suspension between the moistened, roughened surfaces of two slides. The single cell suspension was then passed through a 100 µl thymus. The cell count was determined using the Z2 Schar particle count.

2.2.6 Isolation and accumulation of thymic epithelial cells

2.2.6.1 Enzymatic tissue digestion

The thymus was removed from the upper thoracic cavity, dissected and suspended in preheated in 500µl RPMI medium to 37 ° C with 2% FCS. To remove thymic epithelial cells from the stroma, the medium was supplemented with collagenase (1.2 mg / ml), dispase (1.25 mg / ml), and DNase (1.5 mg / ml). Digestion was then performed in several rounds for 20 minutes each at 37 ° C shaking at 900 rpm (Eppendorf thermomixer comfort) until no undigested tissue was visible.[106] Half the digestion time was used to support tissue dissociation by pipetting up and down with a 1000 µl pipette. After this time, the supernatant was removed, collected in a separate tube and kept on ice, then 20 µl of 0.5M EDTA per ml tissue solution was added and incubated on maximum shaking at 37 °C for 5 minutes. The resulting single cell suspension was passed through a 100 µm cell screen and washed once by adding 50 ml PBS and centrifuging (5 minutes, 1800 rpm, 4 °C) **(Fig.7).**

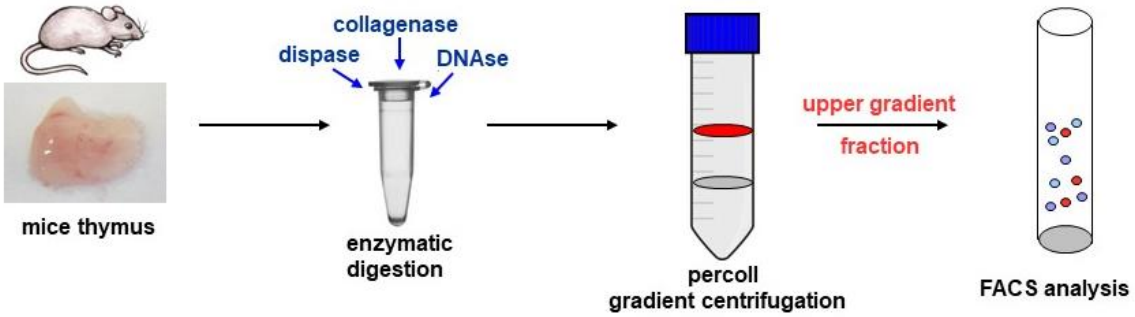

Figure 7. Enzymatic tissue digestion of mouse thymus.

Schematic representation shows the mice thymus enzymatic tissue digestion with dispase, collagenase, and DNase follow by density gradient centrifugation to obtain thymic epithelial cell (TECs), which appear at upper fraction analysis by FACS with specific surface marker antibodies.

2.2.6.2 Enrichment of TECs by percoll gradient centrifugation

The cell pellet washed in PBS was first resuspended in 4 ml dense (1.115 g / ml) percoll. In the meantime, a 15 ml falcon tube was filled with 2 ml FCS and completely wetted with the FCS by rolling on the inside. The serum was disposed, and the percoll cell suspension was pipetted into the serum. The tube was held at 45° and first coated with 2 ml less dense (1.065 g / ml) percoll and then gently coated with 2 ml PBS. After density gradient centrifugation

for 30 minutes at 3030 rpm without brake (Beckman Coulter Allegra® X-15R) at 4°C, the upper Percoll cell fraction (OPF) was removed with a 1000 pipette and added in a 50 ml Falcon tube which was washed once in DPBS and then absorbed into 500 µl PBS.[106, 107] Trypanblau in the Neubauer chamber was used to determine the absolute cell count of OPF, which contains thymic epithelial cells as well as other thymic stromal cells such as dendritic cells, macrophages, fibroblasts, and endothelial cells. To determine the surface markers, the cells were stained and analyzed by the FACS.

2.2.7 FLOW CYTOMETRY

2.2.7.1 Flow cytometric analysis

In this work, the flow cytometer BD LSRII was used for the analysis. The instrument is equipped with the following lasers: a blue laser (488 nm), a red laser (633 nm) and a violet laser (405 nm). The blue laser generates FSC and SSC and stimulates the fluorophores FITC, AlexaFluor 488, PE, PerCP-Cy5.5, PI, and PE-Cy7 used in this work. The red laser stimulates APC, AlexaFluor 647, APC-Cy7, APC-eFluor780 and APC-Alexa Fluor 750, and the violet laser DAPI, Pacific Blue, and PI (violet).

2.2.7.1.1 Cell surface marker analysis

To detect the expression of surface markers, 1×10^6 cells of a unicellular suspension were placed as standard in a 96-well microtiter plate. To block non-specific binding, 100 µl of anti-CD16 / CD32 (antibodies against mouse Fc receptor) (1: 400 in PBS 2% FCS) was added and incubated on ice for 15 minutes. After washing the cells with 100 µl FACS buffer (PBS + 2% FCS + 0.02% NaN_3) and subsequent centrifugation at 1800 rpm for 5 minutes (Beckman Coulter Allegra® X-15R), the supernatant was discarded and the remaining cell pellet was stained with 40 ul of the mixture of fluorochrome-conjugated antibodies of interest followed by incubation for 20 minutes on ice in the dark. DAPI or propidium iodide (PI) was added to the cells immediately before analysis to stain dead cells. If the antibody mixture contained unconjugated biotinylated antibodies, second staining with streptavidin-coupled fluorophores was performed after the first staining and washing step. Streptavidin binds with high specificity to biotin. The recording was then performed in the DAPI / PI-FACS buffer. To achieve a compensation (determination and correction of the signals by

overlapping the impulses, see above), all antibodies contained in the mix as well as DAPI or PI as single color were each led to 1×10^6 cells and read in on the LSRII device.

For the analysis of T cell development and TECs in the thymus, thymocytes were stained with the following fluorochrome antibodies. Early thymic progenitors (ETPs) were identified due to their expression of CD44 (IM7; APC) and C-Kit (2B8; APC-Cy7) antibodies, T cell development was analyzed by staining the thymocytes with anti-CD44 and anti-CD25 (eBio3C7; DAPI), anti-CD4 (RM4-5; PE-Cy-7), anti-CD8 (53-6.7; APC-Cy7) antibodies. DN thymocytes (DN1: CD44+CD25-; DN2: CD44+CD25+; DN3: CD44-CD25+; DN4: CD44-CD25-), and later subpopulations CD4 and CD8 (DP: CD4+CD8+, CD4:SP, CD8:SP) as thymocytes negative for non–T lineage and mature T lineage were stained with anti-CD3e (145-2C11), anti-CD19(6D5), anti-Ter119 (TER119), anti-Mac1 (M1/70), anti-Gr-1 (RB6-8C5), anti-NK1.1 (PK136), and anti-B220 (RA3-6B2). Enzymatically digested TEC suspensions were stain with UEA (Ulex Europaeus Agglutinin) (conjugate protein; Vector Labs), anti- CD326 (EpCAM) (G8.8; eBioscience), anti-Ly51 (BP-1; all from BD Pharmingen), anti-CD45 (30-F11; PE-Cy7) antibodies, TECs were sorted using a FACS Aria II Flow Cytometer (BD). The CXCL10 receptor CXCR3 expression analyzed from thymocytes using mouse anti-CXCR3 (CXCR3-173; BioLegend) and isotype control Armenian hamster IgG (eBio299Arm; eBioscience) antibodies. For the human cell line, we used anti-CXCR3 (G025H7, BioLegend) antibody. To verify NOHCH1 expression on thymocytes, mouse anti-Notch1 (HMN1-12) antibody. An arm. Hamster IgG (eBio299Arm; eBioscience) antibody was used as isotype control **(Table 6**). All data was acquired on a FACS LSRII (BD) and analyzed using FlowJo software.

2.2.7.2 Flow cytometric sorting

The cell sorting was performed at the FACS Aria II Flow Cytometer (BD), at the Institute for Experimental Immunology and Imaging, University Hospital Essen, Essen, Germany. For the isolation of the RNA sorted cells were collected in polypropylene tubes containing 350µl RLT buffers, centrifuged and the cell pellet introduced into the Qiagen QIAamp DNA Micro Kit.

2.2.8 Isolation of RNA from single cell suspensions

The RNeasy® Mini Kit and the RNeasy® Micro Kit from Qiagen were used to isolating RNA from cells. The principal base on selective binding of isolated RNA to membranes based on

silicon gels by microcentrifugation. For the purification of RNA, cells were collected by centrifugation (5 min, 1800 rpm) and taken up in 700 µl RLT buffer enriched with beta-mercaptoethanol, and frozen at -80^{0}C for the further isolation procedure. Dynabeads mRNA DIRECT Kit was used for the isolation of the RNA from sorted thymic epithelial cells (from Invitrogen). Around 5 × 10^5 cells and 350 µl of the buffer were used. After thawing RNA, isolation was carried out according to the manufacturer's protocol. The concentration of the eluted RNA was then determined by measuring the light absorption at 260 nm (A260) on the Beckman spectrophotometer. For further analysis, the RNA was stored at -80 0C. The RNA was then measured at 260 nm (A260) on the Beckman spectrophotometer.

2.2.8.1 cDNA synthesis

The Advantage® RT-for PCR Kit from Clontech was used for the re-transcription of RNA into complementary DNA (cDNA). RNA and primer were first mixed and heated at 70^{0}C to melt the secondary structure of the RNA. The subsequent incubation on ice enables hybridization of the primers. The first strand synthesis is performed with oligo (dT) primers that attach themselves characteristically to the poly-A tail of the messenger RNA (mRNA). Thus, only the transcription of the mRNA within the entire RNA is guaranteed. In the reaction mixture, 1 µg RNA were added in small E-Cups. The thawing of reagents and samples, as well as the implementation, was carried on ice. The cDNA synthesis was carryout into PCR about 1 hour at 42 ^{0}C. The synthesized cDNA was finally diluted 1:5 with nuclease-free water and stored at -80 ^{0}C for further use.

2.2.9 Quantitative real-time PCR

The cDNA derived from reverse transcription was used to quantify gene expression at the mRNA level by qRT-PCR. This was done with TaqMan assays from Applied Biosystems. Subsequently, the expression of mRNA of interest to the expression of housekeeping transcripts was correlated and quantified. In this thesis, gene expression data against hypoxanthine-guanine-phosphoribosyltransferase (HPRT) was normalized as standard. For each TaqMan approach of a sample, a reaction batch without cDNA (no template control, NTC) was used as a control. All reactions were performed in duplicate. For this purpose, each TaqMan approach (TaqMan Assay **Table 8**, PCR protocols in appendix) was pipetted according to the manufacturer's instructions in MicroAmp™ 96-well microtiter plates and amplified in the Applied Biosystems StepOne™ real-time PCR device. The reaction

protocol was based on the following program: 2 minutes at 50^0C, 10 minutes at 95^0C, and 40 cycles of 15 seconds at 95^0C, and 60 seconds at 60^0C. The amplification plots (cycle versus normalized reporter signal) was displayed with the StepOne.

The relative quantification of gene expression was performed using the delta-delta-Ct (ΔΔCt) method. The Ct value corresponds to the PCR cycle in which the fluorescence signal passes the threshold value from background fluorescence to amplification fluorescence. The lower this value, the more DNA copies are present in the original sample. The expression of the target gene was initially based on the expression of an internal standard (housekeeping gene, reference gene) (ΔCt value). The ΔCt value of the sample and the corresponding control was then determined. The difference in the transcription levels of both groups resulted from the formula $2^{-\Delta\Delta Ct}$.

(1) ΔΔCt = ΔCt control - ΔCt test = [Ct control- Ct HPRT (K)] - [CtTest-Ct HPRT (T)]

(2) RQ = 2-ΔΔCt

2.2.10 RT² profiler PCR arrays

The applied RT² Profiler™ Mouse cytokines & chemokines PCR Array (PAMM-150Z), RT² Profiler™ Mouse Notch Signal Way PCR Array (PAMM-059Z) and RT² Profiler™ Mouse Epithelial to Mesenchymal Transition PCR Array (PAMM-090Z) profiles the expression of 84 genes, 5 housekeeping genes, reverse transcriptase, as well as positive controls (**Table 9-10**). Relevant genes from the following signaling pathways were analyzed and standardized to two household genes (β-Actin and Gapdh): The average correlation coefficients of these arrays are higher than 0.99, which provides reliable detection of expression differences between samples. cDNA from *WT/WT* and *SCL/LMO1* mice were used as biological samples in this test. The arrays were performed with 2X SYBR Green PCR Master Mix and QuantStudio™ Real-Time PCR System according to the manufacturer's protocol.

2.2.11 Immunohistochemistry and immunofluorescence on tissue section

2.2.11.1 Tissue embedding and cutting

For the production of histological preparations, the tissue was collected and stored in Sakura Tissue-Tek O.C.T. A compound with water-soluble glycols and anti-freeze resins,

embedded and frozen in a specially prepared aluminum dish over the liquid atmosphere of nitrogen and at - 80^{0}C. With the help of a temperature controlled cryomicrotome (Leica CM1850 UV), 8 µm thin frozen sections were placed on SuperFrost®Plus slides (Langenbrinck). The cryosections were also stored at - 80^{0}C.

2.2.11.2 Hematoxylin & Eosin (HE) staining

To visualize the different tissue structures in the microscopic image, the hematoxylin-eosin (HE) staining was chosen as the overview staining. The staining is based on the principle of impregnation and electrostatic absorption. Hematoxylin is positively charged at low pH and binds to negatively charged basophilic structures such as DNA and RNA of the endoplasmic reticulum, which then appears blue. Eosin is negatively charged, and stains positively charged acidophilic structures such as cytoplasmic proteins and mitochondria in red. First, it is stained with hematoxylin in the desired degree of staining (progressive staining). Then it is overstained with eosin and differentiated into ethanol (regressive staining). For H&E staining, the sections were dried at RT for at least 30 minutes and then stained and covered with the Fast frozen stain Kit (Polysciences) according to the manufacturer's instructions using the supplied CitraMountTM assembly medium.

2.2.11.3 Immunofluorescence staining

For the immunofluorescence staining, the tissue sections were dried at RT for at least 30 minutes, and then fixed in acetone for 10 minutes. The slides were allowed to dry and framed with ImmEdge Pen. It was then washed once with PBS for 3 minutes. To block non-specific binding and minimize background, slides were incubated with 100 µl of 2% FCS in PBS for 20 minutes. The incubation with 100 µl fluorophore-conjugated antibodies in 2% FCS in PBS for 40 minutes at RT in the dark was followed. After this time, unbound antibodies were removed by washing (2 X 3 minutes in 2% FCS in PBS). If the unconjugated antibody was used for primary staining, second staining with the fluorophore-conjugated secondary antibody was performed for another 40 minutes followed by gentle washing with 2% FCS in PBS. The contaminated areas were sealed with VECTASHIELD HardSet Mounting Medium with DAPI and stored at 4^{0}C in the dark. Microscopy and documentation were performed the next day due to possible fading.

2.2.11.4 Microscopy

Fluorescence microscopy aims to excite fluorophores with the light of a defined wavelength (absorption light) and to detect the resulting longer wavelength fluorescent light (emission light) only via transmissive filters. The fluorescence and bright field microscopic examinations and images were performed on the BZ-9000 of Keyence microscope at the Institute of Immunology, University Hospital Essen, Essen, Germany and Zeiss AxioObserverZ1 and Apotome at the ImagingCenter Essen (IMCES), University Hospital Essen, Germany.

2.2.11.5 Image processing

Fluorescent images were processed with ImageJ software. ImageJ was also used to generate masks for each channel. These masks were then overlapped to generate a single overlay image.

2.2.12 Enzyme-linked immunosorbent assay (ELISA)

For the quantification of the concentrations of different factors in the supernatant of cultured cells, we performed different sandwich ELISA assay. ELISA protocols contain the same procedure consisting of coating, blocking, the addition of standard probes and samples in duplicates, detection, enzyme reaction, and development. However, the ELISA kits vary according to the desired factor, particularly in the antibodies and buffers used as well as in the incubation times. Variances of the different ELISA kits were adapted to the specific protocols of the manufacturer. Between the individual working steps, multiple washing steps using a multichannel pipette removed unbound molecules.

2.2.12.1 CXCL10 ELISA

ELISA Duoset kit (DY466) for mouse CXCL10 were obtained from R&D systems and ELISAs were performed according to the manufacturer's instructions. Samples were stored at −20 °C until analysis. Optical density (O.D) of each well was measured immediately using a microplate reader (BioRAD Imark) at 450 nm and 540nm for wavelength correction.

2.2.13 Statistical analysis

Tests for all data were performed using GraphPad prism version 8 (2019) Significance in two-tailed *t*-tests was assumed for *P*-values < 0.05 (*), < 0.01 (**), or < 0.001 (***).

CHAPTER-3

RESULTS

3 RESULTS

3.1 Growth kinetics and gene expression analysis of cortical and medullary thymic epithelial cell lines

First, we validated the TEC nature of the ANV [100] and TE-71 [101] cell lines which were received from the labs which originally generated these cell lines. These cell lines were used as a tool to study T-ALL and TEC interactions *in vitro* throughout the project. ANV cells were derived from a primary murine cTECs while, TE-71 cells evolved from mTECs. Flow cytometric analysis was performed with the cell lines. They were stained with anti-EpCAM, anti-BP1, UEA, and anti-MHCII antibodies. As expected, the mTEC cell line TE-71 showed expression of the epithelial cell marker EpCAM, the mTEC-specific marker Ulex europaeus agglutinin (UEA) and MHC class II. The cTECcell line ANV expressed EpCAM, the cTEC specific marker BP1 and MHC class II molecules **(Fig. 8).**

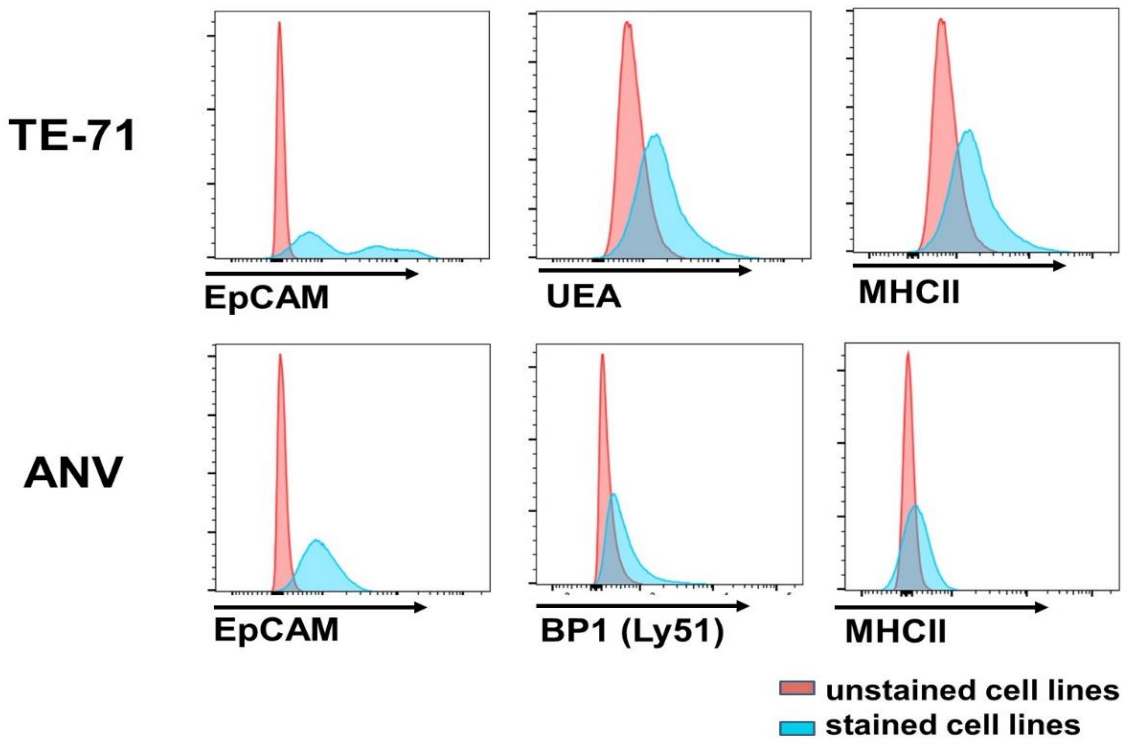

Figure 8. Analysis of cortical and medullary thymic epithelial cell lines.

The cortical and medullary thymus epithelial cell lines ANV and TE-71 were stained with anti-EpCAM, anti-BP1, UEA and anti-MHCII antibodies and analyzed by flow cytometry. The histograms of cell fractions show the stained cells (blue area) against the unstained cells (red area).

The demonstrated expression of these markers confirmed the identity of the TE-71 cell line and ANV cell line as cTEC- and mTEC-derived, respectively. Because it was planned to study the leukemia-supporting potential of TECs we studied previously described factors mediating TEC support for thymic progenitors. The gene expression of these mediators was studied in ANV and TE-71 cell lines by real-time PCR. We analyzed the expression of the NOTCH1 ligand DLL4 representing the key thymic NOTCH pathway activator, chemokine CCL25, stem cell factor (SCF), insulin-like growth factor 1 (IGF-1),

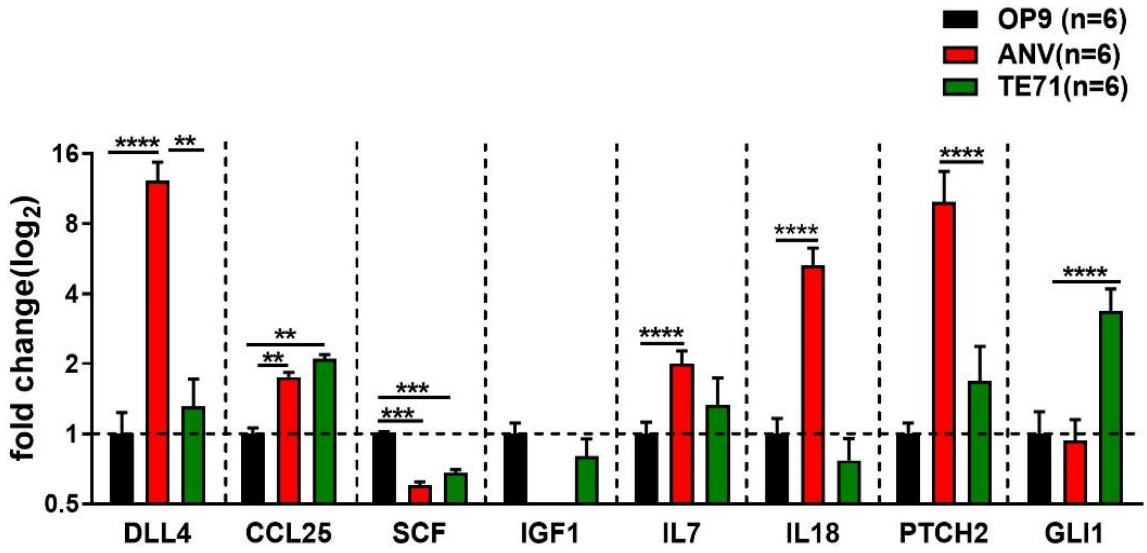

Figure 9. Expression of thymocyte supporting factors by thymic epithelial cell lines.

RT-PCR analysis of the DLL4, CCL25, SCF, IGF1, IL7, IL18, PTCH2, and GLI1 gene expression by the ANV, TE-71, and OP9 cell lines. The analysis was performed in 6 independent duplicates per gene and per cell line, respectively. Expression of target mRNA was normalized against the expression of the housekeeping gene Hprt1. Values represent fold-change in comparison to the expression of the stromal cell line OP9. Graph depicts means +SD; *p< 0.05; **p< 0.005; ***p< 0.001.

interleukin 7 (IL-7), interleukin 18 (IL-18), patched 2 (PTCH2) a negative regulator of the Hedgehog signaling pathway, and zinc finger protein GLI1, an effector of hedgehog signaling. Expression was normalization to the hypoxanthine-guanine phosphoribosyltransferase HPRT 1 housekeeping gene. TEC cell line gene expression was compared to the expression of the murine bone marrow stromal cell line OP9.[102] The OP9 cell line is a widely used mesenchymal cell line with established leukemia supporting potential. The RT-PCR analysis revealed that the expression of DLL4, CCL25, IL7, and IL18 was significantly higher in ANV cell lines compared to OP9 stromal cells. The ANV DLL 4expression was more than 8-fold higher compared to TE71. These data are concordant with the cTEC origin of ANV cells as DLL4 is uniquely expressed by cTECs. On the other

hand, expression of CCl25 and GLI1 was significantly upregulated in TE71 compared to OP9. The expression of the early hematopoietic progenitor supporting SCF was lower in the TEC cell lines compared to OP9 **(Fig. 9).** In summary, the analysis confirmed the TEC identity of the ANV and TE-71 cell lines and demonstrated that primary TEC-defining mediator expression such as that of DLL4 and CCL25 was preserved in ANV and TE-71 cells.

3.2 Characterization of *lck-ERT2-SCL / lck-LMO1 (SCL/LMO1)* transgenic mice

To be able to study TECs during T-ALL leukemogenesis and in established T-ALL, a murine model with short leukemia latency and high penetrance was sought. Previously, it was shown that *SCL/TAL1* is a common genetic aberration in T-ALL.[82, 108, 109] Our group characterized an SCL-induced NOTCH1-activated preleukemic T-developmental phenotype using a tamoxifen-inducible lck-ERT2-SCL transgenic mouse model.[82]

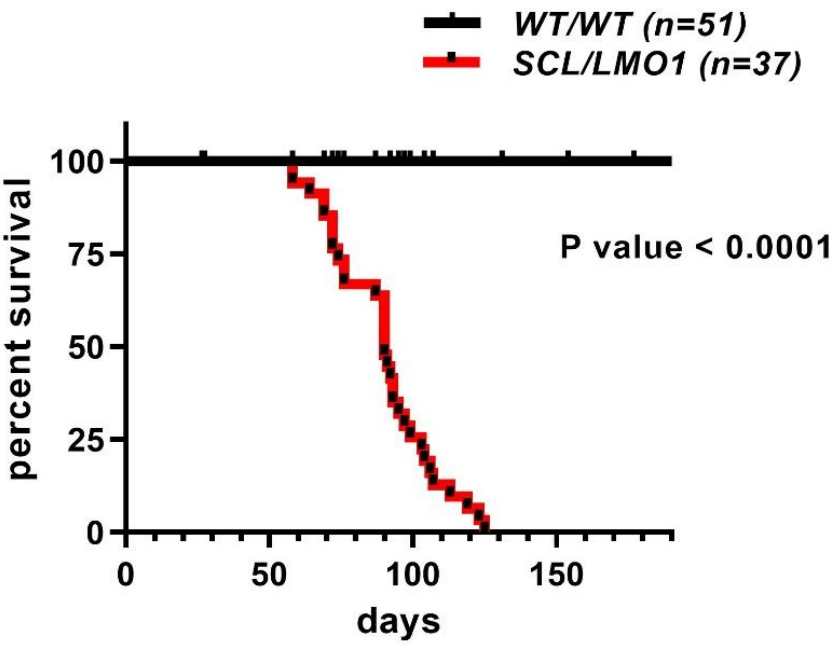

Figure 10. Leuekmia-free survival curves of *lck-ERT2-SCL / lck-LMO1 (SCL/LMO1)* double-transgenic mice.

Kaplan-Meier leukemia-free survival curves of *WT/WT* control (black line) and *SCL/LMO1* mice (red line). The analysis was performed with *WT/WT* (n=51) and *SCL/LMO1* (n=37) mice.

It should be emphasized that increased NOTCH1 signaling by most gain-of-function mutations remains ligand-dependent. Therefore, we hypothesized that TECs expressing the DLL4 NOTCH1-ligand might play a central role in T-ALL leukemogenesis. However, the latency of T-ALL development in *lck-ERT2-SCL* transgenic mice was more than one year with incomplete penetrance. To reduce T-ALL latency and penetrance, we crossed *lck-ERT2-SCL* transgenic mice with *lck-LMO1* transgenic mice to generate *lck-ERT2- SCL*; *lck-LMO1* double transgenic mice (from now on abbreviated as *SCL/LMO1* mice). *LMO1* is an oncogenic transcription factor that interacts directly with *SCL* and is also overexpressed in T-ALL.[84] Surprisingly, we observed T-ALL development in *SCL/LMO1* mice in the absence of any tamoxifen treatment. This could be due to nuclear leakiness of the ERT2-SCL fusion protein in the absence of tamoxifen cooperating with *LMO1* in the nucleus. Another possibility is recently generated cytosolic *LMO1* complexes with ERT2-*SCL* and is dragged into the nucleus by the strong nuclear localization domain of LMO1. Either way, *SCL/LMO1* leukemogenesis allowed us to now abstain from laborious and also side effect-prone tamoxifen treatment of *SCL/LMO1* transgenic mice. The study of ectopic co-expression of *ERT2-SCL* and *LMO1* in mice accelerated the onset of leukemogenesis and reduced T-ALL latency of *SCL/LMO1* mice to 60 to 120 days **(Fig. 10).** Over time, *SCL*/*LMO1* thymi became enlarged compared to *WT/WT* thymi **(Fig. 11)**. Additionally, increased *SCL/LMO1* thymic weight **(Fig. 12 A)** as well as significantly increased thymic cellularity at 4, 6, 8 weeks, and leukemia stage (~11 weeks old) in *SCL/ LMO1* mice compared to control *WT/WT* mice became apparent **(Fig. 12 B).** In summary, it was demonstrated that *SCL/LMO1* mice develop T-ALL in the absence of tamoxifen at the median age of 3 months of age. The penetrance of *SCL/LMO1* T-ALL was 100%.

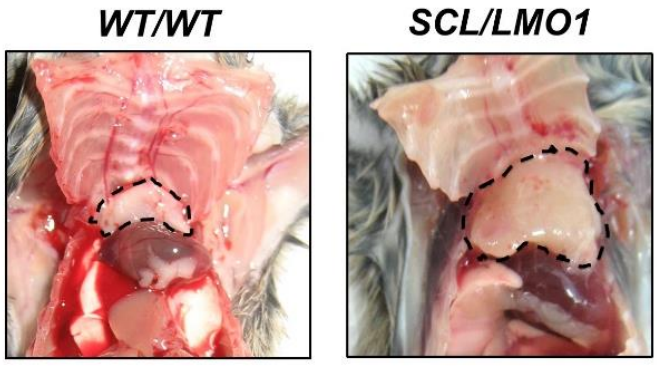

Figure 11. *Lck-ERT2-SCL / lck-LMO1 (SCL/LMO1)* mice macroscopically show an enlarged thymus.

Representative ventral views of the upper mediastinal region of *Lck-ERT2-SCL / lck-LMO1 (SCL/LMO1)* and *WT/WT* (control) mice (age of 6 weeks).

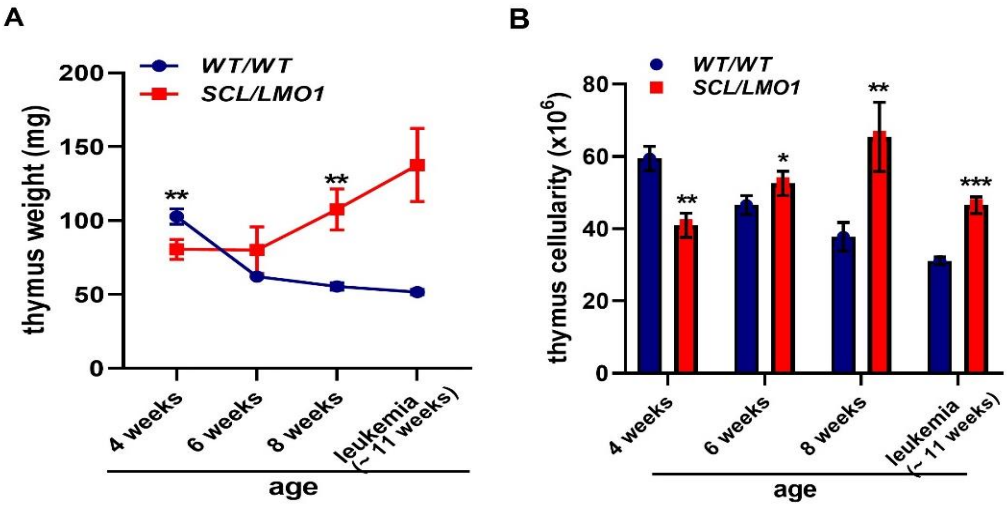

Figure 12. Thymic weight and cellularity are increased in *SCL/LMO1* mice.
Graphs showing (A) thymic weight and (B) total thymic cellularity of *SCL/LMO1* and *WT/WT* mice over time. n=5 *WT/WT* mice; n=5 *SCL/LMO1* mice. Means±SEM are displayed. ***p*<0.01.

3.3 The NOTCH1 aberrant upregulated in *SCL/LMO1* mice

In the majority of T-ALL cases, enhanced NOTCH1 signaling is the primary driver of this malignancy.[65] We previously demonstrated that aberrant *SCL* activation mediated by a presumptive first genetic hit in T-ALL already leads to enhanced NOTCH1 signaling. Therefore, we now aimed to study whether enhanced NOTCH1 signaling is also a feature of the *SCL/LMO1* preleukemic thymus. We performed NOTCH1 and downstream gene expression analysis and immunohistochemistry. First, we harvested total thymocytes from preleukemic *SCL/LMO1* and *WT/WT* control mice at the ages of 4, 6 and 8 weeks to analyze gene expression of NOTCH1 and its target genes HES1 and DTX1.

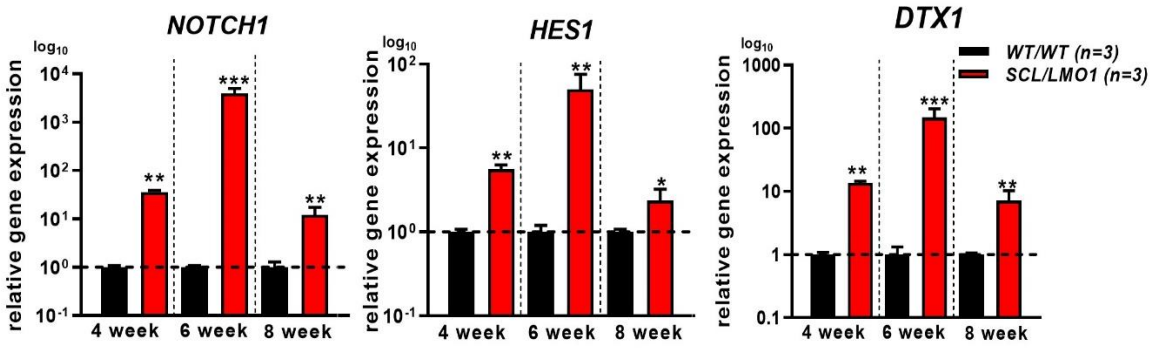

Figure 13. *SCL/LMO1* thymocytes showed higher expression of NOTCH1 and its downstream target genes.

NOTCH1 and its downstream target (DTX1 and HES1) gene expression were analyzed in *SCL/LMO1* mice (n=3) and compared with *WT/WT* mice (n=3) at the age of 4, 6, and 8 weeks. Data represent means±SEM; *p< 0.05; **p< 0.005; N.S., non-significant.

Our results revealed that the expression of NOTCH1, HES1, and DTX1 was significantly increased in *SCL/LMO1* thymocytes. The expression levels were highest in 6 weeks old transgenic mice notably; the expression of NOTCH1 was 1000-folds higher in *SCL/LMO1* transgenic mice compared to *WT/WT* mice **(Fig. 13).** Additionally, to verify NOTCH1 upregulation also at the protein level, we performed immunofluorescent staining of thymic sections. Sections were stained with NOTCH1 and cytokeratin [Pan (C-11)] markers to identify epithelial cells and analyzed by microscopy. NOTCH1 expression increased in *SCL/LMO1* thymic sections during T-ALL leukemogenesis disease while it *WT/WT* thymic sections NOTCH1 expression remained relatively stable over time. As there was not a strong overlap of NOTCH1 and cytokeratin Pan (C-11) staining the increment of NOTCH1 expression was primarily restricted to *SCL/LMO1* thymocytes **(Fig. 14)**. In summary, in line with our previous data demonstrating NOTCH1 upregulation in SCL transgenic thymocytes, we now extended this observation to the *SCL/LMO1* double transgenic thymus.

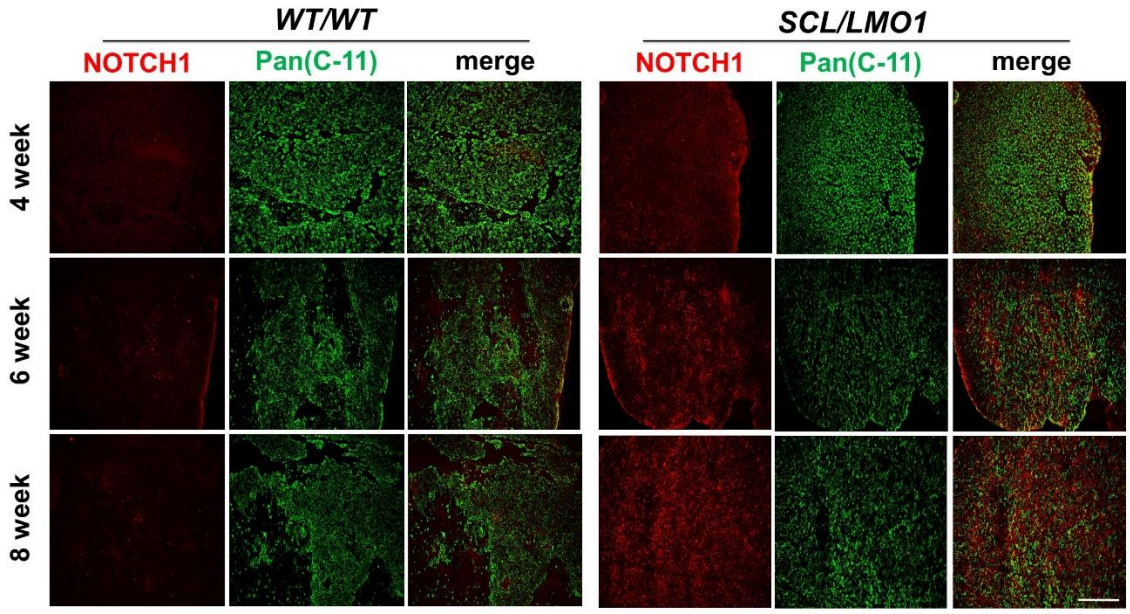

Figure 14. *SCL* and *LMO1* induced T-ALL development leads to NOTCH1 upregulation.

Thymus cryo-transverse sections of *WT/WT* and *SCL/LMO1* mice were stains with ant-NOTCH1 (red), and anti-pan(C-11) (green) antibodies and were analyzed by microscopy. Scale bar: 100µm, representative images of 4, 6, and 8 weeks old mice (n=3 mice per genotype and time point analyzed) are shown.

3.4 T cell development in *SCL/LMO1* transgenic mice is severely perturbed

To determine the impact of the combined *SCL* and *LMO1* transgenes on T-cell development we analyzed the T-cell developmental, subsets of pre-leukemic *WT/WT* and *SCL/LMO1* thymi. T cell development in the thymus initiates from early thymic progenitors (ETPs) which are characterized by CD44 and c-kit surface expression and by the lack of mature T cell markers including CD4, CD8, and TCRβ. ETPs are a sub-fraction of the CD4 and CD8 double negative 1 (DN1) population. The CD4 and CD8 double negative (DN) population is subdivided by the expression of CD44 and CD25 into four developmentally successive subpopulations: DN1 (CD44+CD25-), DN2: (CD44+CD25+), DN3 (CD44-CD25+) and DN4 (CD44-CD25-). A successfully re-arranged TCRβ chain complexed with preTCRα drives DN cells to upregulate CD8 and later CD4 to become CD4 and CD8 double positive (DP) thymocytes. The TCRα chain is re-arranged, and DP cells are selected to finally mature into single-positive (SP) CD4 and CD8 T-cells. To characterize these T-cell developmental steps in our newly established *SCL/LMO1* model, we analyzed thymi by 7-color-flow cytometry **(Fig. 15)**.

We found that in *SCL/LMO1* mice, the absolute number of the earliest thymic T-developmental stage, the ETPs, was increased compared to *WT/WT* control mice. Furthermore, the total number of DN cells was more than 5-fold increased **(Fig. 15, 16A).** On the other hand, the absolute number of DP thymocytes was significantly reduced in *SCL/LMO1* mice **(Fig. 15, 16B).** Total numbers of CD8SPs and CD8SPs TCRβ+ showed an increase in *SCL/LMO1* mice **(Fig. 15, 16C)** while total CD4SP and CD4SP TCRβ+ cells were decreased in *SCL/LMO1* mice compared to control *WT/WT* mice **(Fig. 15, 16D).** These results demonstrated that aberrant expression of the *SCL* and *LMO1* oncogenes leads to the expansion of early T progenitor populations (ETPs and DNs). In contrast, terminal developmental stages such as DPs and CD4SP TCRβ+ cells were significantly decreased. This increase of early and decrease of terminal developmental stages point at a blockade in *SCL/LMO1* T cell development. Developing T progenitors in the transit from the DN to the DP stage upregulate CD8 followed by CD4. Thus, the expansion of the CD8 SP is most likely due to a significant deceleration of DN to DP transition. Indeed, within the *SCL/LMO1* CD8SP TCRβ+ gate the majority of cells appeared to be TCRβ intermediate rather than high **(Fig. 15)** indicating that these *SCL/LMO1* cells might be unable to up-regulate TCRβ to the level of *WT/WT* cells.

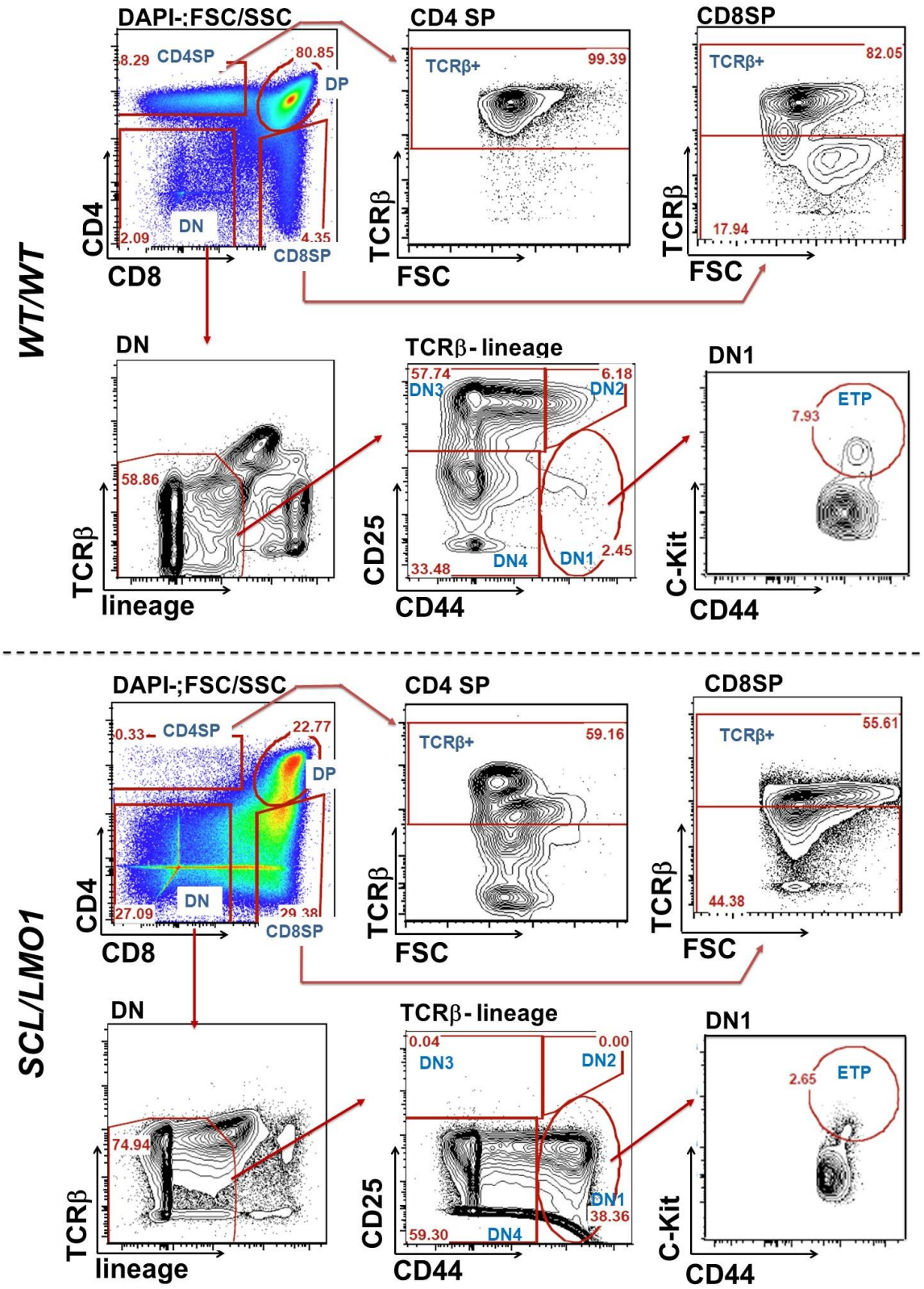

Figure 15. Flow cytometric analysis of thymic T-cell developmental stages of *WT/WT* in comparison to *SCL/LMO1* mice.

Representative flow cytometry plots displaying the gating strategy to define thymic subpopulations of *WT/WT* and *SCL/LMO1* mice (age: 6 weeks). The thymocytes were stained with antibodies against CD4, CD8, CD44, CD25, c-kit, TCRβ, and lineage-specific markers.

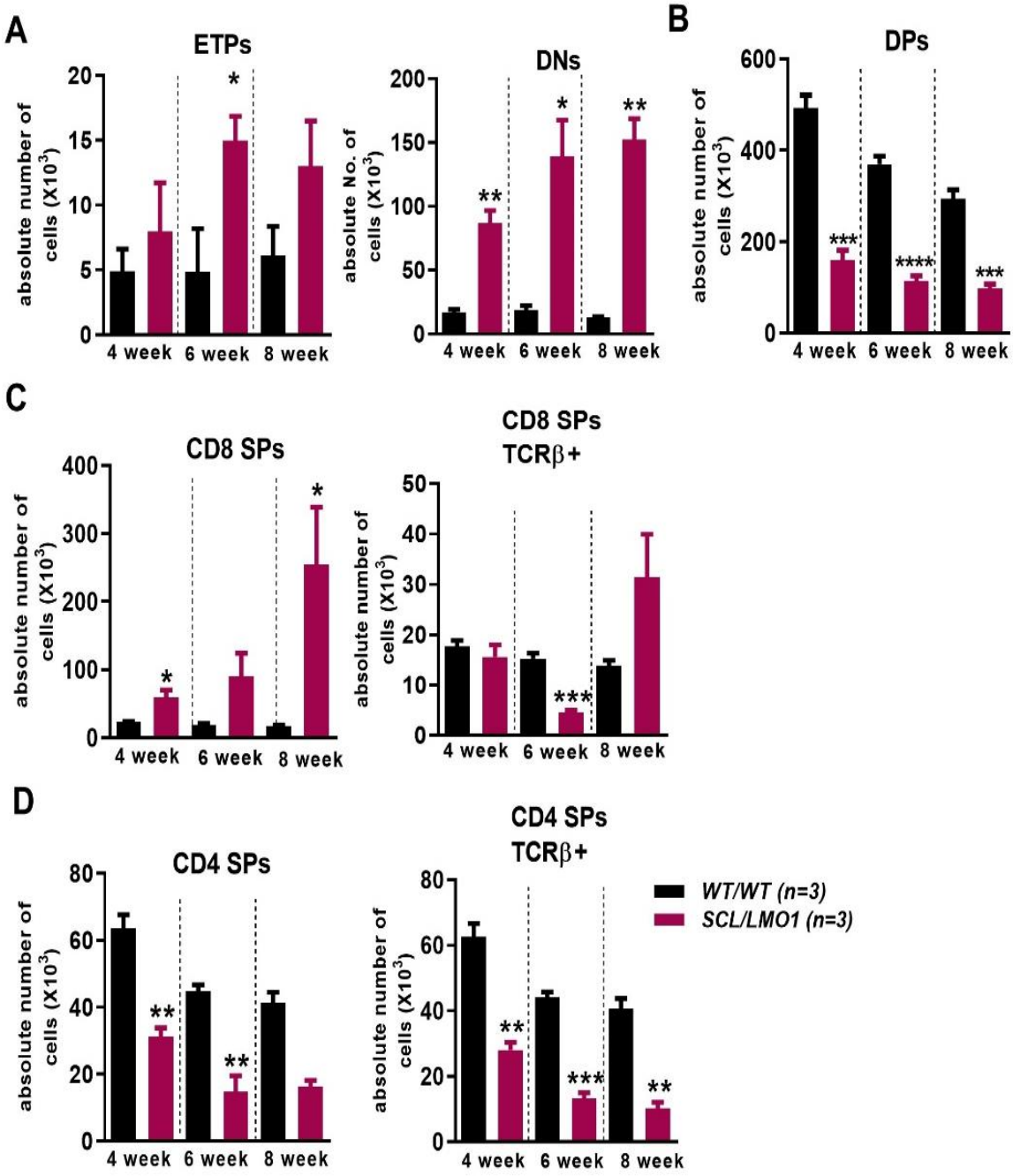

Figure 16. The thymic progenitors are extended and inhibit the transition of single positive cells in *SCL/LMO1* mice thymus.

The absolute numbers of (A) ETPs [DN1], total DN, (B) DP, (C) CD8SPs, CD8SPs TCRβ+, (D) CD4SPs and CD8SPs TCRβ+ subpopulations of 4-, 6-, and 8-week-old *WT/WT* (n=3) and *SCL/LMO1* (n=3) mice. Graph depicts means ±SEM, *p<0.05, **p<0.01, ***p<0.001 and ****p<0.0001. ETPs, early thymic progenitors; DN, double negative; DP, double positive; SP, single positive thymocytes.

3.4.1 Accumulation of abnormal NOTCH1-expressing TCRβintm CD4^{-}CD8^{low} thymocytes in *SCL/LMO1* mice

To quantify and to further characterize the possible origin of the mentioned CD8SP TCRβ^{intermediate} cells **(Figure 15 A)** we gated on a more immature CD4^{-}CD8^{low} population, which was expanded in the majority of *SCL/LMO1* mice **(Fig. 17 A)**. This population was very small in *WT/WT* mice; however, expanded dramatically in *SCL/LMO1* mice **(Figure 17 AB)**. At early stages of T cell development cells pass through phases that are critically dependent on NOTCH1 signaling. When reaching the DP stage of development, cells become independent from NOTCH1 signaling.[110] Because of its central role in normal T cell development and de-regulation in T-ALL, we analyzed NOTCH1 expression of these aberrant *SCL/LMO1* CD4^{-}CD8^{low}TCRβ^{intermediate} cells. Strikingly, compared to *WT/WT* mice, these expanded cells showed a more than 3-fold higher NOTCH1 expression **(Fig. 18 AB)**. In summary, we identified an aberrant NOTCH1+ thymocyte population in the *SCL/LMO1* thymus, which is presumably dependent on a NOTCH1 signal from the microenvironment. The main known provider for such a signal are TECs expressing NOTCH1-ligands such as DLL4**.**

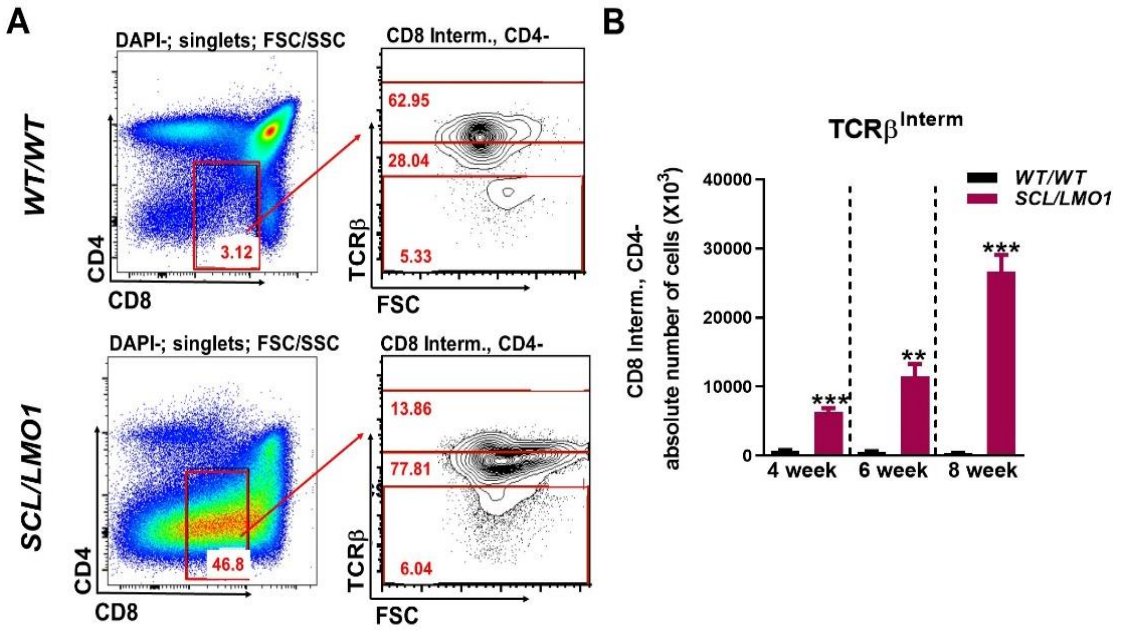

Figure 17. Immature CD4^{-}CD8^{low}TCR ^{intermediate} thymocytes accumulate in *SCL/LMO1* thymi.

A) Representative FACS plots and gating strategy of CD4^{-}CD8^{low} cells displaying differential TCRβ expression. In contrast to *WT/WT*, in *SCL/LMO1* mice, a clear TCR ^{intermediate} population with big cellular size was demarcating [FSC^{high}]. (B) The absolute numbers of CD4^{-}CD8^{low}TCR^{intermediate} were

determined in the thymus of *WT/WT* and *SCL/LMO1* mice. *SCL/LMO1*, n=3; *WT/WT*, n=3; means±SD are displayed. **p<0.01 and ***p<0.001.

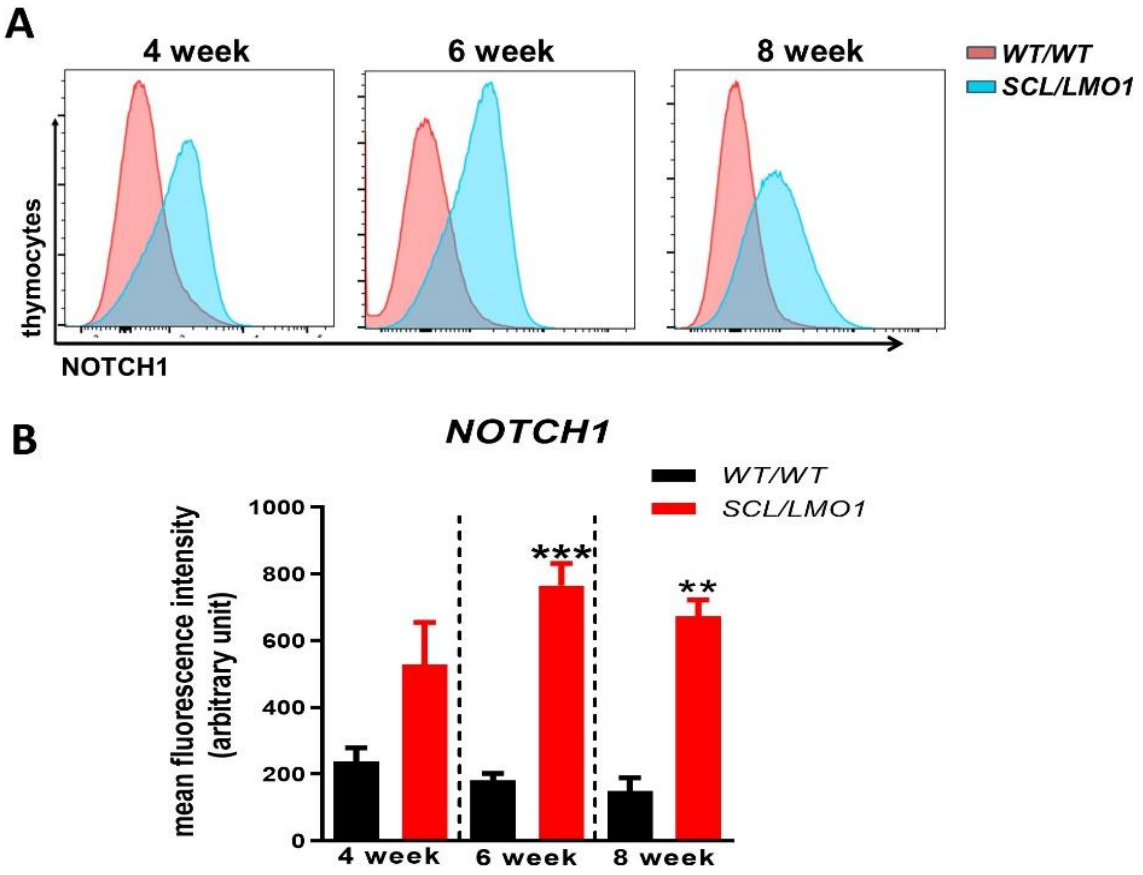

Figure 18. NOTCH1 is upregulated in CD4^{-}CD8^{low}TCR ^{intermediate} of *SCL/LMO1* mice.

(A) Representative histogram and (B) mean fluorescence intensity (MFI) showing NOTCH1 expression of the CD4^{-}CD8^{low}TCR^{intermediate} thymocyte subpopulation *WT/WT* (red area) and *SCL/LMO1* (blue area) mice at the indicated age. *SCL/LMO1*, n=3; *WT/WT*, n=3; means±SD are displayed. **p<0.01 and ***p<0.001.

3.5 The T-ALL supporting potential of TEC cell lines

As now the *SCL/LMO1* was established as a reliable T-ALL model triggered by genomic events frequently observed in genuine human T-ALL, leukemic thymocytes of this model were used to investigate the *in vitro* leukemia-supporting potential of TECs. This was undertaken by culturing primary *SCL/LMO1* leukemic cells on the thymic epithelial cell lines ANV and TE-71. Culturing *SCL/LMO1* leukemic thymocytes on the stromal BM cell line OP9 served as a positive control. Culturing *SCL/LMO1* leukemic thymocytes without any supporting cell line was the negative control of the experiment. After seventy-two hours

of co-culture, a high number of leukemic thymocytes were observed in close interaction with the OP9 control stromal cells as well as with the TEC cell lines TE-71 and ANV.

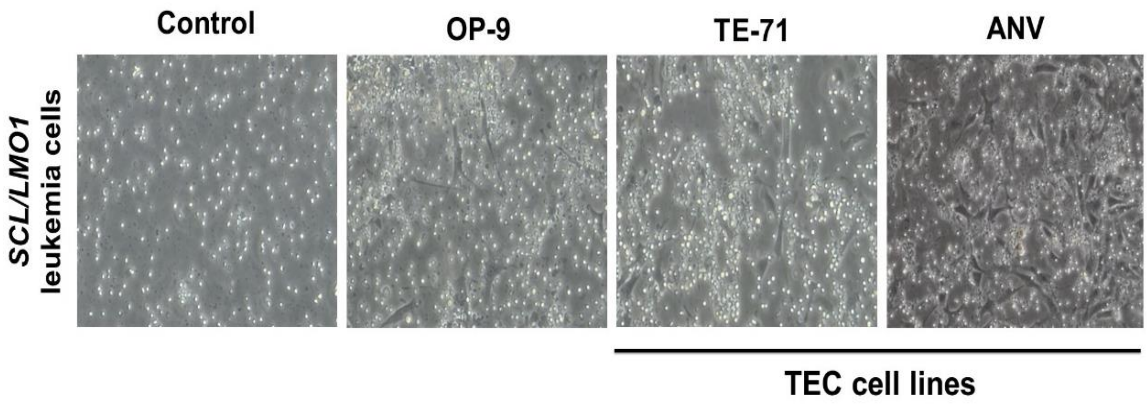

Figure 19. T-ALL *in vitro* supporting potential of the thymic epithelial cell lines ANV and TE-71.

Representative images showing co-cultured *SCL/LMO1* leukemia cells on the stromal OP9 and the epithelial TEC cell lines ANV and TE-71, respectively, after 72h. T-ALL cells from n=7 individual *SCL/LMO1* mice (6 to 8 weeks old) were used. Images were taken with a light field microscope.

These interactions appeared to result in increased cellular viability **(Figure 19)**. Because we incubated total thymocytes potentially still including a fraction of non-transformed, normal CD4+ T- and CD4+CD8+ DP-thymocytes, we stained the remaining cells after 72-hour culture with anti-CD4 and anti-CD8 antibodies and analyzed by flow cytometry. The proportion of *SCL/LMO1* transformed cells not resembling CD4+ T, and CD4+CD8+ DP cells were determined and used to calculate the absolute number of remaining leukemic cells after co-culture **(Fig. 20 A)**. The experiment resulted in a dichotomous finding. While n=4 T-ALLs showed increased leukemic thymocyte numbers after cell line co-incubations, n=3 T-ALLs neither showed relevant cell number changes after OP9 nor after TE-71 or ANV co-culture. As expected, the highest T-ALL supporting potential was mediated by the positive control OP9 cell line. However, the TE-71 and the ANV cell line displayed relevant T-ALL supporting potential of n=4 T-ALLs **(Fig. 20 B).** These findings indicate that thymic epithelial cells are capable of providing *in vitro* support to T-ALL leukemia cells.

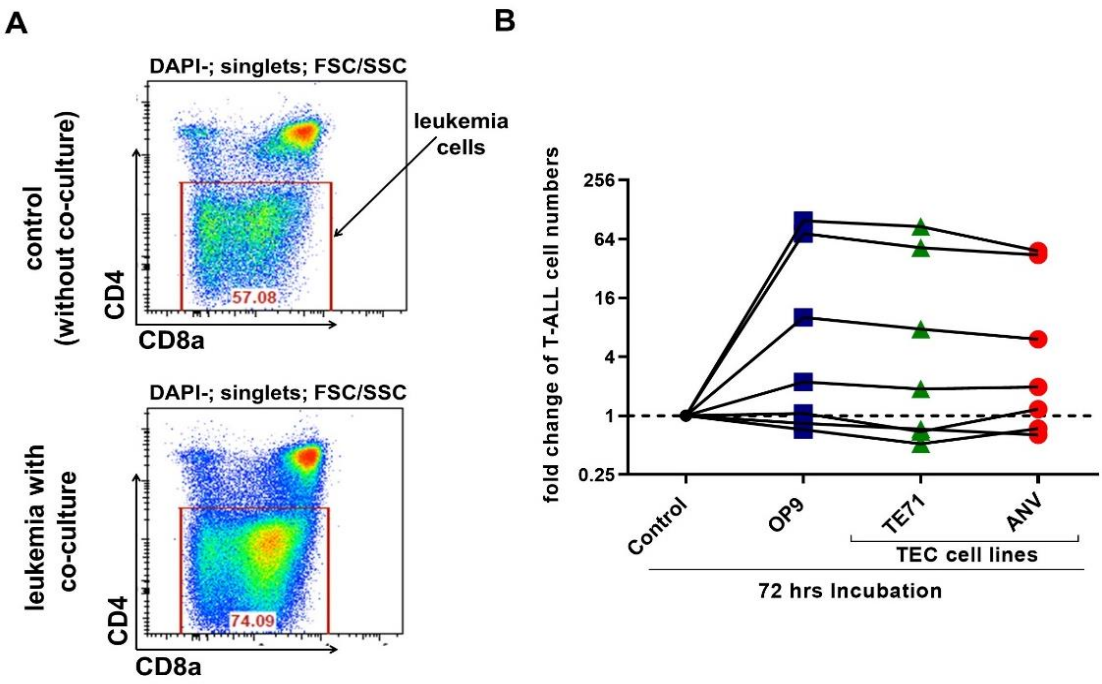

Figure 20. *In vitro* thymic epithelial cell line support of *SCL/LMO1* T-ALL cells.

(A) Representative flow cytometry plots showing the gating strategy to differentiate co-cultured CD4-negative transformed T-ALL cells from co-cultured normal CD4+ T- and CD4+CD8+ DP-thymocytes. (B) Graph showing fold change of co-cultured leukemia cell numbers compared to the corresponding control leukemic cell numbers of cultures without any stromal or epithelial cell line support. Fold change data of T-ALLs derived from n=7 *SCL/LMO1* mice. Each line depicts data of an independent *SCL/LMO1* leukemia. Each data point represents mean data derived from triplicate cultures.

3.6 Disrupted thymic architecture in *SCL/LMO1* transgenic mice

As the *SCL/LMO1* T-ALL model was extensively characterized and some *in vitro* evidence of TEC T-ALL supporting potential was acquired, we now studied whether developing T-ALL is associated with alterations of the TEC compartment *in vivo*. We investigated compositional modifications of the TEC microenvironment in *SCL/LMO1* mice. First, we evaluated the thymic architecture by H&E staining before the onset of leukemia at different ages (4, 6, and 8 weeks). H&E analysis revealed that *SCL/LMO1* transgenic mice showed morphological alterations of the thymic architecture. The medullary regions of the *SCL/LMO1* mice appeared to be reduced and more segregated into small areas. In contrast, the cortical areas were expanded in *SCL/LMO1* mice. Furthermore, at 6 and increasingly at 8 weeks, the cortical and medullary junction (CMJ)

blurred in *SCL/LMO1* mice. Overall, the discrimination between cortical and medullary areas faded out **(Fig. 21).**

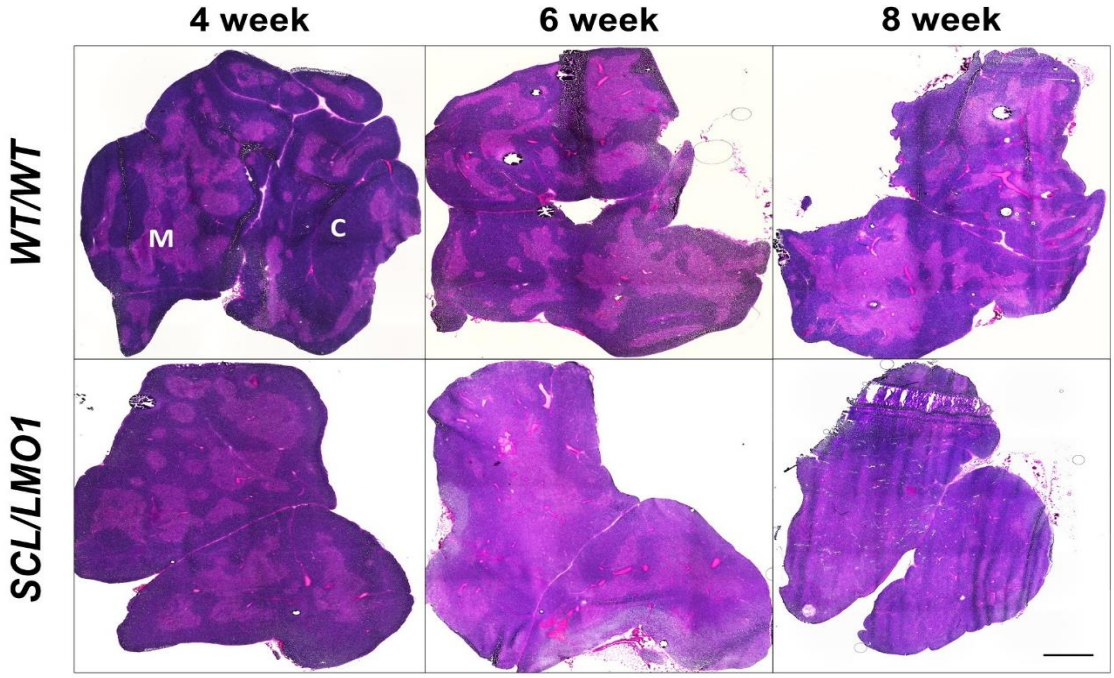

Figure 21. Microanatomic disruptions increase with age in in *SCL/LMO1* mice.

Transverse cryo-sections of *SCL/LMO1 and WT/WT* thymi at 4, 6, and 8 weeks of age were H&E stained and examined by light microscopy. Scale bar: 20µm. M indicates medulla; C, cortex. Representative images of n=3 mice per genotype and age are shown.

Next, we analyzed the distribution of the TEC sub-populations, cortical thymic epithelial cells (cTEC) and medullary thymic epithelial cells (mTEC) by fluorescent microscopy. For this purpose, thymus sections were stained with fluorophore-conjugated antibodies/ligands such as UEA to identify mTECs)[24] and BP1 to identify cTECs.[111] Nuclei were stained with DAPI. The immunofluorescent analysis revealed that the thymic architecture was disrupted in *SCL/LMO1* mice during T-ALL leukemogenesis. At younger age (4 weeks), cTEC regions appeared expanded at the expense of mTEC regions. mTEC regions in *SCL/LMO1* mice diminished and were gradually disorganized with increasing age. They appeared as scattered and isolated small nests of mTECs **(Fig. 22AB)**. With progressing leukemogenesis areas within the thymus appeared, which were completely devoid of thymic epithelial cells **(Figure 22A)**. This suggested that in these areas TECs either changed their marker expression or even transdifferentiated into a different cell-type. Taken together, these results demonstrated that the ratio of cortical (cTEC) to medullary (mTEC) thymic epithelial cells is shifted towards cTECs in the early preleukemic *SCL/LMO1* thymus. At later stages just before the onset of leukemia thymic areas containing phenotypic TECs declined.

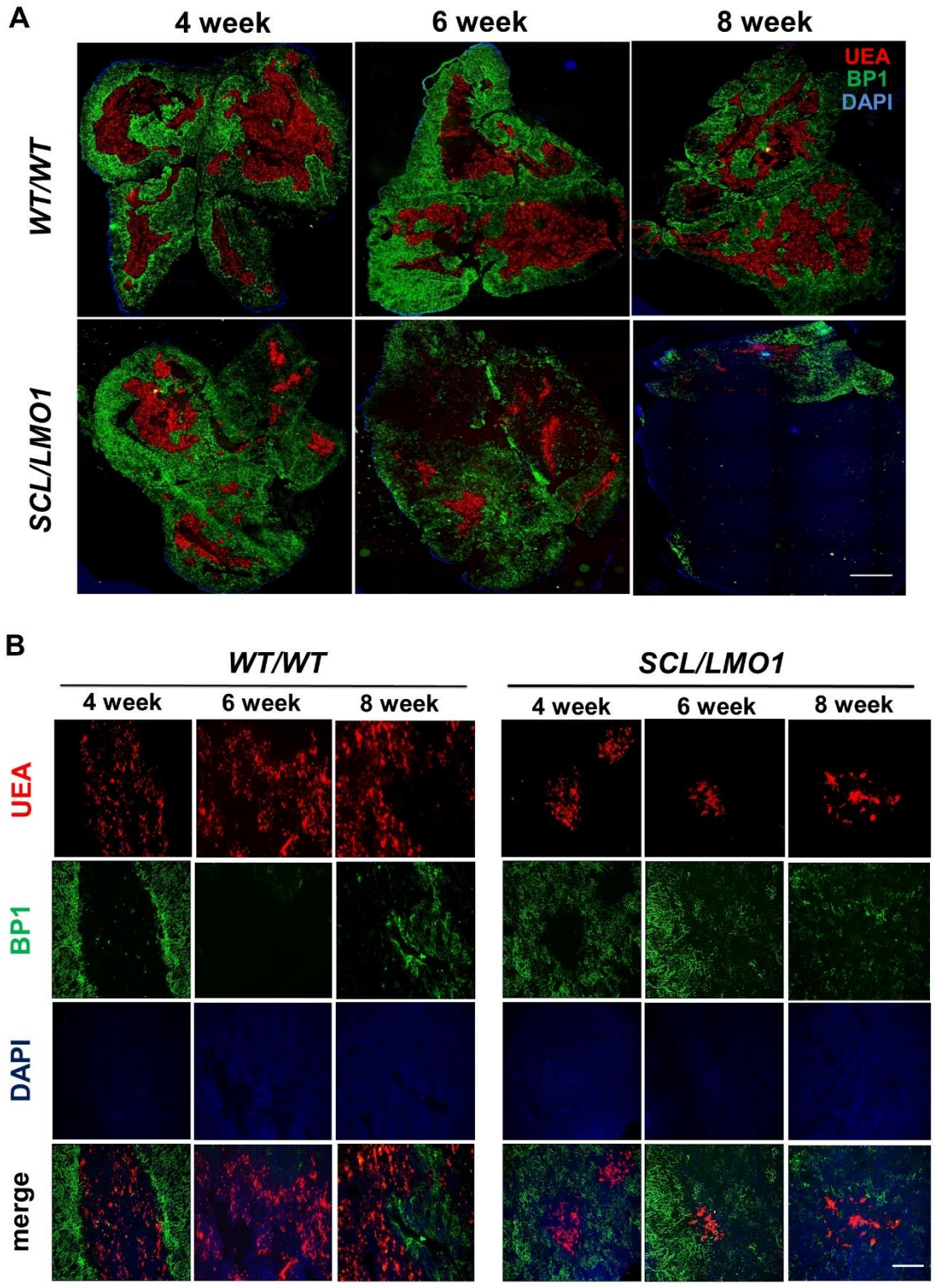

Figure 22. The cortex–medulla architecture in the thymus of the adult mouse.

Immunofluorescence of thymus sections from *WT/WT* and *SCL/LMO1* mice at an indicated time point, stained for UEA (mTEC, red), BP1 (cTEC, green) and DAPI (blue). (A) Images are captured at 10X zoom and (B) Images were captured at 20X zoom. Scale bar 300μm. One representative slide of three independent experiments is shown here.

3.6.1 Flow cytometric characterization of the *SCL/LMO1* thymic epithelial compartmen

Next, we characterized TECs by flow cytometry staining for EpCAM, and CD45 markers post enzymatic dissociation of the thymus **(Fig 5).** TECs are characterized by their expression of the epithelial marker EpCAM. However, they are negative for the pan-hematopoietic marker CD45. Therefore, we analyzed the EpCAM+CD45- the population at different time-points of *SCL/LMO1* leukemogenesis. *SCL/LMO1* mice showed a comparable EpCAM+CD45- fraction at an early age but a decreased fraction at later stages of leukemogenesis **(Fig. 23A).** Absolute *SCL/LMO1* TECs numbers were slightly higher (though not significant) compared to *WT/WT* TECs at an early stage (4 weeks) however over time the *SCL/LMO1* thymic TEC counts gradually decreased **(Fig. 23B).** Overall, TEC cell counts per mg of thymus showed a similar trend throughout the analysis. These results emphasize that TECs numbers show a slight early expansion in *SCL/LMO1* mice; however, throughout leukemogenesis, they show a gradual decrease **(Fig. 23B).**

Within the TEC population, cortical TECs (cTEC) can be distinguished from medullary TECs (mTECs) by their expression of BP1 or UEA, respectively **(Fig. 24A).** Antibodies against these markers were used in addition to anti-EPCAM and anti-CD45 for the flow cytometric analysis to determine the cellularity of the TEC (EPCAM+CD45-) sub-fractions cTEC (BP1+UEA-) and mTEC (UEA1+ BP1-). Remarkably, at initial stages of T leukemogenesis in 4 and 6 week old *SCL/LMO1* mice, when the thymic cellularity and weight were still unaltered, the numbers of *SCL/LMO1* cTECs was significantly increased compared to *WT/WT* mice. This *SCL/LMO1* cTEC number increase did not prevail in the later 8-week time point and also not when mice suffered from overt leukemia **(Fig. 24B)**. In contrast to the observed initial cTEC expansion, *SCL/LMO1* mTEC numbers decreased rapidly with progressing leukemogenesis from the age of 6 weeks onwards **(Fig. 24B).** Upon maturation, cTECs as well as mTECs upregulate MHC class II expression. In order to explore whether the described alterations in the cTEC and mTEC compartments are due to a possible maturation defect, we additionally stained cTECs and mTECs for MHC class II. Here, comparable alterations to the whole cTEC or mTEC compartment data evolved **(Fig. 24C).** Therefore, the dynamic alterations of the *SCL/LMO1* cTEC and mTEC compartments were most likely not due to a maturation defect. The thymic T cell output is normally governed by the ratio of the number of mTECs to the number of cTECs. In concordance with the described data, the *SCL/LMO1* mTEC/cTEC ratio was dramatically

shifted towards cTECs at all evaluated time points **(Fig. 25).** Taken together, the flow cytometric data confirm the TEC immunofluorescence microscopy data of increasing cortical TEC areas during early T-ALL leukemogenesis. Strikingly, during early leukemogenesis cTEC numbers increased while mTEC numbers decreased. Hence, the decrease of absolute total thymic epithelial cell numbers throughout leukemogenesis is primarily due to the loss of mTECs. We hypothesize that early increased *SCL/LMO1* cTEC numbers foster T-ALL leukemogenesis by providing an increased NOTCH1 signal via their DLL4 expression.

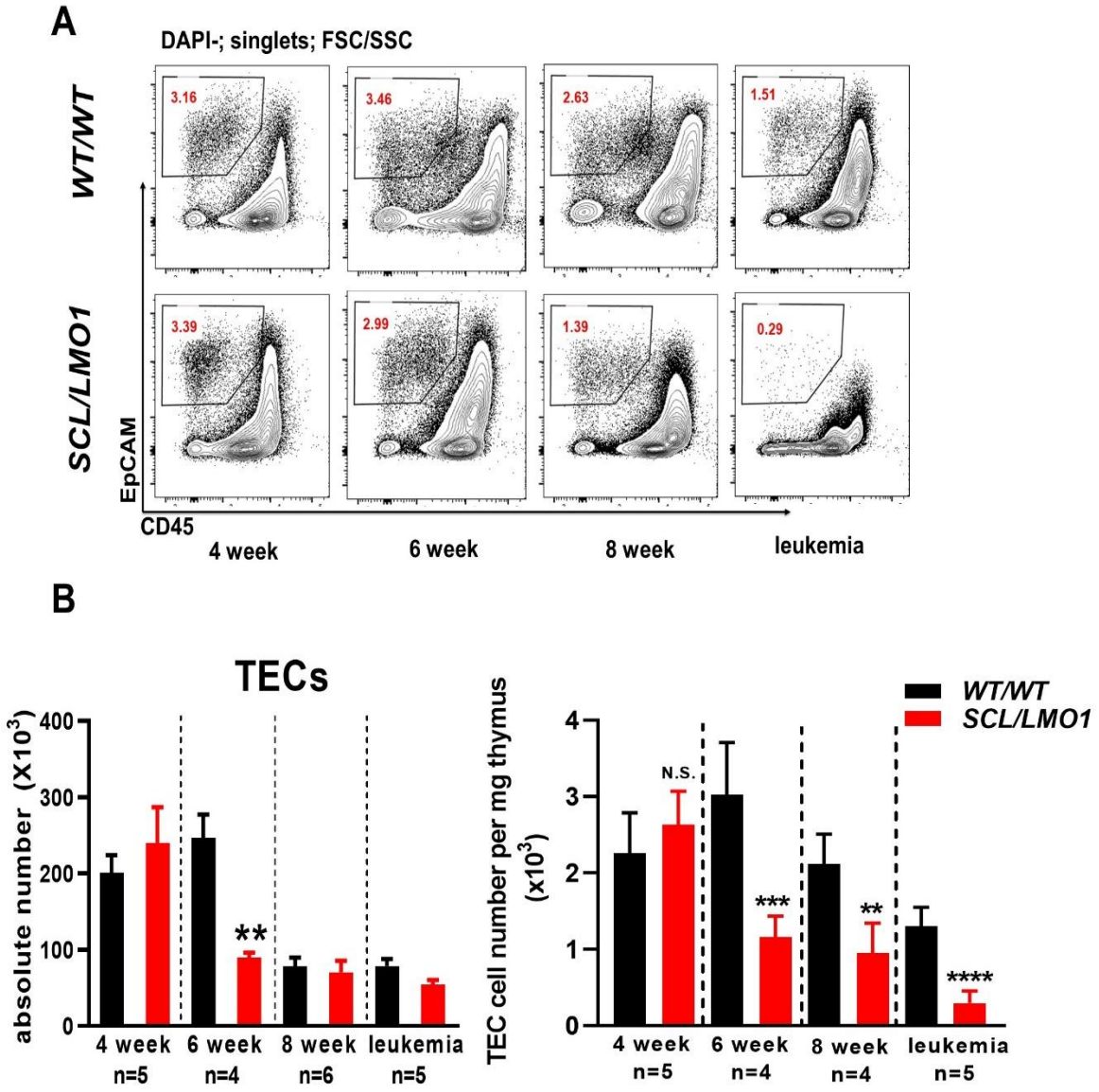

Figure 23. Flow cytometric characterization of TECs in *SCL/LMO1* mice.

(A) Representative flow cytometric analysis of thymic TECs (EpCAM+CD45-) of *WT/WT* and *SCL/LMO1* mice. (B) Quantification of absolute TEC numbers analyzed at the ages of 4, 6, and 8 weeks. Graphs display means+SEM; *p<0.05, **p<0.01 and ***p<0.001.

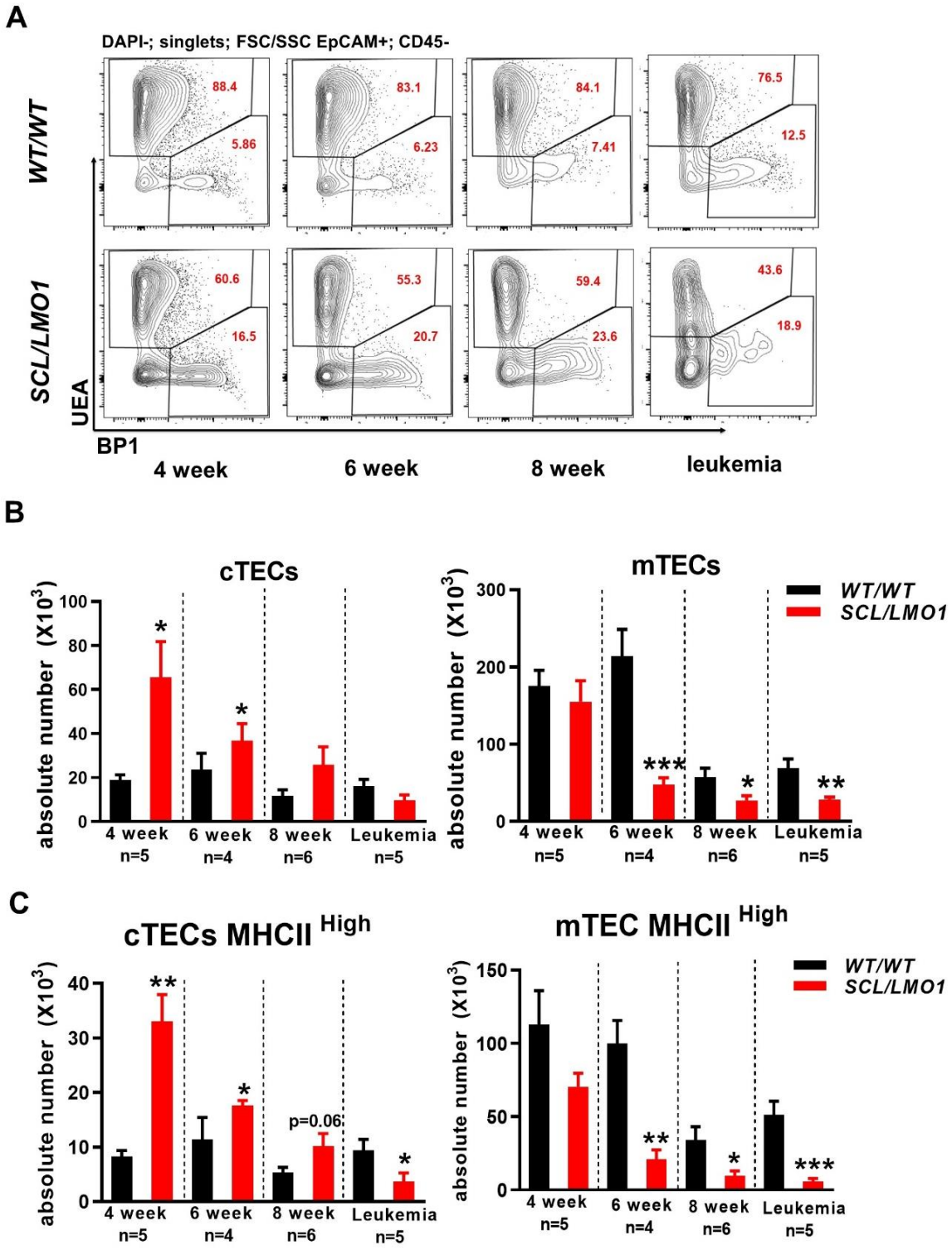

Figure 24. TECs subset analysis of *SCL/LMO1* and control *WT/WT* mice.

(A) Representative flow cytometric analysis of the thymic TEC subpopulations cTECs (Ly51+UEA-) and mTECs (UEA+Ly51-). (B) Absolute numbers of cTECs and mTECs and (C) absolute numbers of mature (MHCII high) cTECs and mTECs at the ages 4, 6 and 8 weeks. Means+SD; *p<0.05, **p<0.01 and ***p<0.001.

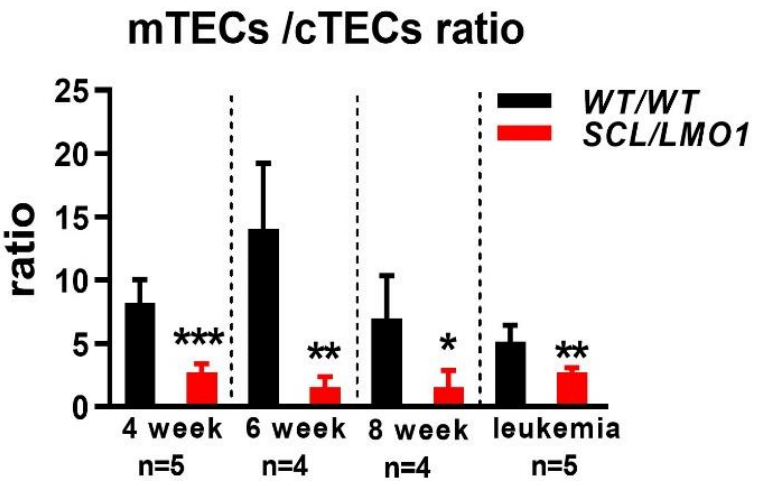

Figure 25. The ratio of mTECs to cTECs *WT/WT* in comparison to *SCL/LMO1* mice.

The analysis was performed at the ages 4, 6, and 8 weeks and in mice which developed leukemia. Data shown here represent means ±SD; *p<0.05, **p<0.01 and ***p<0.001.

3.7 The non-TEC stromal compartment of *SCL/LMO* mice during T-ALL leukemogenesis

During the flow cytometric TEC (EpCAM+ CD45-) analysis, we observed that the EpCAM negative and CD45 negative fraction appeared to increase over time in *SCL/LMO1* mice. Previous studies have shown that Ly51+ cells among EpCAM-CD45-CD31- cells express mesenchymal markers such as PDGFRβ in the thymus. Therefore, the EpCAM- CD45- Ly51+ population was defined as a mesenchymal, fibroblast-like population of the thymus.[28] Based on this, we studied these mesenchymal (EpCAM- CD45- Ly51+) cells in *SCL/LMO1* mice **(Fig. 26A)**. We found that during the progress of leukemogenesis, the absolute number of Ly51+ cells was highly variable but appeared to increase in *SCL/LMO1* mice compared to *WT/WT* mice. However, this increase did not achieve statistical significance. It remains problematic that thymic mesenchymal cells remain poorly defined. Thus, thymic *SCL/LMO1* fibroblast-like cells might have been missed by the EpCAM- CD45- Ly51+ analysis. Therefore, the obtained data do not exclude the existence of a mesenchymal cell type, which is increased in *SCL/LMO1* thymi. We still favor a hypothesis in which the loss of TECs could be due to TECs differentiating into mesenchyme-/ fibroblast-like cells via a process similar to the well-described epithelial-mesenchymal-transition (EMT) of cancer.

3.7.1 TGFβ expression in *SCL/LMO1* leukemia mice

In order to study factors, which are known inducers of EMT, we decided to measure TGFβ expression by *SCL/LMO1* thymocytes. TGFβ was shown to induce EMT in immortalized mammary epithelial NMuMG cells. [112] **(Fig. 27).** The expression of TGFβ was significantly upregulated in 4-week-old *SCL/LMO1* mice, however was highly variable there after. Possibly, early TGFβ upregulation could induce an EMT-like process in *SCL/LMO1* thymi.

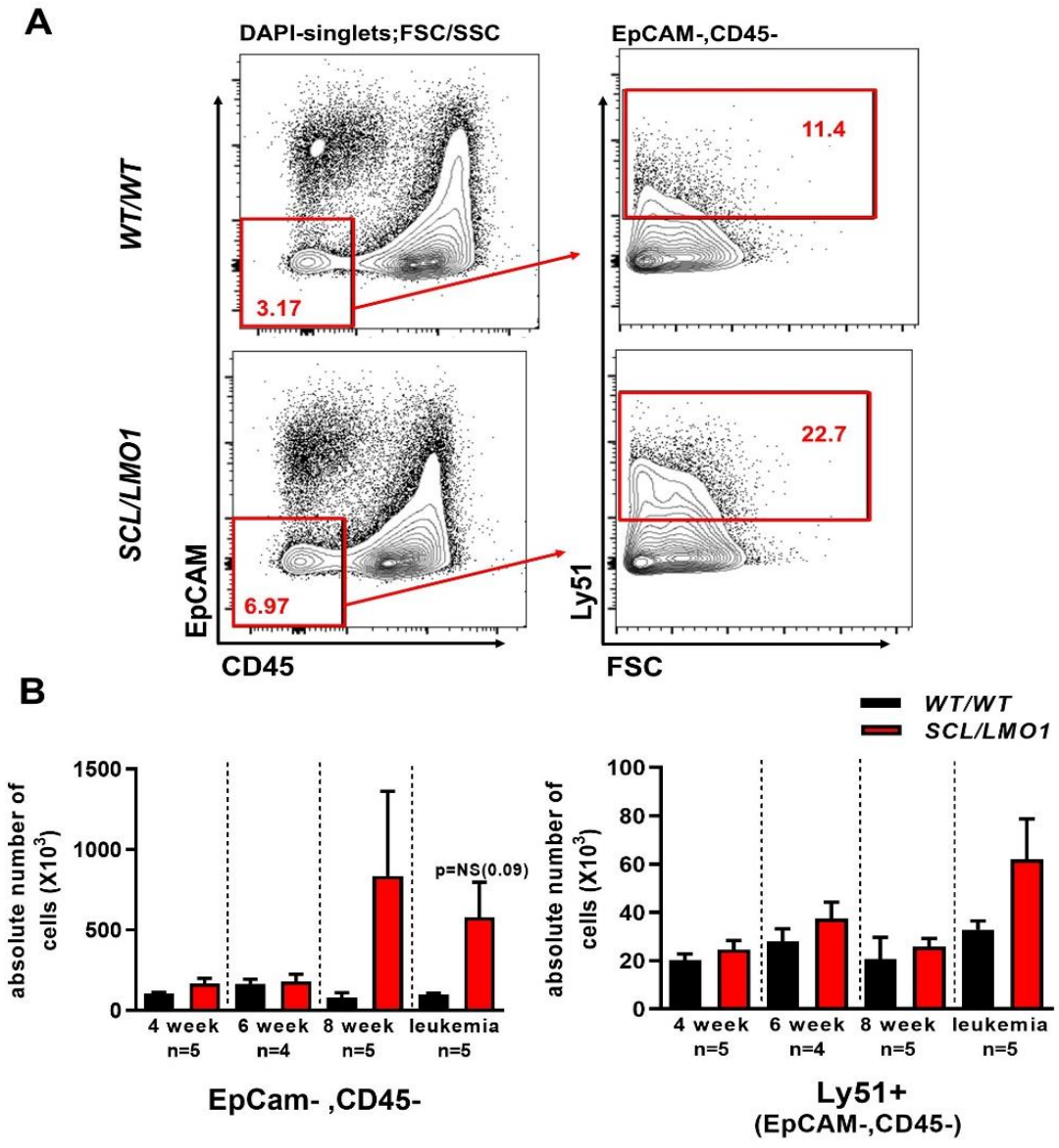

Figure 26. Mesenchymal (EpCAM- CD45- Ly51+) cells in *SCL/LMO1* leukemogenesis.

(A) Representative gating strategy for the flow cytometric analysis of the mesenchymal (EpCAM- CD45- Ly51+) cell in *SCL/LMO* and *WT/WT* mice. (B) Absolute numbers of EpCAM- CD45- cells

and mesenchymal cells (EpCAM- CD45- Ly51+) of 4, 6, and 8-week-old *SCL/LMO1* and *WT/WT* mice. Mean+SEM are displayed.

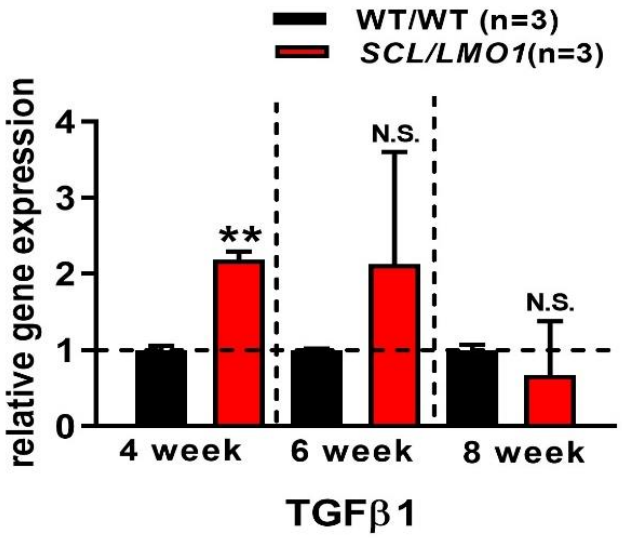

Figure 27. TGFβ expression by *SCL/LMO1* compared to *WT/WT* thymocytes.

Bar diagram showing thymocyte TGFβ gene expression in *SCL/LMO1* and *WT/WT* mice at different ages (4, 6, and 8 weeks). ***p*< 0.01; N.S., non-significant.

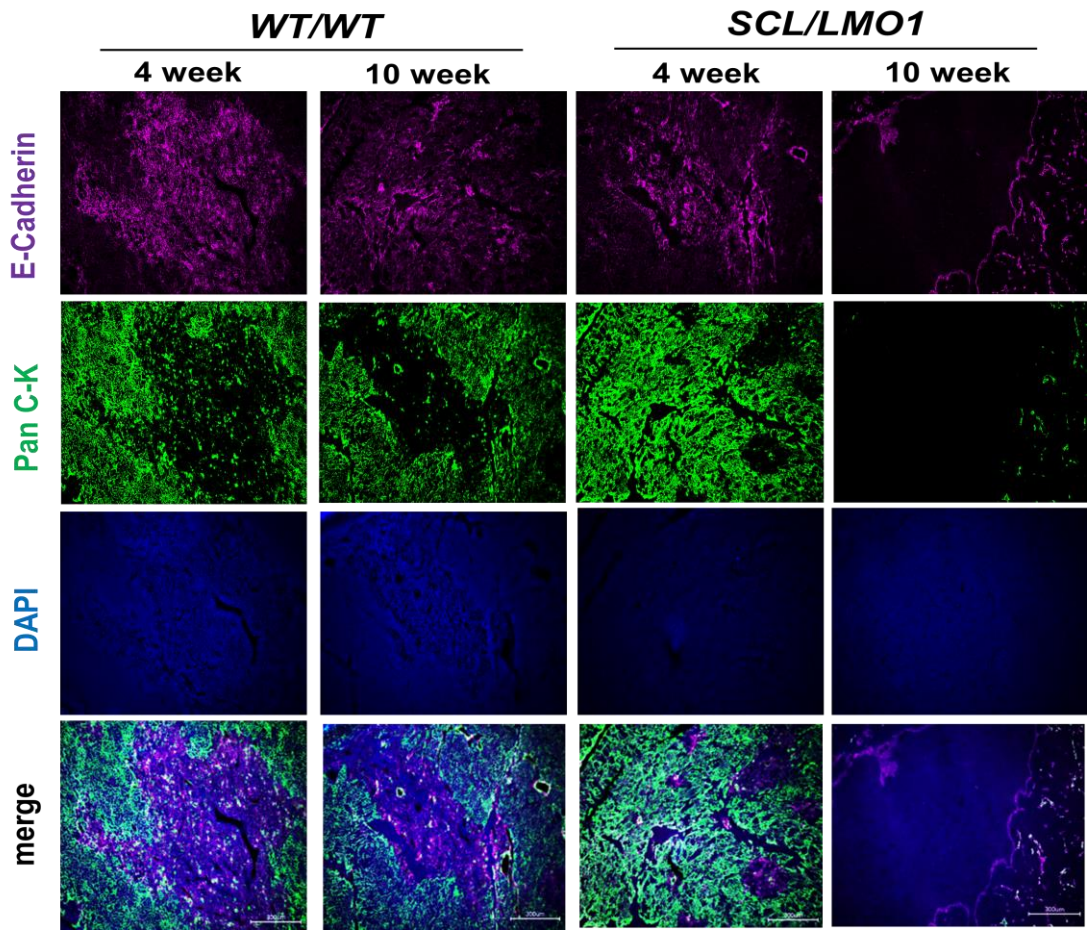

Figure 28. Thymic immunofluorescent staining for E-cadherin.

Representative immunofluorescence of sections from the thymus of naive wild-type (*WT/WT*), and *SCL/LMO1* transgenic mice after staining for epithelial cells (E-cadherin, violet), and pan CK (C-11) (green) ($n = 4–5$ per group). Scale bar, 300 μm. One slide representative of four or five slides is shown.

3.7.2 Analysis of *SCL/LMO1* thymic E-cadherin and ER-TR7 expression

To further gain insight into the decreasing TECs numbers during progressing T-ALL leukemogenesis, we performed additional immunofluorescence staining of thymic sections from *SCL/LMO1* and *WT/WT* mice. The sections were stained with additional antibodies against epithelial markers (E-Cadherin and Pan C-K) to confirm the TEC data were so far mainly collected with an anti-EpCAM antibody. The up to now collected *SCL/LMO1* data were confirmed with the anti-E-Cadherin and anti-pan C-K antibodies: immunofluorescent thymic staining with these antibodies progressively decreased in *SCL/LMO1* mice compared to *WT/WT* mice during leukemogenesis (**Fig. 28**). In order to use an alternative approach to identify potential stromal thymic mesenchymal cells in developing T-ALL thymic sections were stained for the ER-TR7 pan-mesenchymal marker. Because ER-TR7 also stains perivascular cells, we performed co-staining for the endothelial cell marker CD31. In 8-week-old *SCL/LMO1* mice thymic, CD31+ vascular density appeared increased compared to *WT/WT* mice. Around these *SCL/LMO1* vessels, strong ER-TR7 staining was observed most likely representing perivascular mesenchymal cells (**Fig.29**). Taken together, these results confirm epithelial cell depletion with progressing *SCL/LMO1* leukemogenesis. Mesenchymal cells appear to expand in the perivascular space of *SCL/LMO1* thymi.

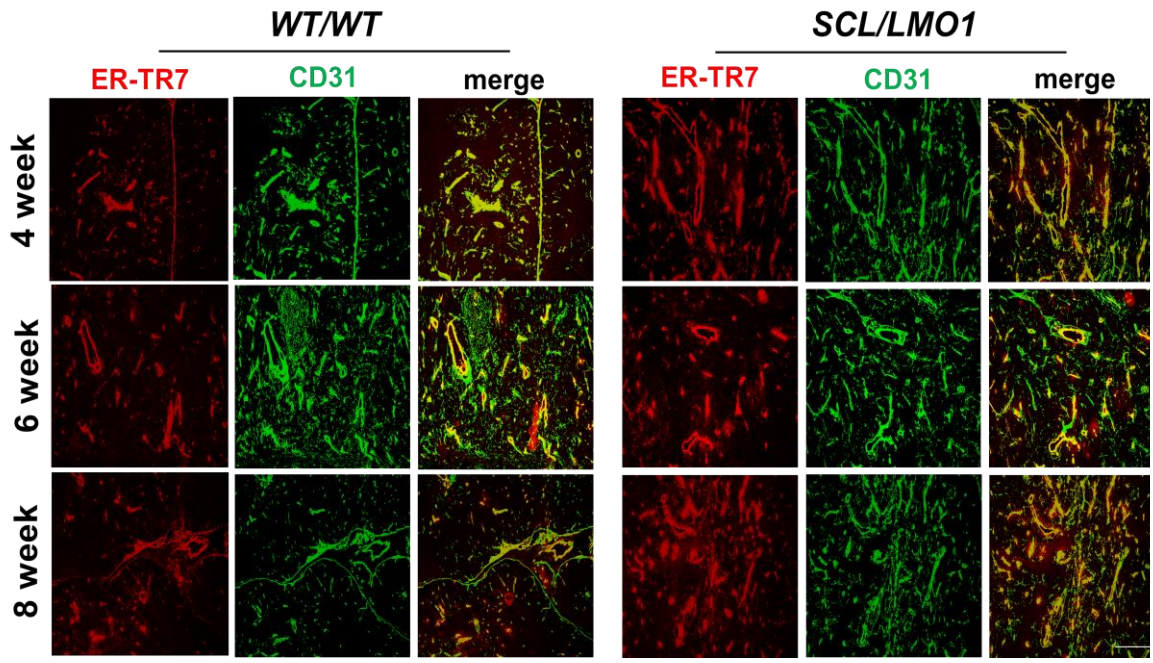

Figure 29. *SCL/LMO1* mice showed upregulation of ER-TR7 expression.

Representative immunofluorescent staining of thymic sections from wild type (*WT/WT*) and *SCL/LMO1* mice with ant- ER-TR7 (mesenchymal marker), anti-CD31 (endothelial cell marker) and DAPI. Scale bar 100 µm. Representative images from three independent mice per age group and genotype.

3.8 GENE EXPRESSION ANALYSIS OF SORTED TECS AND LY51+ MESENCHYMAL CELLS

Next, we investigated whether T-ALL leukemogenesis altered the expression of T-cell development-promoting factors by stromal cells such as TECs and mesenchymal cells. For this, we flow cytometry-sorted TECs and Ly51+ mesenchymal cells according to the gating strategy shown **(Fig. 30**). The purity of sorted TECs and Ly51+ mesenchymal cells was greater than 90%. Sorted TECs cells were analyzed for their expression of CXCL12, CCL25, SCF, IL7, IL18, and IGF1. By RT-PCR analysis, we found that all these genes were upregulated in *SCL/LMO1* TEC cells compared to *WT/WT* TECs cells. In particular, the upregulation of CXCL12 and IL-18 within *SCL/LMO1* TECs reached statistical significance (**Fig.31**). These results show that secreted factors critical for thymic T cell development were upregulated in TECs during leukemogenesis

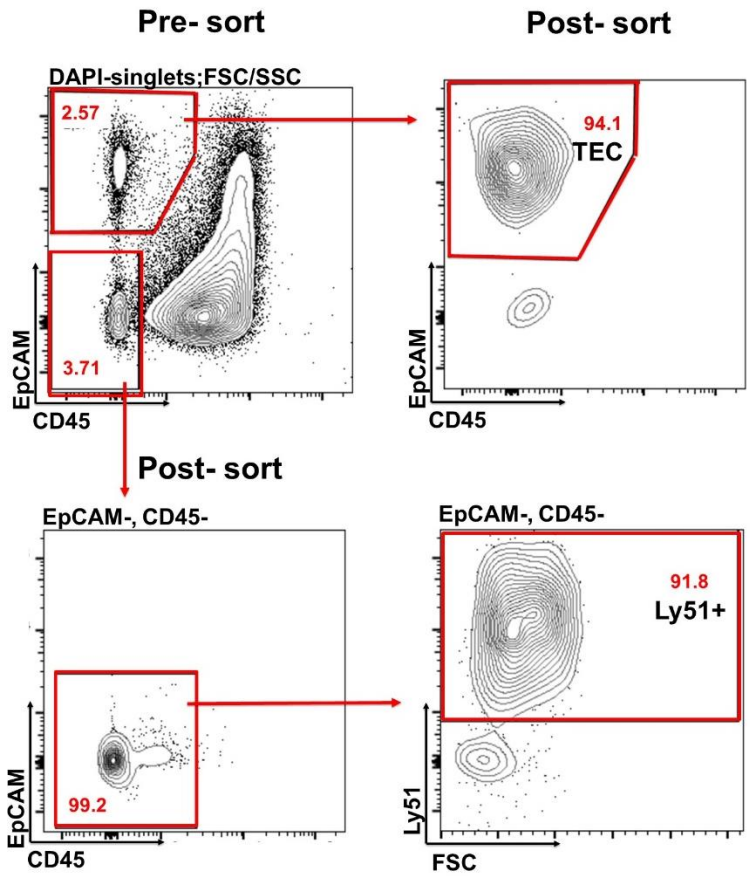

Figure 30. Flow cytometry-sorting strategy and post-sort purity of TECs and thymic Ly51+ mesenchymal cells.

Gating strategy for the FACS purification of thymic TECs and Ly51+ mesenchymal cells. Representative contour plots for pre- and post-sort cell populations are shown. Cells were sorted from n=3 *WT/WT* and n=3 *SCL/LMO1* mice.

A similar analysis was performed with Ly51+ mesenchymal cells from *SCL/LMO1* mice. RT-PCR analysis showed that the NOTCH1 receptor was significantly upregulated by Ly51+ cells. The NOTCH1 ligand DLL4 and the downstream NOTCH-genes HES1 and DTX1 only showed a trend towards upregulation within *SCL/LMO1* mesenchymal cells **(Fig. 32).** As shown before, early preleukemic thymocytes express higher levels of TGFβ **(Fig. 27)**. Now to study the expression of TGFβ in mesenchymal cells, we analyzed the expression of TGFβ in *SCL/LMO1* mesenchymal cells. RT-PCR analysis showed a significantly higher expression of TGFβ while vascular endothelial growth factor (VEGF) was unaltered in mesenchymal cells from *SCL/LMO1* mice **(Fig.33).** In summary, TECs of the preleukemic *SCL/LMO1* thymus upregulated CXCL12 and IL-18, which both are factors known to promote normal T cell development. Moreover, thymic mesenchymal cells upregulated the NOTCH1 receptor and the cytokine TGFβ.

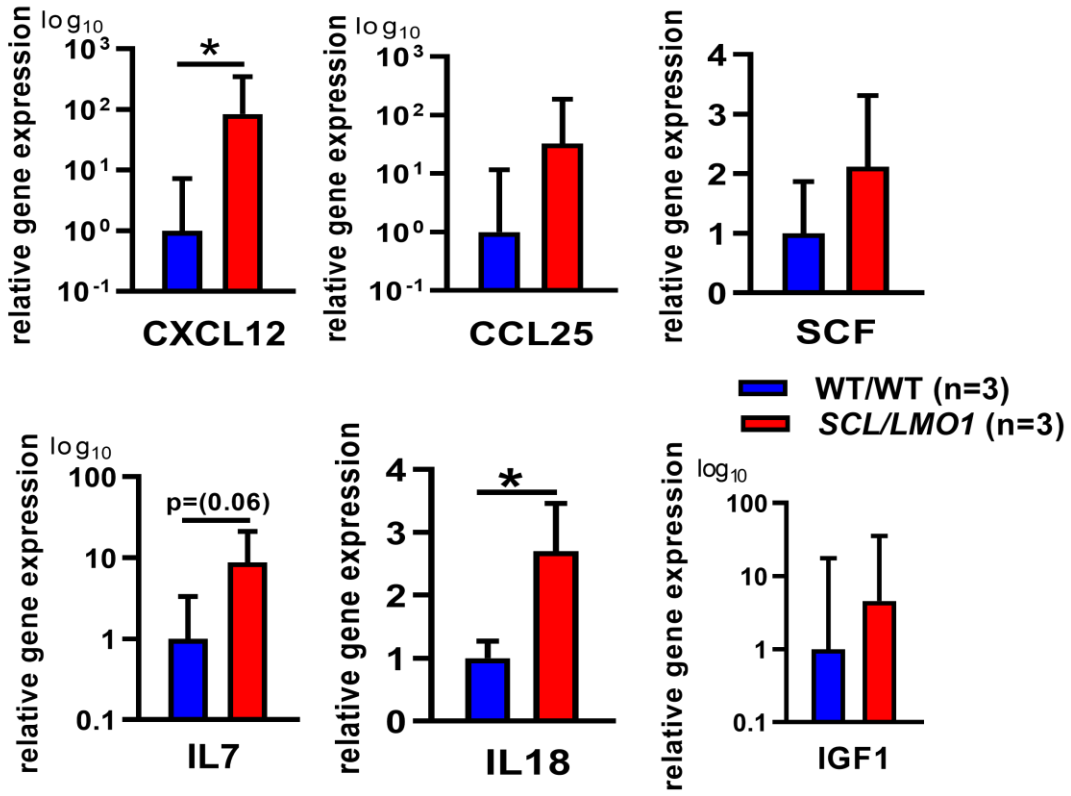

Figure 31. Gene expression analysis of T cell development-promoting factors by *SCL/LMO1* preleukemic TECs cells.

Bar graphs showing gene expression by sorted TECs from the thymus of *SCL/LMO1* and *WT/WT* mice. Target mRNA was normalized against the expression of Hprt-mRNA as the housekeeping transcript. The cells were isolated from 6-week-old mice. Mean+SD displayed, *p<0.05.

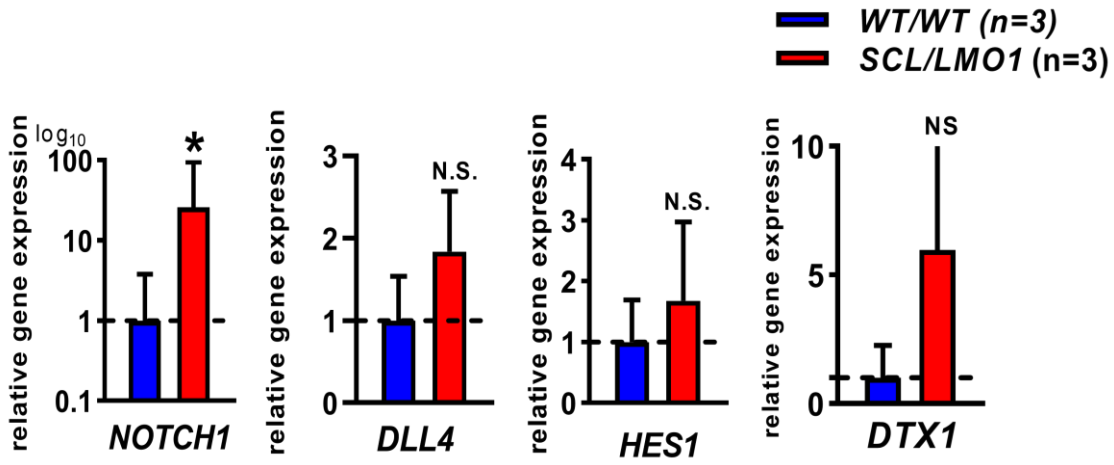

Figure 32. Ly51+ mesenchymal cells from *SCL/LMO1* mice showed upregulation of NOTCH1 receptor expression.

Bar diagrams displaying an expression of NOTCH1, DLL4, HES1, and DTX1 of sorted Ly51+ cells from the thymus of *SCL/LMO1* and *WT/WT* mice. Target mRNA was normalized against the expression of Hprt-mRNA the housekeeping transcript. Cells were sorted from the 6-week-old mice. Mean+SD displayed, *p<0.05, N.S., non-significant

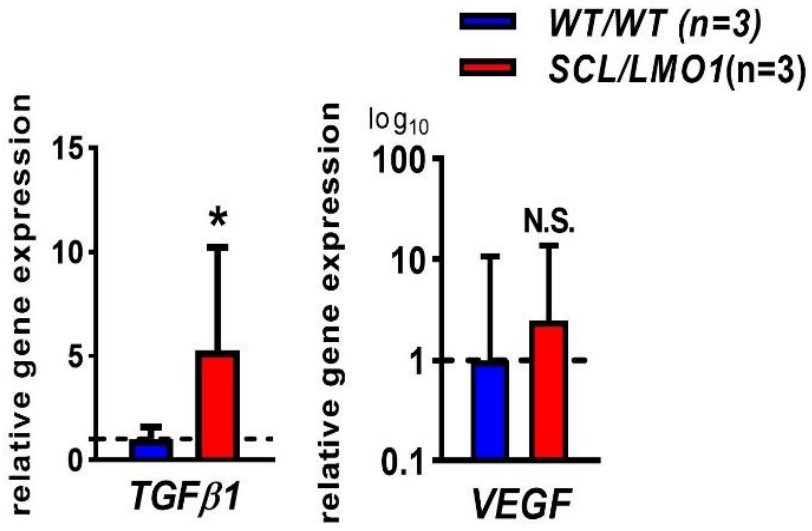

Figure 33. Ly51+ (mesenchymal) cells from *SCL/LMO1* mice showed upregulation of TGFβ.

Bar diagrams showing expression of TGFβ and VEGF on sorted Ly51+ cells from the thymus of *SCL/LMO1* and *WT/WT* mice. Target mRNA was normalized against the expression of Hprt-mRNA as control. The cells were isolated from the 6-week-old mice. Data is representative of three experiments. Mean ±SD, *p<0.05, N.S., non-significant

3.9 RT^2 profiler PCR array analysis of preleukemic TECs

3.9.1 Expression of NOTCH pathway components in preleukemic TEC

Notch ligand expressing TECs initiate and sustain NOTCH signaling in thymocytes. We have shown that within the pre-leukemic TEC compartment, there is a dramatic shift towards NOTCH-ligand expressing cortical TECs. These dynamic cellular changes are presumably associated with changes in the TEC expression of NOTCH pathway components. Therefore, we next investigated the expression of 84 genes involved in the NOTCH signaling pathway with a commercially available PCR array in sorted *WT/WT* and *SCL/LMO1* TECs. Remarkably, NOTCH signaling pathway components were primarily upregulated in *SCL/LMO1* compared to *WT/WT* TECs. The top significantly upregulated genes included the NOTCH1 receptor and the NOTCH-ligands DLL4 and DLL3 **(Fig. 34)**. These results are in line with our previous data of expanded preleukemic cTEC, as these cells are known to express high levels of DLL4.

3.9.2 Cytokine and chemokine expression profile of preleukemic TECs

Cytokines and chemokines secreted and expressed by TECs are central to T cell development and are essential for the migration and maturation of thymocytes. In our preliminary data, we showed that preleukemic TECs upregulated chemokines such as CXCL12 **(Fig. 31)**. Therefore, we decided to investigate the expression pattern of 84 cytokine or chemokines in TECs using the mouse RT^2 Profiler PCR array.

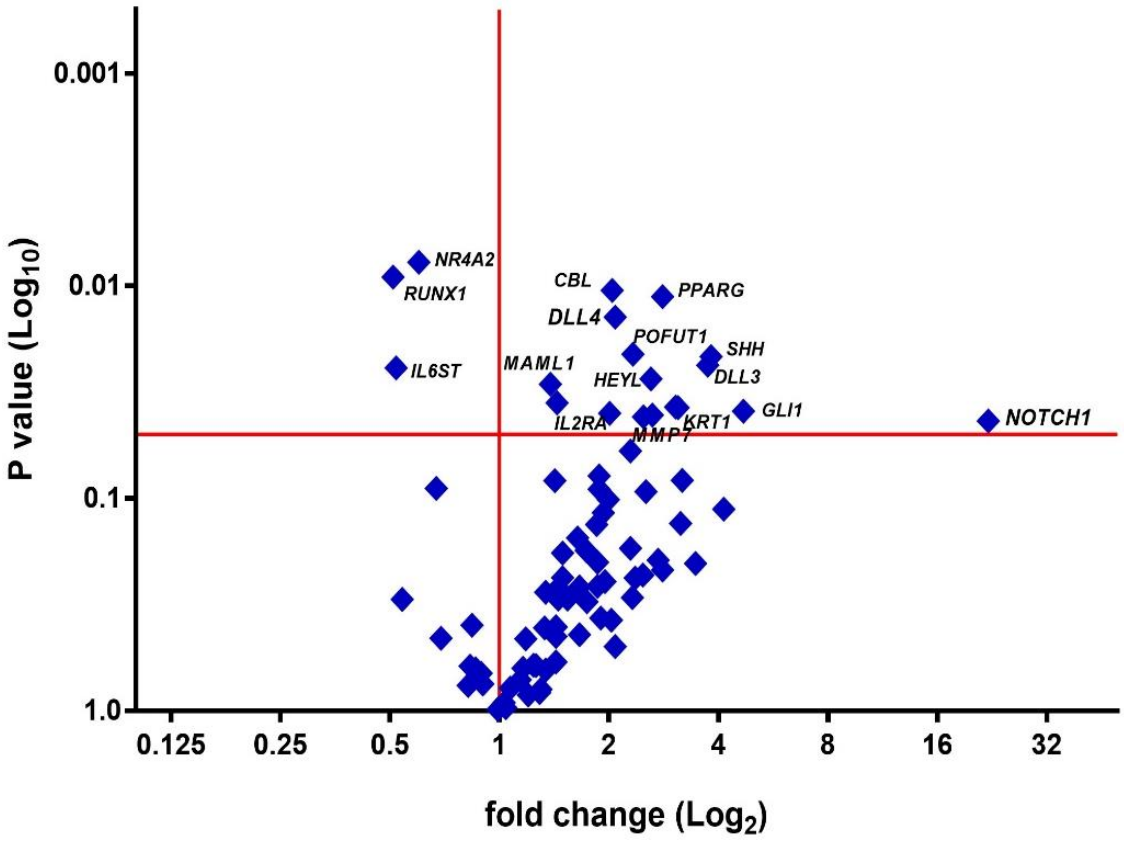

Figure 34. PCR expression array of NOTCH pathway components of normal versus preleukemic TECs.

Volcano plot showing up- and down-regulated genes in sorted TECs from *SCL/LMO1* mice (n=4) compared to sorted TECs from *WT/WT* mice (n=4). Mice were 6 months old. Data are shown as log_2 (n-fold) values plotted against negative Log_{10} ($p<0.05$).

Various cytokines and chemokines were differentially expressed by *SCL/LMO1* versus *WT/WT* TECs. The analysis revealed significant ($P< 0.05$) preleukemic TEC upregulation of chemokines in particular, including CXCL10, CXCL12, CCL2, CXCL1 and CCL9 **(Fig. 35)**. These data confirm our preliminary results of upregulated CXCL12 by preleukemic TECs **(Fig. 31)**.

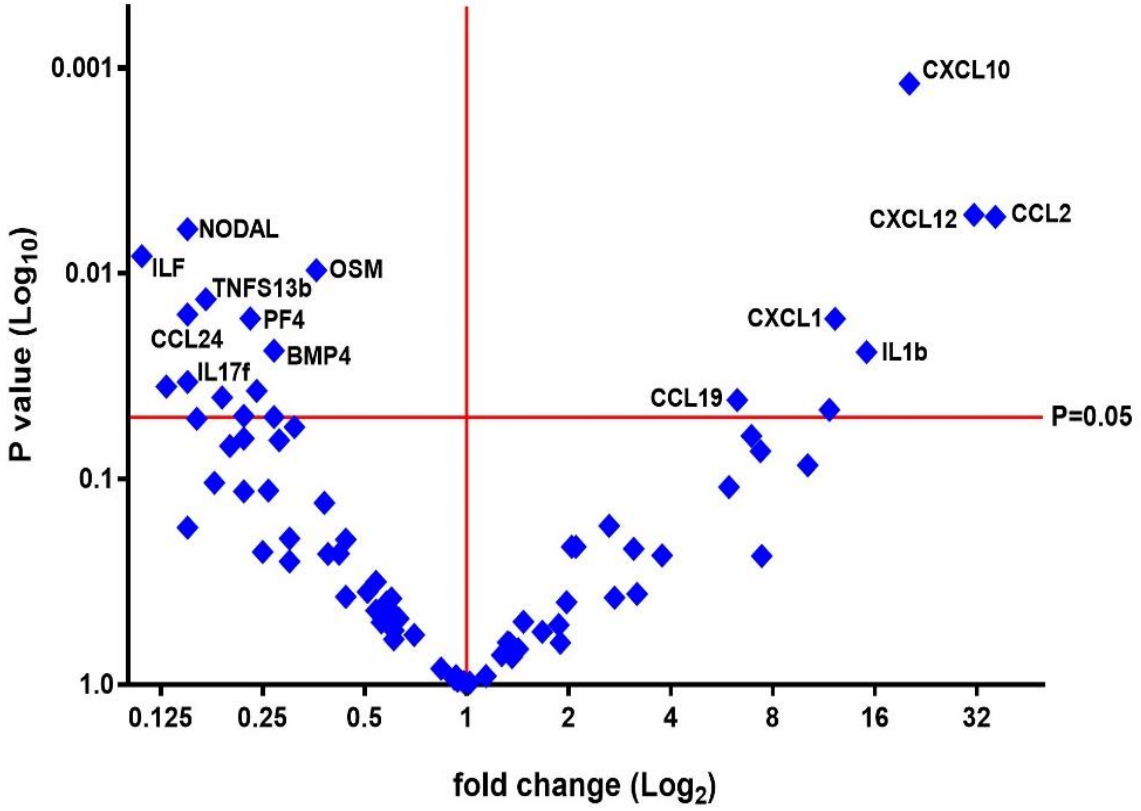

Figure 35. PCR expression array of cytokines and chemokines of normal versus preleukemic TECs.

The volcano plot showing up- and down-regulated genes in sorted TECs from *SCL/LMO1* mice (n=4) compared to sorted TECs from *WT/WT* mice (n=4). Mice were 6 months old. Data is shown as log_2 (n-fold) values plotted against negative Log_{10} ($p<0.05$).

3.10 Chemokine CXCL10 is upregulated in preleukemic cTECs and thymi.

The PCR array assay resulted in several chemokines, which were upregulated by preleukemic TECs. In order to investigate whether cortical or medullary subsets or both were responsible for this upregulation, we sorted mTECs and cTECs from thymi of 6-week-old *SCL/LMO1* and *WT/WT* mice, respectively. Next, we used alternative real-time PCR assays to determine the expression levels of CXCL10, CXCL12, CCL25, and CCL2 within sorted cTECs and mTECs **(Fig.36).** In *SCL/LMO1* preleukemic, thymi the significant upregulation of CXCL10, CXCL12, CCL25, and CCL2 was restricted to cTECs **(Fig. 37)**. Previous studies reported the expression of factors such as CXCL12 and CCL25 by cTECs as essential for normal T cell development.[113] Additionally, it was already shown that CXCL12 is an

essential factor for T-ALL maintenance, especially in the bone marrow.[114] Remarkably, we found significant upregulation of CXCL10 within *SCL/LMO1* preleukemic cTECs. Therefore, we decided to investigate further the role of TEC-derived CXCL10 in promoting T-ALL development and maintenance. First, we asked whether we would also detect high CXCL10 levels within the interstitial fluid of preleukemic *SCL/LMO1* thymi. For this, we determined CXCL10 protein levels in the thymic interstitial fluid (TIF) by ELISA. Strikingly, the CXCL10 concentration within *SCL/LMO1* TIF was significantly higher compared to *WT/WT* TIF (**Fig. 38).** We confirmed the finding of high CXCL10 concentrations within the preleukemic thymus by immunofluorescent staining of thymic sections from *WT/WT* mice and *SCL/LMO1* mice. Interstitial cells with positive CXCL10 immunofluorescence appeared more frequently in *SCL/LMO1* than in *WT/WT* thymi **(Fig. 39).** In summary, we identified a number of chemokines, including CXCL10 upregulated within preleukemic TECs. We found that CXCL10 is primarily upregulated within preleukemic cTECs. Strikingly, we further demonstrated high CXCL10 chemokine levels within the pre-leukemic thymus.

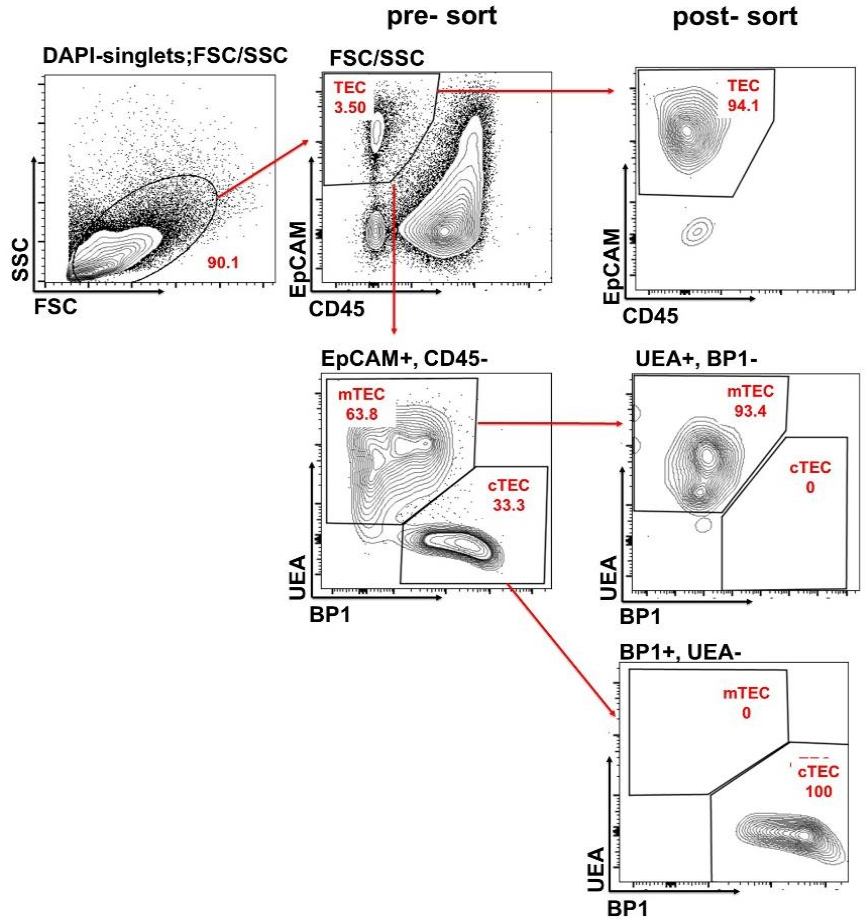

Figure 36. FACS plot of pre- and post-sorted TEC, cTECs and mTECc fractions.

FACS plots showing the sorting scheme for TECs and TEC subpopulations. Representative contour plots for pre- and post- sort of TECs, mTEC and cTEC cell populations are displayed. The sort was carried out with thyme from 6-week-old mice. n=3 mice per genotype. The purity of sorted cells was above 93%. FSC = forward scatter, SSC = side scatter.

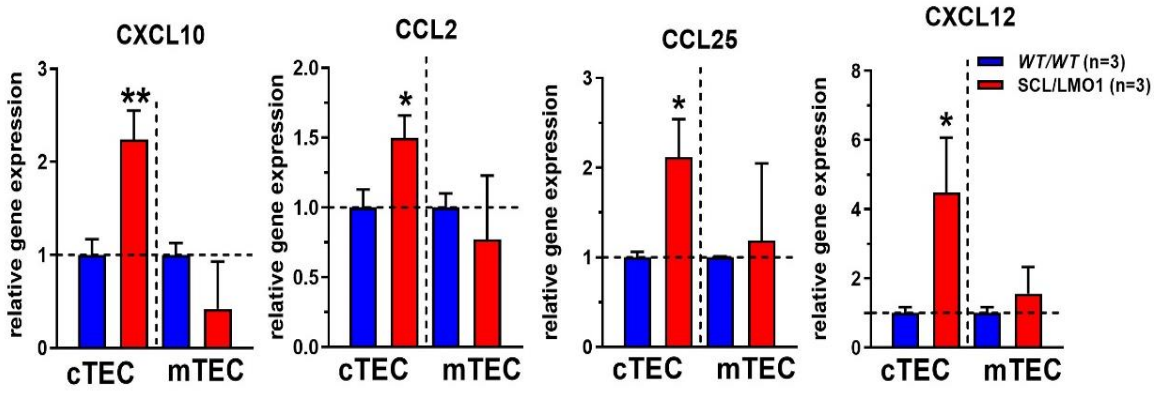

Figure 37. Chemokine upregulated in cTECs of *SCL/LMO1* mice.

Bar graph showing the expression of chemokines by sorted cTECs and mTECs from the thymi of *SCL/LMO1* and *WT/WT* mice. Target mRNA was normalized against the expression of Hprt-mRNA. Six week old mice of indicated genotypes were used for the sorting. mean ± SD, *P<0.05, and **P<0.01.

.

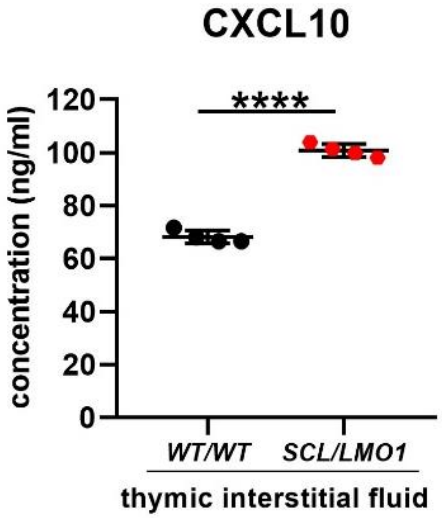

Figure 38. CXCL10 level within the thymic interstitial fluid of *SCL/LMO1* mice.

Graph showing the CXCL10 concentration within the thymic interstitial fluid of *SCL/LMO1* and *WT/WT* mice measured by ELISA. n=4 mice per genotype, mean ± SD; ****P <0.0001.

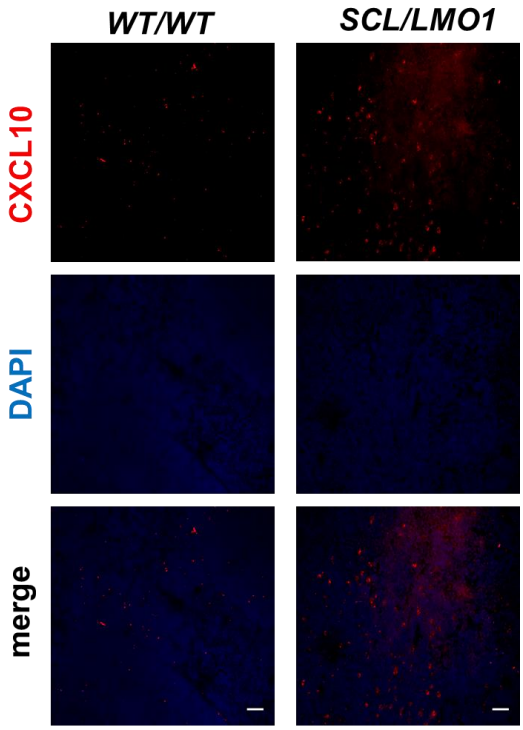

Figure 39. CXCL10 immunofluorescence within *WT/WT* and *SCL/LMO1* thymic sections.

Representative immunofluorescence of sections from the thymi of wild-type (*WT/WT*) and *SCL/LMO1* mice after staining for CXCL10 (red) and DAPI (blue) ($n = 3$ per group). Scale bar, 100 µm. Representative images of n=3 mice per genotype are shown.

3.11 Preleukemic thymocytes induce CXCL10 expression by TECs

To explore whether preleukemic thymocytes directly induce CXCL10 expression by preleukemic TECs, we co-cultured the TEC cell lines (ANV and TE-71) together with primary *SCL/LMO1* or *WT/WT* thymocytes. For this, we utilized two co-culture system approaches. One was direct contact (cell to cell) and the second was indirect contact (transwell) co-culture system as shown in the methods section **(Fig. 5).**

3.11.1 *SCL/LMO1* thymocytes induce CXCL10 expression in TEC cell lines via direct cell to cell contact

The expression of CXCL10 by the TEC cell lines (ANV and TE-71) was determined after 24 hours of co-culture (direct or indirect contact condition) by RT-PCR. Remarkably, we found that CXCL10 was significantly upregulated in both TEC cell lines (ANV and TE-71) by direct contact with *SCL/LMO1* preleukemic compared to *WT/WT* thymocytes. Indirect

contact between *SCL/LMO1* thymocytes and TE-71 cells, however was capable of inducing a slightly higher CXCL10 expression level than indirect contact between *WT/WT* thymocytes and TE-71 **(Fig. 40AB).** Our data argue for a model where specifically *SCL/LMO1* thymocytes induce CXCL10 expression within TECs by direct cellular contact.

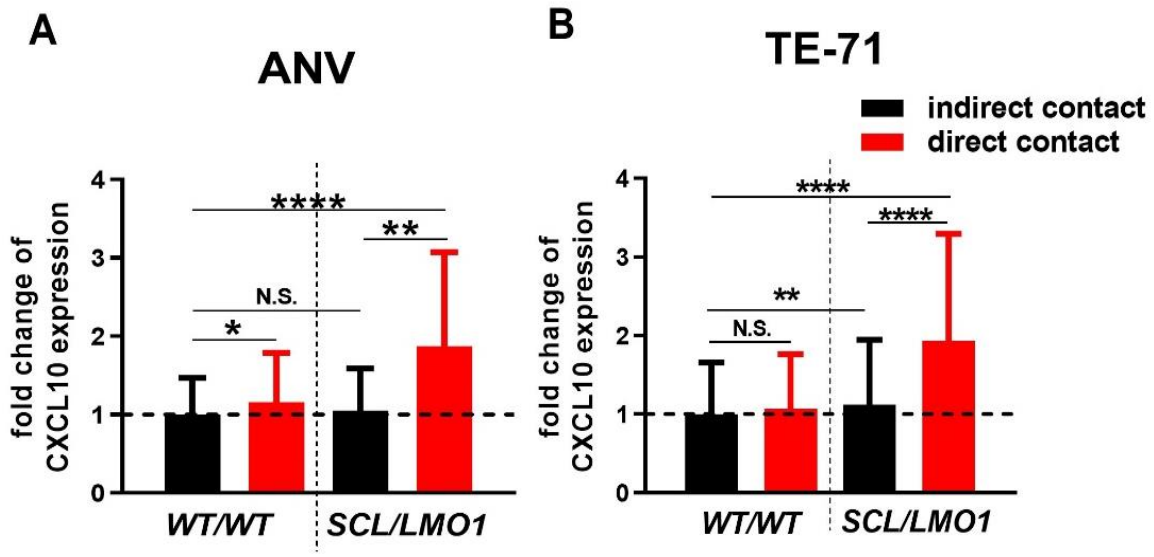

Figure 40. *SCL/LMO1* cells induce CXCL10 expression in TEC cell lines.

Expression levels of CXCL10 analyzed in TEC cell lines (A) ANV and (B) TE-71 by RT-PCR post co-cultue with *WT/WT* or *SCL/LMO1* thymocytes. The data are expressed as mean+SD from data derived from three independent wells per experimental condition. *P<0.05, **P<0.01 and ***P<0.001.

3.11.2 *SCL/LMO1* thymocytes induce CXCL10 chemokine secretion by TECs via direct cellular interaction

In order study whether *SCL/LMO1* thymocytes were also, capable of inducing CXCL10 secretion by TECs, we measured the CXCL10 in the co-culture supernatants by ELISA. Indeed, levels of CXCL10 protein were significantly increased in the supernatants from direct co-cultures between preleukemic *SCL/LMO1* cells and TEC cell lines **(Fig. 41AB).** This finding demonstrates that direct cell-to-cell contact between preleukemic thymocytes and TECs induces the secretion of CXCL10 by TECs.

3.11.3 INFγ and IL1β expression by *SCL/LMO1* is not responsible for TEC CXCL10 induction

Others have shown that interferon-γ (IFNγ) and interleukin-1β (IL1β) is capable of inducing CXCL10 expression in human intestinal epithelial cells.[93] Therefore, we examined if

SCL/LMO1 thymocytes express higher levels of IFNγ and IL1β than *WT/WT* thymocytes. High *SCL/LMO1* IFNγ and IL1β expression could then be responsible for CXCL10 secretion by TECs. However, IFNγ and IL1β expression levels within *WT/WT* and *SCL/LMO1* thymocytes did not differ significantly **(Fig. 42)**. Hence, it is unlikely that IFNγ and IL1β produced by *SCL/LMO1* thymocytes is responsible for the CXCL10 induction within TECs.

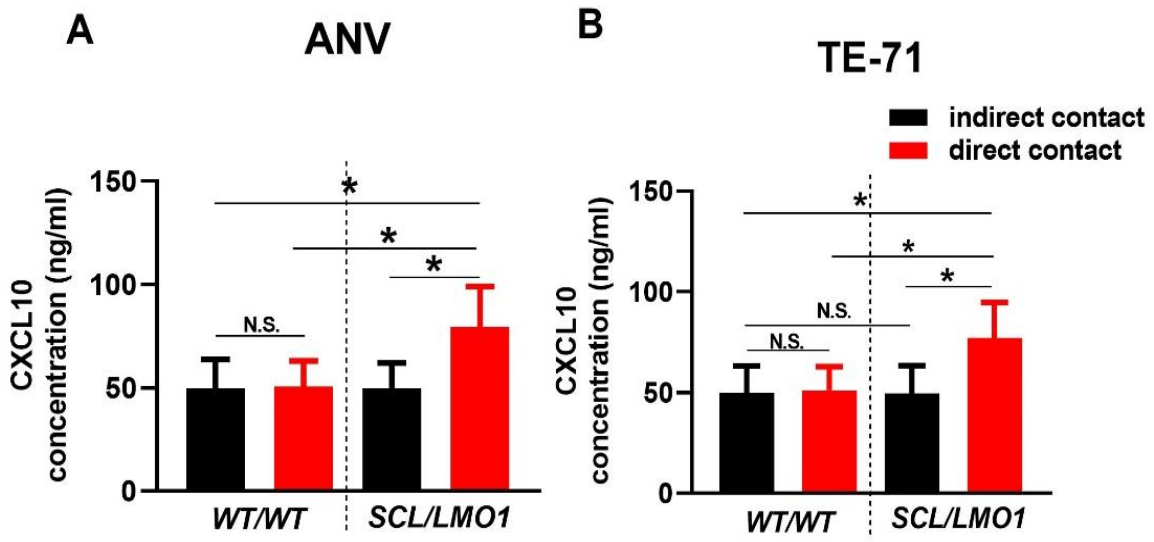

Figure 41. Supernatant CXCL10 chemokine levels after co-cultures between *WT/WT* or *SCL/LMO1* thymocytes and TEC cell lines.

Bar graphs showing CXCL10 protein concentrations determined in the supernatants from direct contact (cell to cell) and indirect contact (through transwell) co-culture systems between thymocytes (*WT/WT* or *SCL/LMO1*) and TEC cell lines (ANV or TE-71) by ELISA. The data are expressed as mean+SD from data derived from three independent wells per experimental condition. *P<0.05, N.S. = not significant.

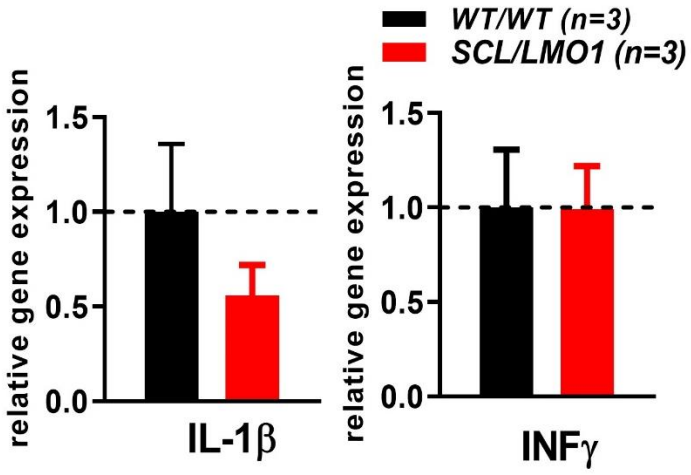

Figure 42. IFN-γ and IL1β expression by *WT/WT* and *SCL/LMO1* thymocytes.

INFγ and IL-1β expression were analyzed by real-time PCR in *WT/WT* and *SCL/LMO1* mice. The data are expressed as mean+SD derived from n=3 mice per genotype. Target mRNA was normalized against the expression of Hprt-mRNA. N.S= not significant.

3.12 CXCR3 expressed by *SCL/LMO1* thymocytes during leukemogenesis

We have demonstrated that preleukemic thymocytes induce CXCL10 within TECs by direct interaction. Moreover, we demonstrated increased CXCL10 chemokine levels in the preleukemic thymic microenvironment. To now test whether there is the possibility of TEC-derived CXCL10 feeding back to preleukemic thymocytes, we determined if preleukemic thymocytes express the CXCL10 receptor CXCR3. We performed flow cytometric analysis of thymocyte CXCR3 expressions by *SCL/LMO1* and *WT/WT* mice. This analysis revealed that the proportion, as well as the absolute number of CXCR3 expressing thymocytes, was significantly increased in *SCL/LMO1* compared to *WT/WT* mice (**Fig.43 AB).**

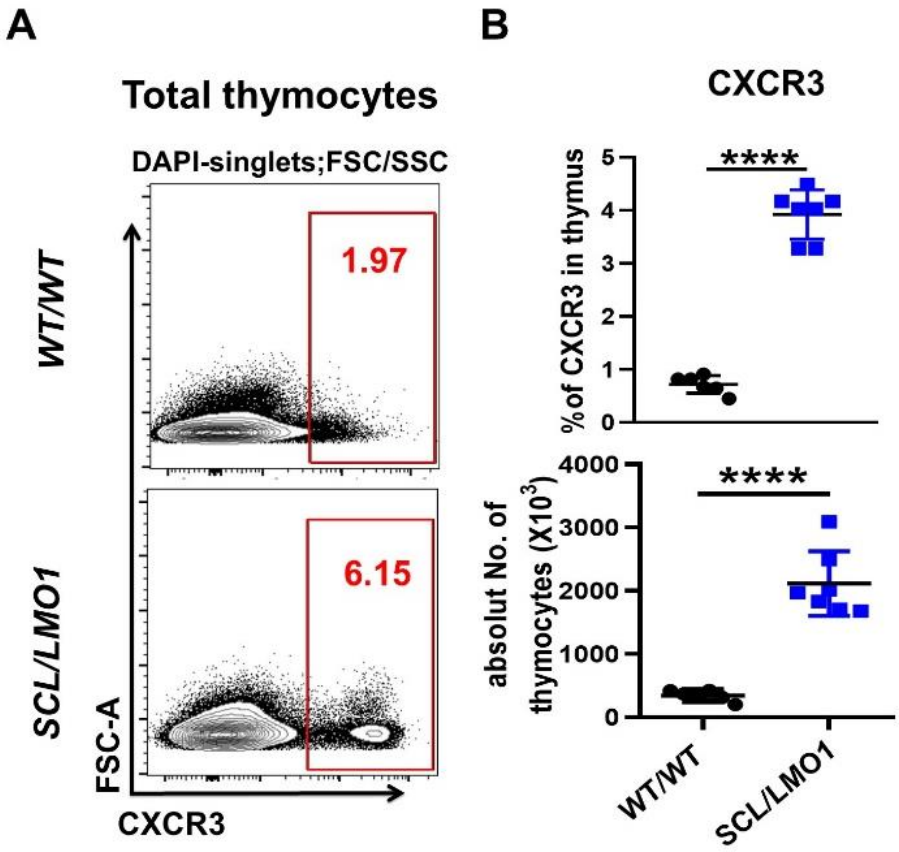

Figure 43. CXCR3 expression in *SCL/LMO1* thymus.

Gating strategy (A) and the total number of thymocytes (B) stained with anti-CXCR3 antibody and measured by flow cytometry in *SCL/LMO1* and *WT/WT* mice. Cells were gated on CXCR3 positive fraction. The data are expressed as mean ±SD from three independent experiments. ****P<0.0001

SCL/LMO1 mice had four times more CXCR3 expressing cells within their thymus **(Fig. 43B).** We have shown that the preleukemic thymus is characterized by accumulating abnormal TCRβ^{intm} thymocytes **(Fig. 19)**. Thus, we analyzed if these TCRβ^{intermediate} *SCL/LMO1* cells are also characterized by CXCR3 expression. Indeed, we found that *SCL/LMO1* TCRβ^{intermediate} thymocytes were higher in their CXCR3 percentage. Moreover, the absolute number of TCRβ^{intermediate}CXCR3+ thymocytes was significantly higher in *SCL/LMO1* than in *WT/WT* thymi (**Fig. 44 AB).**

To determine whether CXCR3 upregulation was specifically prominent in certain *SCL/LMO1* T cell developmental subset, we analyzed the CXCR3 expression in thymic DN, DP, CD4SP, and CD8SP subsets using flow cytometry. We observed throughout all subsets that the CXCR3 fraction was higher in *SCL/LMO1* than in *WT/WT* mice **(Fig. 45 A**). The absolute number of CXCR3+ DN cells was significantly higher in *SCL/LMO1* mice compared to control mice **(Fig. 45 B).** Taken together, these results indicated that immature T cells in preleukemic mice show a significantly higher proportion of CXCR3-expressing cells. These increased number of CXCR3-expressing thymocytes might well be responding to the increased CXCL10 ligand concentration within the *SCL/LMO1* thymus.

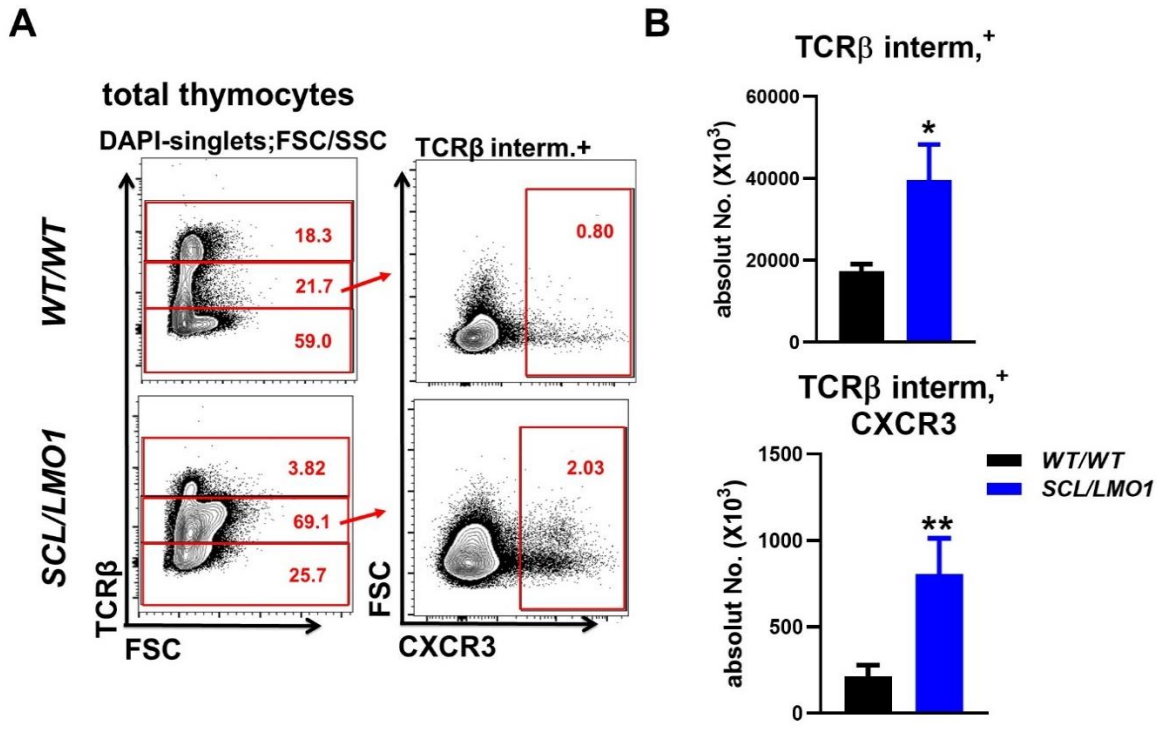

Figure 44. CXCR3 expressing TCRβ^{intermediate} cells within the *SCL/LMO1* thymus.

(A) FACS plots showing the gating strategy of thymocytes from *SCL/LMO1* and *WT/WT* mice stained with anti-TCRβ and CXCR3 antibodies. (B) Quantification of absolute numbers of TCRβ^{intermediate} (upper panel) and TCRβ^{intermediate}CXCR3+ cells. The data are expressed as mean+SD from three independent mice per genotype. **P*<0.05, and ***P*<0.01.

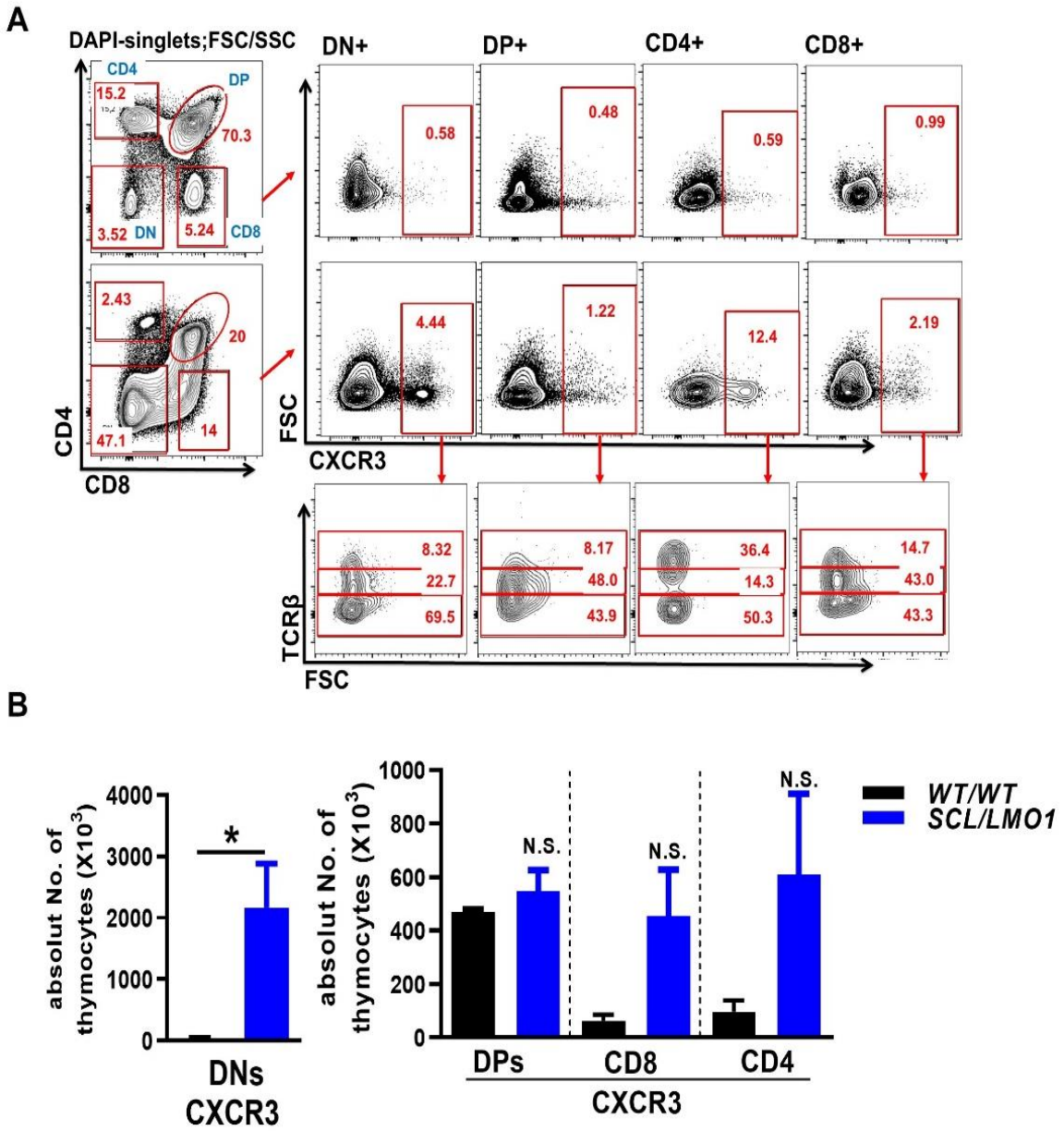

Figure 45. CXCR3-expression throughout T cell developmental stages.

(A) FACS plots showing the gating strategy of thymocytes stained with anti-CXCR3, TCRβ, CD4, and CD8 antibodies. CXCR3 expression was analyzed on DN, DP, CD4SP, and CD8SP sub-populations. CXCR3+ cells were further gated for their expression of TCRβ. (B) Bar diagrams depicting the absolute number of CXCR3+ cells within different sub-populations of thymocytes in *SCL/LMO1* and *WT/WT* mice. The data are expressed as mean+SD from three mice per genotype. **P*<0.05, N.S= not significant.

3.13 CXCL10/CXCR3 signaling induces cell survival and activates NOTCH1 signaling

We have shown that preleukemic T-ALL thymocytes induce TEC CXCL10 expression by direct interaction *in vitro*. In concordance with these data, the CXCL10 thymic concentration and numbers of thymocytes expressing the CXCL10 receptor CXCR3 are increased in *SCL/LMO1* thymi. These data pointed at a role for TEC-derived CXCL10 in promoting T-ALL leukemogenesis via CXCR3.[115] To study this hypothesis, we studied the impact of increasing CXCL10 concentrations on *SCL/LMO1* thymocytes *in vitro*. We isolated primary thymocytes from *SCL/LMO1* transgenic mice and cultured these cells in the presence of recombinant CXCL10. Eight hours post incubation we analyzed the thymocytes by flow cytometry.

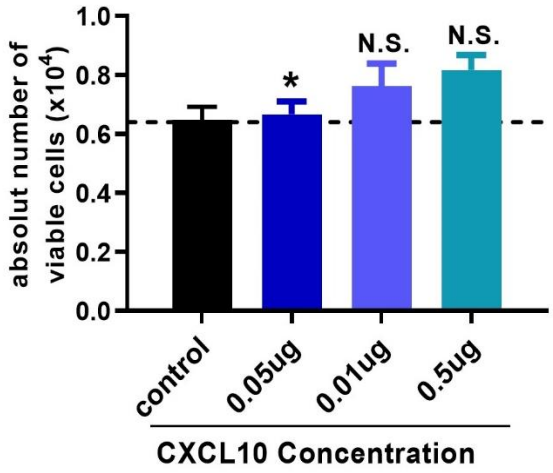

Figure 46. Recombinant CXCL10 induces cell survival of *SCL/LMO1* thymocytes *in vitro*.

Bar diagram showing fold change in the number of viable cells from *SCL/LMO1* thymocytes upon culture with recombinant CXCL10 at indicated concentrations. The data are expressed as mean +SD derived from n=3 *SCL/LMO1* mice. **P*<0.05; N.S. = not significant.

3.13.1 The chemokine CXCL10 supports the survival of *SCL/LMO1* cells *in vitro*

First, we analyze the effect of recombinant CXCL10 on the viability of *SCL/LMO1* thymocytes in culture. We found that there supplying exogenous CXCL10 resulted in an increase *in vitro* viability of *SCL/LMO1* cells compared to cells cultured without CXCL10 **(Fig 46).** Additionally, the apoptosis rate of cells was measured by Annexin-V / DAPI staining by flow cytometry. Cultured *SCL/LMO1* cells were stained with Annexin-V and

DAPI to measure the rate of apoptosis in T-ALL cells. A decrease of apoptosis in cells that were cultured in the presence of recombinant CXCL10 was noted. The absolute number of dead (Annexin-V+ DAPI+) cells was significantly reduced when T-ALL cells were cultured in the presence of CXCL10.

Similarly, the proportion of early apoptosis cells (Annexin V +, DAPI -) was also reduced in the presence of CXCL10 **(Fig. 47A).** The survival rate of *SCL/LMO1* cells was significantly increased, and apoptosis decreased with an increasing concentration of CXCL10 in culture **(Fig. 47B).**

3.13.2 Recombinant CXCL10 enhances NOTCH1 signaling within *SCL/LMO1* cells

As the above results clearly show that CXCL10 affects survival, we now investigated whether CXCL10 chemokine alters NOTCH1 signaling in *SCL/LMO1* thymocytes. For this purpose, we followed similar culture conditions, as described previously (3.13). Twenty-four hours post culture with CXCL10 the T-ALL were harvested and subject to expression analysis of NOTCH1 and Notch target genes by real-time PCR. We found that CXCL10 treatment showed a significant increase in the expression of NOTCH1 and NOTCH1 targeting genes HES1 and DTX1.

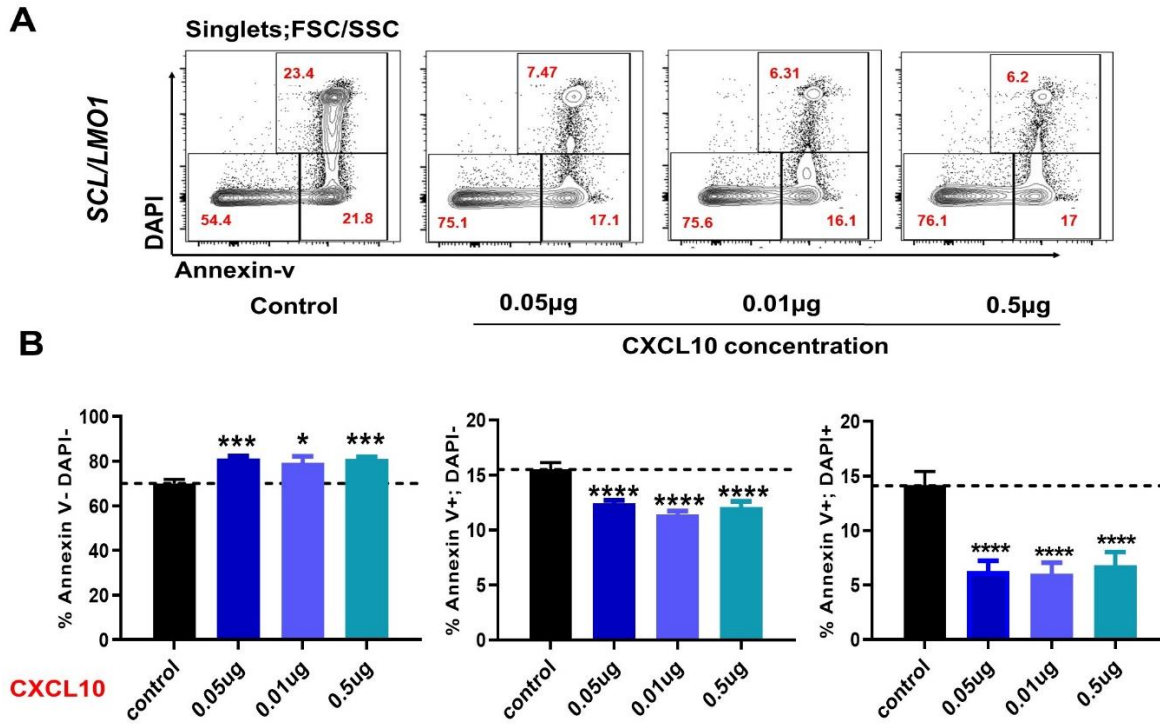

Figure 47. Recombinant CXCL10 decreases the *in vitro* apoptosis rate of *SCL/LMO1* cells.

SCL/LMO1 leukemia cells were cultured with recombinant CXCL10 at indicated concentrations. (A) FACS plots showing the survival of *SCL/LMO1* leukemia cells assessed by Annexin-V and DAPI staining. (B) Bar diagram showing the proportion of cells assessed with the Annexin V assay. Graphs were showing dead Annexin V+, DAPI+, apoptotic Annexin V+, DAPI- and viable annexin V-, DAPI- populations following treatment with recombinant CXCL10. The data are expressed as mean+SD from n=3 *SCL/LMO1* mice. *P<0.05, **P<0.01 and ***P<0.001.

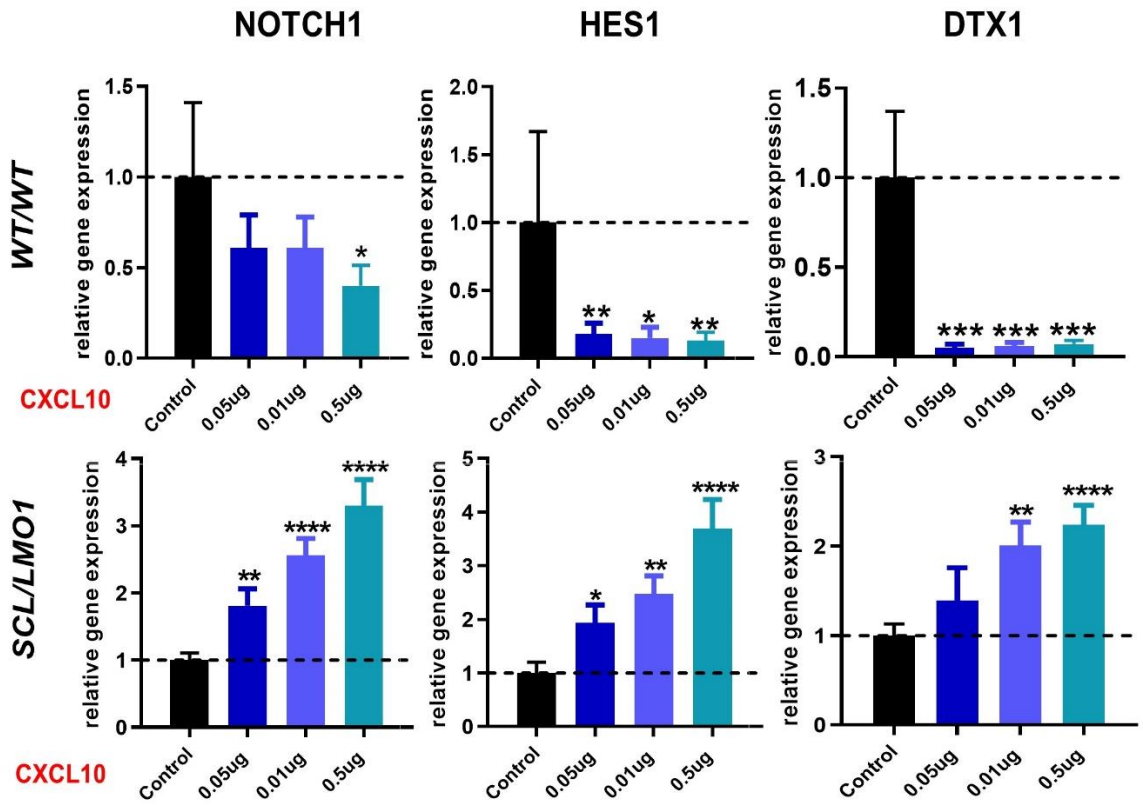

Figure 48. Recombinant CXCL10 increases the expression of NOTCH1 and downstream targeting gene in *SCL/LMO1* mice.

Bar diagram showing NOTCH1 and downstream targeting gene (HES1 and DTX1) expression of cells from *SCL/LMO1* thymocytes upon culture with recombinant CXCL10 at indicated concentrations. The data are expressed as mean ±SD from three independent experiments. *p<0.05, **p<0.01 and ***p<0.001.

Strikingly, incubation with CXCL10 downregulated the expression of NOTCH target genes in *WT/WT* cells **(Fig. 48)**. This result suggests that CXCR3-CXCL10 interaction upregulates NOTCH signaling in *SCL/LMO1* cells.

3.14 Human T-ALL cell lines activate the NOTCH1 signaling pathway upon CXCL10 exposure

Because of our previous results implying a role for the CXCR3/CXCL10 axis in controlling cell survival and NOTCH1 signaling of preleukemic thymocytes, we now studied this axis in human T-ALL. To uncover the involvement of CXCL10/CXCR3 axis in human T-ALL we first determined the expression of CXCR3 on different human T-ALL cell lines.

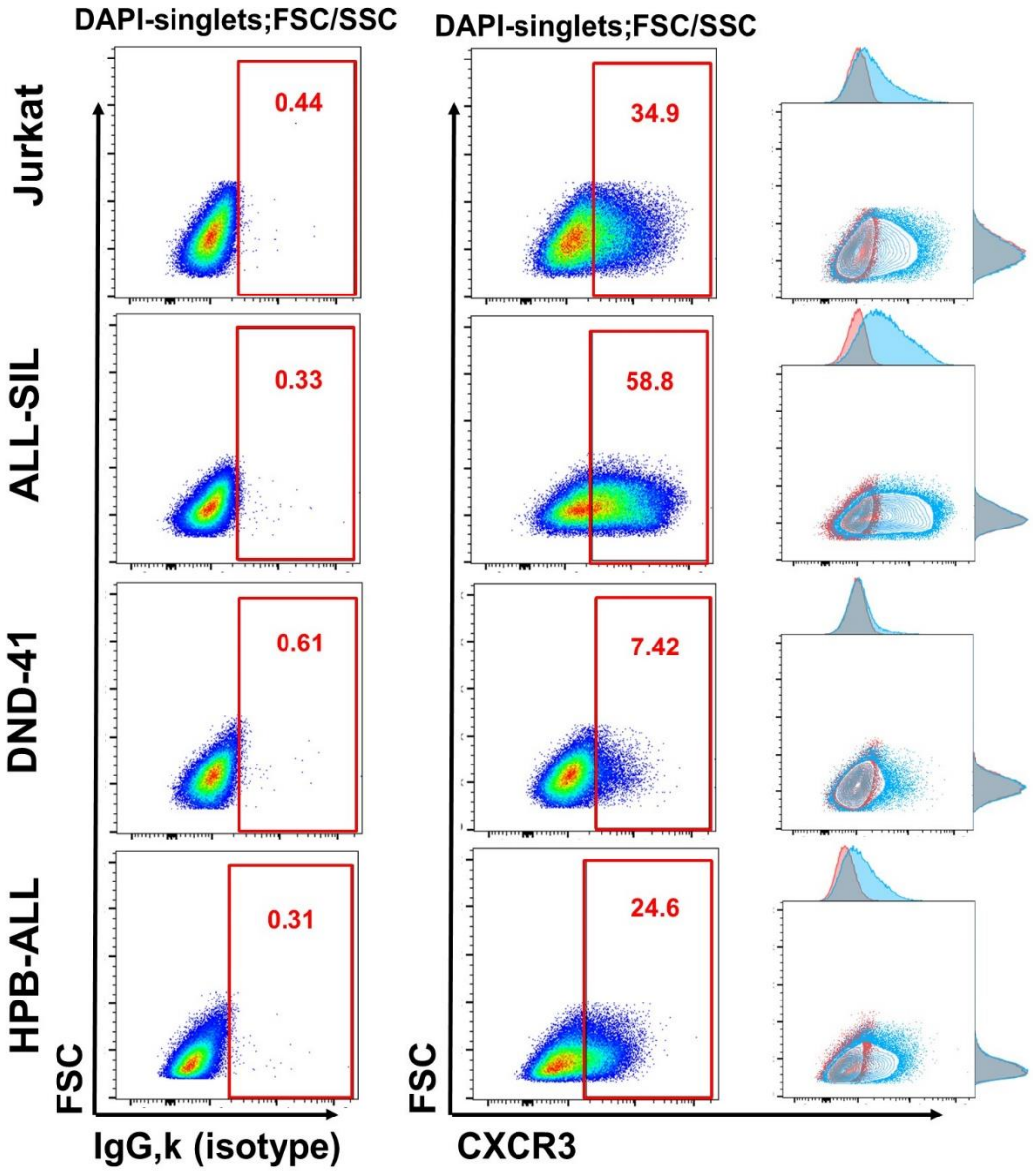

Figure 49. Human T-ALL cell lines express the CXCR3 receptor.

FACS blot showing the gating strategy of CXCR3 cell-surface expression on Jurkat, ALL-SIL, DND-41, and HPB-ALL cell lines analyzed by FACS with anti –CXCR3 antibody (blue line) and control IgG isotype antibody (red line).

3.14.1 CXCR3 is expressed by human T-ALL cell lines

First, we checked the surface expression of CXCR3 on the human T-ALL cell lines Jurkat, ALL-SIL, DND-41, and HPB-ALL. Subfractions of all human T-ALL cell lines were positive for the expression of CXCR3. Among all cell lines tested, the ALL-SIL cell line showed more than 50% of cells expressing CXCR3. Jurkat and HPB-ALL showed 25 to 35%, and DND-41 cells exhibited a relatively low proportion of cells (around 8%) expressing CXCR3. These results indicate that in addition to preleukemic murine thymocytes, human T-ALL cells also express CXCR3 **(Fig. 49).**

3.14.2 NOTCH signaling pathway analysis in human T-ALL cell lines after *in vitro* incubation with CXCL10

Furthermore, we analyzed the NOTCH signaling pathway in human T-ALL cell lines (Jurkat, ALL-SIL, DND-41, and HPB-ALL) when cultured in the presence of recombinant CXCL10 at different concentrations for 48 hours. We analyzed the expression of NOTCH1 and downstream target genes such as HES1 and DTX1 by real-time PCR. We found that the expression of NOTCH1, HES1, and DTX1 was significantly upregulated in Jurkat and ALL-SIL cell lines. The degree of NOTCH1 pathway activation correlated with the concentration of recombinant CXCL10 in the culture. The expression of NOTCH1, HES1, and DTX1 was not significantly altered in HPB-ALL and DND-41 cell lines **(Fig. 50).** These results indicated that the CXCL10/CXCR3 axis regulates the NOTCH signaling pathway also in overt human T-ALL. These data imply that the CXCL10/CXCR3 axis data acquired in the preleukemic murine T-ALL setting might also be valid in overt human T-ALL.

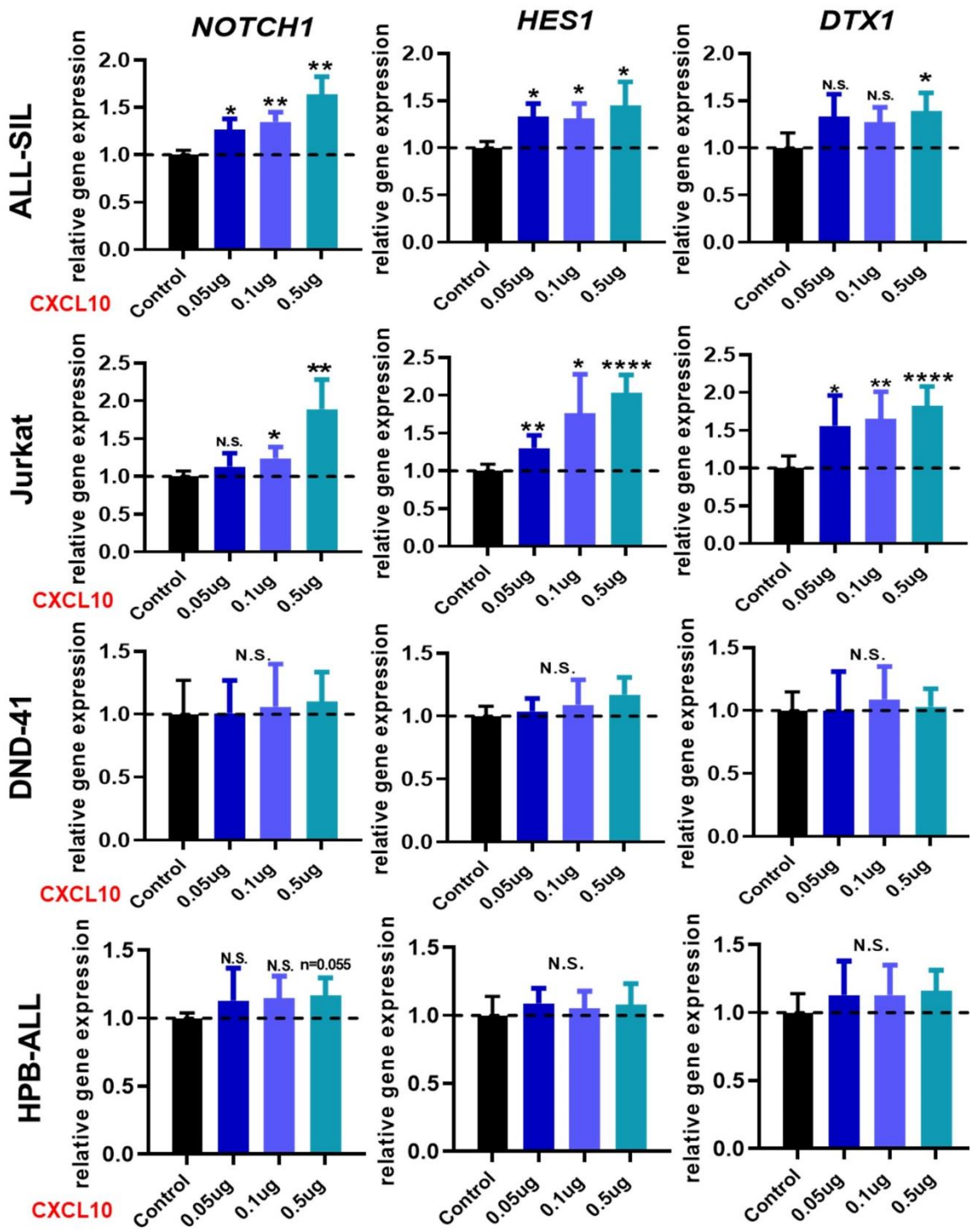

Figure 50. *In vitro* recombinant CXCL10 increases the expression of NOTCH1 and downstream target genes in Jurkat and ALL-SIL human T-ALL cell lines.

Bar diagrams showing NOTCH1 and downstream target gene (HES1 and DTX1) expression of human T-ALL cell lines (Jurkat, ALL-SIL, DND-41, and HPB-ALL) in culture with recombinant CXCL10 at indicated concentrations. means+SD are displayed. The data were derived from three independent wells per experimental condition. The statistical significance was calculated versus the control without added CXCL10. *p<0.05, **p<0.01 and ***p<0.001.

CHAPTER-4

DISCUSSION

4 DISCUSSION

T-ALL arises in the thymus, where the development of T-cells occurs, and it propagates via the blood to the rest of the body. The thymus contains stromal cells, mainly consisting of a functionally central cellular component, the thymic epithelial cells (TECs). TECs fulfill an essential function in regulating T cell development and thymocyte migration via the expression of NOTCH membrane ligands (DLL4), cytokines [e.g., interleukin-7 (IL-7)], stem cell factor (SCF) and chemokines (e.g., CXCL12 and CCL25). [11, 30, 33] The infiltration of leukemic T cells in peripheral organs is one of the most crucial causes of relapse and is correlated with a poor prognosis in patients with T-ALL. The migration of leukemia cells via the bloodstream is essential to invade target organs. The mechanisms by which normal T-cells migrate to the periphery are well understood, but the mechanism by which leukemic T-cells migrate to peripheral organs remains unclear. However, the interactions of malignant cells with the cellular microenvironment via chemokines, interferons, and Notch signaling play a critical role in malignant cell survival, migration and invasion. In the present study, we identified various cellular alterations within the thymic microenvironment, which are associated with the development and progression of *SCL/LMO1* T-ALL. Here, we aimed to delineate a previously unknown role of chemokine secreting TECs, which are crucial for the early survival and proliferation of T-ALL cells. Here, we have shown that cellular crosstalk via CXCL10/CXCR3 signaling between developing leukemia cells and TECs contributes to the survival of leukemic T cells, particularly by regulating NOTCH1 signaling in T-ALL cells.

In the work of Triplett, T.A. *et al*. was shown that the thymic epithelium is gradually lost, expanding epithelial free regions in LN3 T-ALL mice.[116] Additionally, they demonstrated that primary human T-cell blasts require a stromal derived signal to survive and proliferate. [116] These data already suggested that T-ALL influences thymic structure and TECs. However, in the LN3 T-ALL mouse, model endogenous TCRα/β loci are pre-rearranged, and therefore normal T cell development is perturbed beginning at early embryonic stages. As all developing T cells are monoclonal normal selection checkpoints, do not have to be passed by developing T cells. Therefore, we decided to study the role of thymic epithelial cells in the *SCL/LMO1* mouse model in which steps of human T-ALL development are reproduced. [1] *SCL/LMO1* double transgenic mice developed T-ALL within 2 to 3 months with large mediastinal thymic tumors and significant infiltration of leukemic cells in the bone marrow. T-ALL formation in the double transgenic *SCL/LMO1* model was no longer

tamoxifen-dependent, as a small amount of SCL entering the nucleus in the absence of tamoxifen is presumably sufficient to induce T-ALL together with *LMO1*. Furthermore, our data indicate that leukemogenesis caused by the *SCL* and *LMO1* oncogenes results in increased in thymic cellularity. It was shown that NOTCH1 mutations are common in human T-ALL and were also demonstrated to occur in *SCL/LMO1* transgenic mice by others. [108, 109] In addition, we showed that upregulated NOTCH1 expression in *SCL/LMO1* lymphocytes per se increased gene expression of HES1 and DTX1 suggesting direct NOTCH1 pathway activation by the aberrant expression of the transcription factors *SCL* and *LMO1*.

The characterization of thymic epithelial cell lines

The cortical and medullary thymic epithelial cell lines ANV and TE-71 used in our experiments were initially obtained from Andrew G. Farr, University of Washington, WA, USA. The ANV cell line is derived from the thymus epithelium of the k14 E6/E7 transgenic hyperplastic thymus and has the properties of cTECs.[100] The TE-71 cell line was derived from enzymatically dissociated murine thymus stroma and exhibited medullary TEC characteristics. These include the expression of mTEC-specific keratins and ER-TR5 as well as the ability to agglutinate UEA.[101] To confirm this, we first examined the cell lines for their TEC characteristics. As expected, positive expression of EpCAM and UEA was found in TE-71 cells and although the potential to bind BP1 was low, this confirmed the cortical origin of ANV cells. The distinct TE-71 and ANV specific expressions of EpCAM were compatible with a comparatively strong adhesion behavior in cell culture. We observed reduced expression of MHC class II molecules in both ANV and TE71 cell lines.

We are not aware of studies, which investigated the expression of T cell development-promoting factors in the cortical or medullary cell lines ANV and TE71, respectively. Therefore, here we compared the expression of T-cell supportive factors such as DLL4, CXCL12, IL-7, IL-18, and IGF-1 between thymic epithelial cell lines (ANV and TE71) and a stromal (OP9) cell line. Our results showed that ANV cells expressed significantly higher levels of factors essential for T cell development compared to TE-71 cells. Additionally, the ANV cortical TEC cell line showed high expression of DLL4 as well as the interleukins IL-7 and IL-18, and protein-coding gene Patched 2 (PTCH2) involved in the Hedgehog signaling pathway illustrating the characteristics of cortical TECs (cTEC).

Role of the thymic microenvironment/stroma in T-ALL development

Previous studies have shown that primary human T-cell blasts require a stromal-derived signal from healthy human thymic epithelial cells and T-ALL-LN3 mice epithelial cells to survive and proliferate. However, these studies primarily showed that this thymic epithelial cell-derived signal operates via IL7 and IGF1R, respectively.[116, 117] Thymic epithelial cells which are susceptible to the growth of T-ALL, lacking exogenous cytokines, have not yet been identified. In this study, utilizing an *in vitro* system, we demonstrated the ability of monolayer TEC cell lines (ANV and TE71) to regulate the survival of leukemic T cells comparable to the standard OP9 culture system. We found that the *in vitro* microenvironment created by the interaction of ANV and TE71 TEC cell lines with murine T-ALL cells promoted survival and proliferation.

SCL and LMO1 inhibit normal T-cell differentiation in T-ALL

Others previously investigated pre-leukemic T-cell development of *SCL/LMO1* mice. [109, 118, 119] These results were acquired with *SCL* and *LMO1* transgenic mouse thymocytes. In these studies, SCL-transgenic mice showed neither T-cell abnormalities nor clonality at the age of 4-12 weeks. In addition, single LMO1-transgenic mice were also devoid of abnormalities and clonality at the age of 4 weeks, and rarely showed evidence of clonal propagation at the age of 12 weeks. [119] In line with these findings, Chervinsky DS. *et al.* showed that *SCL/LMO1*/Scid mice had increased thymic cellularity and a comparative deceleration of $CD4^{-}$ $CD8^{-}$ to $CD4^{+}CD8^{+}$ cell transition. These data suggested that TCRβ gene rearrangements might be required for the oncogenic potential of *SCL* and *LMO1* to unfold.[118]

Here, we described reproducible findings of T cell developmental data obtained in *SCL/LMO1* mice. We showed that the oncogenic activity of the *SCL* and *LMO1* transcription factors leads to an increase in the cellularity of the ETP (DN1) cell population in young mice. Our results further showed a significant increase in the T cell developmental DN stage. Mostly, the cells were accumulated at the DN4 stage of T lymphocyte development. In contrast, the number of DP cells was significantly reduced. Taken together, these results indicate that *SCL* and *LMO1* block the differentiation between DN and DP stages of thymocyte development. As a result, the cells further accumulated at the DN stage and thus probably promoting to the occurrence of further mutations. The significant reduction of mature CD4+ and CD8+ T cell in the thymus is indirect evidence of the disturbances of

thymus function and architecture. Therefore, this significant decrease of other thymocyte subpopulations indicated dysfunction of T cell development occurring in the *SCL/LMO1* thymus.

In the initial phases of T cell development, thymocytes pass through phases that are decisively dependent on NOTCH signaling. Finally, at the terminal maturation stages, the cells become autonomous. It is well established that the immature to mature transition of thymocytes depends on NOTCH signaling.[110] Based on these findings, we investigated NOTCH1 expression of cells in transition between DN and DP stages. Here, the transgenic expression of *SCL* and *LMO1* led to the upregulation of NOTCH1. However, our data in *SCL/LMO1* mice suggested that upregulated NOTCH1 in immature thymocytes induced a block in thymocyte differentiation.

Alterations of thymic epithelial cells in *SCL/LMO1* mice

The activation of the NOTCH1 signaling pathway not only increases the proliferation and survival of normal T cell progenitors but also that of the T lymphoblasts.[120] Therefore, we postulated that at least in the early phase of leukemogenesis DLL4 expressing TECs are of central importance for the establishment of T-ALL. Consequently, we investigated the TEC populations in pre-leukemic *SCL/LMO1* mice, and we found various thymic microenvironment cellular alterations, which were associated with the development and progression of thymic lymphoma. These were associated with the loss of a defined cortico-medullary junction and increased with the disruption of the thymic lobes. Interestingly, immunohistological analysis of thymus sections revealed that in *SCL/LMO* transgenic mice, the cortico-medullary junction was increasingly blurred. This phenomenon was accompanied by a dramatic decrease in medullary regions and expansion of the cortical region in at preleukemic stages followed by the development of distinctive epithelial-negative regions. The observation of distinctive epithelial-negative regions were also shown in T-ALL leukemia in other mouse models such as LN3 and AKR/J (H-2k).[116, 121]

Furthermore, we investigated the TECs subpopulations cortical and medullary thymic epithelial cells (cTECs and mTECs, respectively) in *SCL/LMO1* transgenic mice. We observed a dispersed medullary architecture and reduced numbers of UEA+MHCIIhi mTECs during progressing T-leukemogenesis. MHC molecules on the surface of mTECs are required for efficient negative selection of thymocytes expressing potentially autoreactive TCRs. Our results show reduced mature mTEC numbers, which may contribute

to a defective negative selection process. In contrast, the cortical architecture expanded and an increased number of BP1+ MHCIIhi cTECs in early T-ALL development were observed. Given the NOTCH-ligand expression by cTECs, this finding indicated that the expanded cTECs compartment might be involved in increasing the NOTCH1 signal in developing leukemia. Maturation of cTECs requires cellular and molecular interactions with early thymocytes (**Fig. 51**).[30] Thus, expanded cTECs might well be functionally constrained by the disturbed *SCL/LMO1* thymocyte differentiation. Moreover, the loss of interactions with normal mature thymocytes might have an inhibitory effect on the development of the mTECs in *SCL/LMO1* mice. Previously, it was reported that TGFβ signaling negatively modulates the mTEC populations in the thymus.[122] As we demonstrated upregulated TGFβ expression by *SCL/LMO1* TECs, this might have resulted in the reduction of mTEC numbers during progressing leukemogenesis. During the progression of leukemia total TEC numbers decreased, which was mainly due to the reduction of the mTEC subpopulation. On the other hand, there was a trend towards increasing mesenchymal (EpCAM- CD45- Ly51+) cells with progressing leukemogenesis. A previous study has confirmed the mesenchymal nature of thymic Ly51+ EpCAM- CD45- CD31- cells by their expression of the mesenchymal marker PDGFRβ.[28]

Mesenchymal cells during *SCL/LMO1* leukemogenesis

As TEC numbers decreased, we were hypothesizing that thymic fibroblast-like cells might expand and take over the T-ALL-supporting role of previously expanded cTECs. Studying other cell types besides TECs, we discovered an expanding CD31-positive vascular network within the thymus. Perivascular areas stained positive with the thymic mesenchymal marker ER-TR7. However, there was no vascular-independent ERTR7-staining areas observed. This finding suggests that ERTR7-positive mesenchymal cells possibly represent pericytes, which might have a role in supporting angiogenesis or stabilizing newly generated vasculature. However, the anatomic location of ERTR7-positive cells did not suggest that these cells fulfill a key T-ALL supporting function even though the proliferation of supportive stromal fibroblasts is frequently linked to cancer progression. [123] Thus, it remains possible that Sirpα-positive DCs reported by Triplett T.A. *et al*.[116] support leukemic T cell survival by IGF-1 and PDGF (platelet-derived growth factor) also during *SCL/LMO1* lymphomagenesis.

During the oncological process, epithelial-mesenchymal transition (EMT) transmits migratory and invasive properties to epithelial cancer cells that are mediated by transcriptional proteins that suppress the cell-cell adhesion molecule E-cadherin in multiple invasive carcinomas.[124] EMT is induced in cancer cells by various highly conserved signaling pathways involved in embryonic development. TGFβ and NOTCH signaling induce direct transcriptional regulators of E-cadherin, including snail/mouth and twist.[124, 125] Reports indicate that the NOTCH dependent up-regulation of TGFβ expression mediates induction of EMT through the NOTCH signaling pathway.[126] We hypothesized that in *SCL/LMO1* leukemogenesis TECs, representing unusual epithelial cells without a clear lumen or surface confining function, might transdifferentiate into mesenchymal cells by an EMT-like process as we found upregulated NOTCH1-expression on sorted thymic *SCL/LMO1* Ly51+ mesenchymal cells and *SCL/LMO1* thymocytes providing increased TGFβ expression. To further gain insights into possible EMT-like transdifferentiation of T-ALL, we investigated the epithelial markers E-cadherin and Pan C-K expression by immunofluorescence. Our results showed that epithelial markers were expressed at an early age (4 weeks) however as previously observed with other TEC markers with leukemia progression E-Cadherin and Pan C-K expression levels were declining in *SCL/LMO1* thymi. However, we did not observe any vessel-independent appearance of ERTR7-positive mesenchymal-like cells. Therefore, our data argue against the transdifferentiation of TECs towards fibroblasts by an EMT-like process.

Altogether, the findings of this study argue for altered TECs playing a crucial role within the microenvironment of thymocytes situated in the transformation to T-ALL. Identification of the crucial molecular signals generated by stromal cells will not only further elucidate the mechanisms of T cell leukemogenesis but may also uncover options for novel therapies against this cancer type. Although the complex mechanisms of TEC-mediated support in T-ALL largely remain to be resolved, it is possible that the development of leukemic cells is even more sensitive than the development of normal thymocyte to changes therapeutically triggered in TECs.

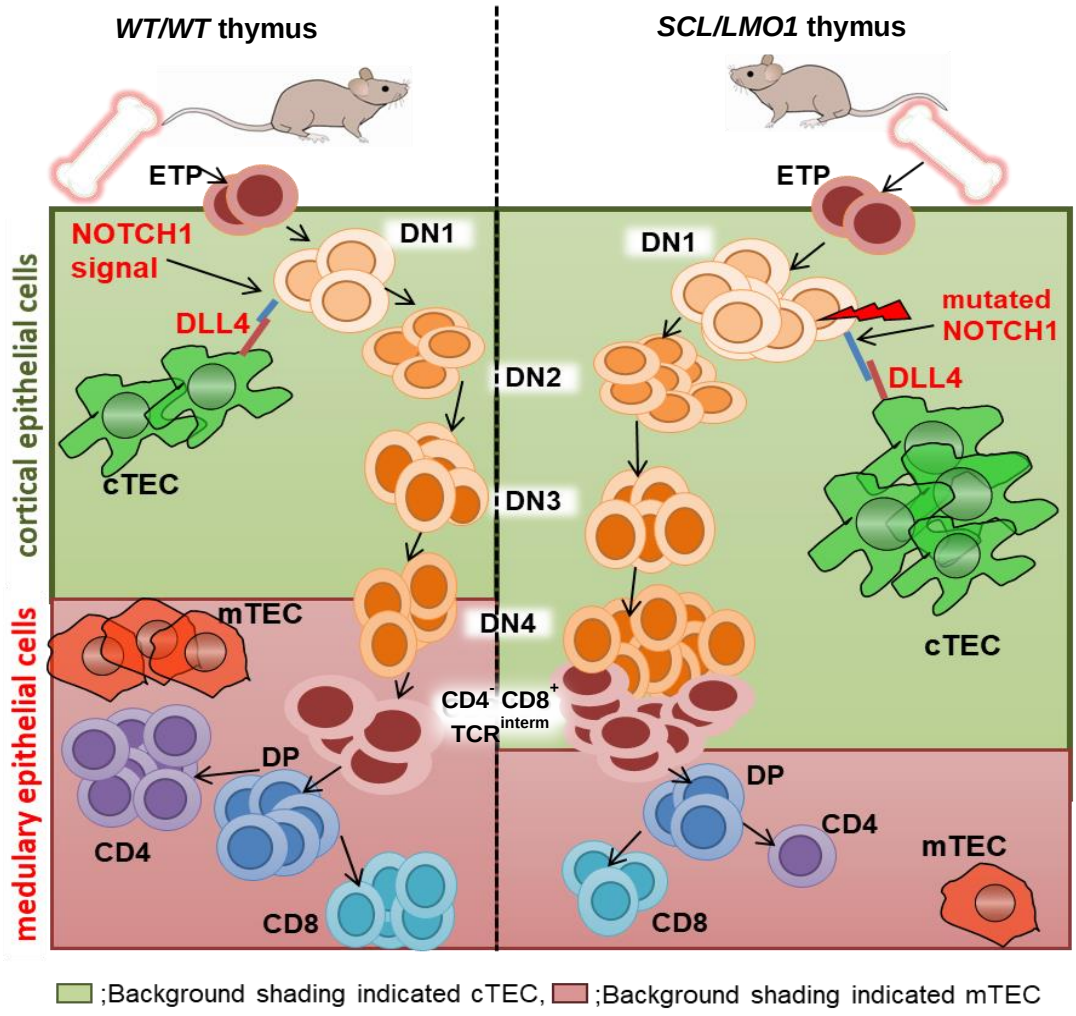

Figure 51. Altered T-cell development and thymic architecture of *SCL/LMO1* mice.

Schematic representation of the *SCL/LMO1* versus the *WT/WT* thymus. The *SCL/LMO1* thymus is dramatically larger than the *WT/WT* thymus at the leukemia stage. A dramatic decrease in *SCL/LMO1* medullary regions (red area) and expansion of the cortical region (green area) was observed. The DLL4/NOTCH1 axis is abundantly upregulated in the *SCL/LMO1* thymus. The NOTCH1-dependent thymopoiesis most likely receives an increased cTEC-derived DLL4 signal as *SCL/LMO1* TEC numbers are increased. *SCL* and *LMO1* oncogenes expand early thymic precursor (ETP)/DN1 thymocytes and block the transition between DN and DP stages of thymocyte development.

The role of TEC-derived chemokines involved in T-ALL development and maintenance

During normal T-cell development, chemokines have a key role in guiding the migration of immature lymphocytes during their thymic maturation and differentiation. Chemokines such as CCL25 and CXCL12 coupled with the expression of the corresponding chemokine receptors on thymocytes, including CXCR4 and CCR9 play a central role.[127] CXCL12 primarily attracts both double negative (DN) and double positive (DP) immature thymocytes

enhancing their migration within the cortical region.[128] In addition to promoting T cell development, cTECs are the primary source of the chemokine CCL25 and cytokines such as IL-7 and SCF.[29-31] CCL25 is crucial for the homing of lymphocyte progenitors migrating from the bone marrow to thymus.[35] However, chemokine and chemokine receptor interactions have recently also been considered essential for the development and progression of leukemogenesis. The chemokine receptors upregulated during T-ALL progression might be associated with a specific genetic alteration. Alternatively, leukemic cells could co-opt these genuinely expressed molecules to promote transformation.

In this study, we investigated the cytokine and chemokine gene profile axis in *SCL/LMO1* sorted TECs cells. Here, we found that leukemic thymic epithelial cells expressed high levels of chemokines and cytokines such as CCL25, CXCL12, CCL2, IL-1b, and CXCL10. Additionally, we have shown that the increased TEC chemokine expression was mainly derived from cTECs in the T-ALL leukemic *SCL/LMO1* mouse model.

Indeed, there are previously recognized roles of CXCL12, CCL25, and CCL2 within T-ALL.[114, 129, 130] The CXCR4/CXCL12 axis is one of the most studied chemokine/ receptors in metastasis. CXCR4 is commonly expressed in hematologic malignancies and acute lymphocytic leukemia. [131-133] Vascular endothelial cells in T-ALL showed an increase in the expression of ligand CXCL12, which was crucial in controlling T-ALL maintenance.[114] The effect of CXCL12/CXCR4-mediated signaling on the Notch pathway has been demonstrated in the migration and growth of ovarian cancer cells.[134] Additionally, Hu *et al*. showed that the CXCL12/CXCR4 axis promotes epithelial to mesenchymal transition (EMT) in colorectal cancer and facilitates progression by activating Wnt/β-catenin signaling. [135] Similarly, it was shown that CCR9/CCL25 axis induces metastasis in MOLT4 cells via the RhoA-ROCK-MLC signaling cascade.[129] CCL2, along with its receptor CCR4, is important for the homeostasis of immune cells but is also involved in T-cell acute lymphoblastic leukemia and Hodgkin's lymphomas.[136] Bai M et al. also demonstrated a role for the expression of CXCR4 and CXCR3 in ALL relapses.[137] In pro-inflammatory environments, CXCL10 is secreted by several cells such as epithelial cells, endothelial cells, fibroblasts, and keratinocytes in response to IFN-γ and IL-1β.[138] In the normal human thymus, TEC CXCL10 expression can be induced by IFN-γ and I-TAC via their receptor CXCR3.[139] Signaling through the CXCL10/CXCR3 axis normally modulates migration, differentiation and activation of immune cells. CXCL10 produced by tumor or host cells can target CXCR3 tumor-infiltrating T cells, causing tumor

suppression.[140-142] So far there are no studies available on CXCL10 chemokine secreted by thymic epithelial cells in T-ALL leukemia. In this study, immunohistochemistry and gene expression analysis showed an upregulation of CXCL10 in *SCL/LMO1* cTECs upon cellular interaction. Strikingly, CXCL10 upregulation was also detected in the *SCL/LMO1* thymic interstitial fluid. Altogether, these results indicated that thymic epithelial cells are characterized by upregulated CXCL10 expression in *SCL/LMO1* leukemia.

Direct interaction between *SCL/LMO1* thymocytes and TECs induces TEC CXCL10 expression

Previous studies have shown that specific stimuli can induce CXCL10 expression by epithelial cells. For example, IFN-γ and IL-1β mediate activation of the CXCL10/CXCR3 axis in human intestinal epithelial cells.[93] Similarly, Boorsma et al. showed that IFN-γ secretion leads to an increase in CXCL10 expression levels by skin keratinocytes.[143] To investigate the mechanism of CXCL10 induction by aninteraction between TECs and T-ALL cells, we utilized a direct and an indirect (transwell) co-culture system of T-ALL lymphoblasts and the TEC cell lines (ANV and TE71). The experimental result demonstrated that the chemokine CXCL10 mRNA expression significantly increased in ANV and TE71 TEC cell lines when T-ALL lymphoblasts were cultured in direct cell-to-cell contact with the TEC cell lines. Furthermore, chemokine CXCL10 protein levels were also increased in the supernatants of direct contact co-cultures of T-ALL with TEC cells. Therefore, a soluble mediator secreted by the T-ALL cells was most likely not responsible for the CXCL10 induction within the TECs. Rather a T-ALL surface-bound molecule must be responsible for the TEC CXCL10 induction. However, we also studied the expression of IFN-γ and IL-1β by *SCL/LMO1* thymocytes, which were not upregulated compared to control thymocytes making it unlikely that these cytokines induced TEC CXCL10 expression. Collectively, these results demonstrated that direct cell-to-cell communication between T-ALL cells and TECs led to the increased expression of the chemokine CXCL10 by TECs.

Developing and established T-ALL blast express the CXCR3 receptor

It was shown by others that CXCR3 expression by T-ALL blasts is associated with central nervous system relapse and chemo-resistance.[115] The CXCR3 receptor is explicitly expressed on the surface of lymphocytes, monocytes, T cells, NK cells, dendritic cells, and tumor cells.[144] A recent report demonstrated CXCR3 expression on CD8+ T cells and to

a lesser extent on CD4+ T cells.[139] The results of this study showed that a sub-fraction of immature T-ALL lymphoblasts expressed the CXCR3 receptor. The expression of CXCR3 was mainly present on preleukemic immature DN and CD8+TCRβintermediate cells in transition between the DN and DP stage of development. In addition, we also observed CXCR3 expression by the human T-ALL cell lines (Jurkat, ALL-SIL, DND-41, and HPB-ALL) however, to different degrees. These data demonstrated that T-ALL cells express the CXCR3 receptor.

The CXCL10/CXCR3 axis is capable of promoting T-ALL survival

Depending on the cellular context, CXCL10 can exert differential effects on growing tumor cells. The effect can either be proliferation-promoting or -inhibiting.[145] The question of whether the CXCR3 receptor expression is regulated in a tumor-dependent cell-autonomous fashion or activated by host-derived ligands remains unclear. To better understand the biological functions of TEC-secreted CXCL10, we investigated its effects on *in vitro SCL/LMO1* thymocyte survival. Remarkably, developing T-ALL lymphoblast survival was promoted by recombinant CXCL10.

The CXCL10/CXCR3 axis induces activation of NOTCH signaling in T-ALL

Previous studies have reported that inhibition of NOTCH signaling in macrophages regulates the expression of cytokines such as CXCL10, IL6, IL12, MCP-1, and VEGFR1.[146] Qin Y et al. showed the NOTCH1 pathway in endothelial cells was capable of increasing the expression of CXCL10.[147] However, there is no evidence so far that the CXCL10/CXCR3 axis mediates NOTCH pathway activation. To investigate this in the T-ALL context, we studied the NOTCH1 target gene expression post CXCL10 exposure of *SCL/LMO1* lymphoblast and a panel of human T-ALL cell lines (Jurkat, ALL-SIL, DND-41, and HPB-ALL). Strikingly, we observed activation of the NOTCH1 pathway by CXCL10 in T-ALL cells expressing CXCR3 on a major proportion of T-ALL cells. These results indicate that the CXCL10/ CXCR3 axis regulates the NOTCH signaling pathway in T-ALL. In summary, our data argue for a model of T-ALL where direct cell-to-cell communication between T-ALL cells and TECs induces secretion of the chemokine CXCL10. CXCL10 then feeds back to CXCR3 receptor expressing leukemic cells resulting in NOTCH1 pathway activation and increased survival (**Fig.52**).

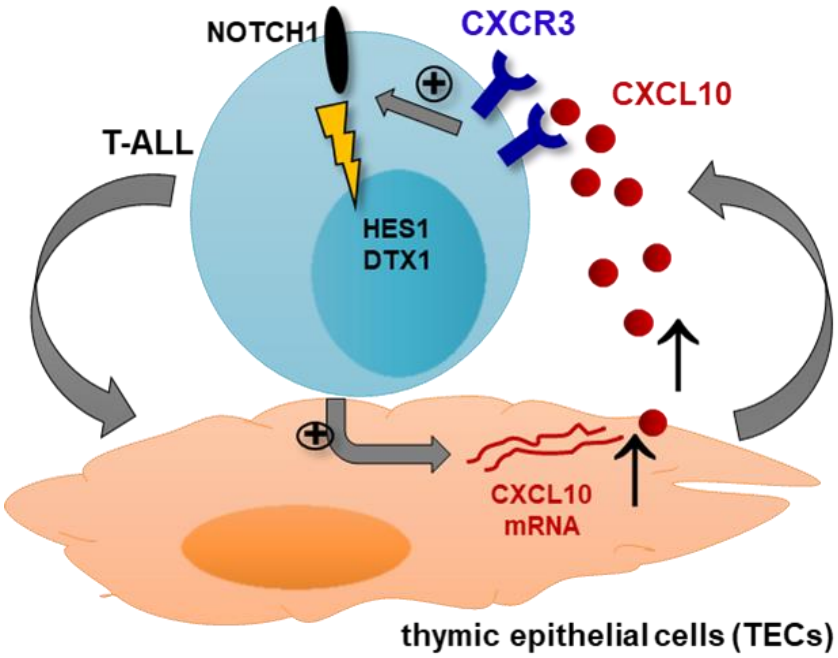

Figure 52. The direct crosstalk between emerging T-ALL cells and TEC promotes leukemogenesis via the CXCL10/CXCR3 axis.

The figure shows the interaction of TECs and T-ALL cells leading to chemokine CXCL10 secretion. CXCL10 is capable of acting on CXCR3 expressing leukemic cells triggering NOTCH1 signaling and increased survival of T-ALL cells.

5 OUTLOOK

Previously published data and the data of this project argue for the role of specific chemokines and their receptors in T-ALL. To our knowledge, the presented data provide the first evidence of a TEC-derived chemokine promoting T-ALL leukemogenesis. Thus, more studies are necessary to unravel the mechanisms and signaling pathways involved in the interaction of thymic stromal cells and developing T-ALL cells. These studies would potentially identify new targets for T-ALL therapy. In line with this notion, several studies reported the CXCL10/CXCR3 axis as a promising target of novel therapeutic approaches. There is a rational for blocking or alternatively even activating the autocrine and paracrine signaling in different diseases. Additionally, in several tumor models agents that deactivate the expression of CXCR3 on cancer cells or even improve paracrine CXCL10 signaling have demonstrated anti-tumor activity.[148-151] Investigations of retroviral CXCL10 gene transduction have demonstrated the utility of CXCL10 overexpression in suppressing tumor growth within lung cancer and melanoma models.[150, 151] Anti-CXCR3 therapies reduced tumor growth and the development of metastases in murine models. The CXCR3 antagonist AMG487 inhibited the growth and implantation of colorectal cancer and osteosarcoma cells and suppressed lung metastasis in an *in vivo* model as well as liver metastasis and growth of metastatic tumors.[148, 149, 152] However, these approaches have not yet been studied in hematologic malignancies. The approach of CXCR3 targeted therapy based on the inhibition of tumor metastasis and invasiveness might partially be transferable to T-ALL as this malignancy infiltrates non-hematopoietic organs such as the brain. Therefore, new studies should evaluate the potential of a CXCR3-specific small molecule antagonist to inhibit the invasive potential of T-ALL cells. In fact, our results provide a strong rationale for further studies of CXCL10/CXCR3 axis inhibition in the context of T-ALL. Specifically, the results of this project warrant future experiments aiming at inhibiting the CXCL10/CXCR axis in T-ALL leukemia models. A genetic approach would be to study leukemogenesis in mice with CXCL10 or CXCR3 knockout alleles in the SCL/LMO1 transgenic background. Furthermore, in preclinical experiments diseased SCL/LMO1 T-ALL mice could be treated with the previously mentioned CXCR3 antagonist AMG487.

6 SUMMARY

Within the thymus, the development of T-cells is controlled by specialized thymic epithelial cells (TECs). Based on their function and anatomic location TECs are separated into cortical and medullary subsets (cTECs and mTECs). cTECs express the indispensable NOTCH-ligand DLL4 controlling T cell lineage commitment while mTECs play a central role in T-cell negative selection. Acquired NOTCH1 gain-of-function mutations play a key role in acute T cell lymphoblastic leukemia (T-ALL) development. During T-ALL leukemogenesis aberrant expression of transcription, factors such as SCL and LMO1 block T cell differentiation and increased self-renewal. Since acquired NOTCH1 mutations are ligand-dependent to exert augmented signaling, we proposed DLL4-expressing TECs playing a critical role in T-ALL leukemogenesis. In the present study, we used the *SCL/LMO1* T-ALL mouse model, murine TEC cell lines and human T-ALL cell lines to investigate TEC dynamics and function in the T-ALL context. First, we demonstrated in co-cultures that TEC cell lines possess *in vitro* T-ALL supporting potential, which was comparable to the mesenchymal cell line OP9. Next, we showed in the *SCL/LMO1* T-ALL mouse model that preleukemic thymocytes displayed a striking upregulation of NOTCH1 target genes. Interestingly, fluorescence microscopy revealed a relative expansion of cortical and a relative reduction of the medullary thymic areas in *SCL/LMO1* thymi. Correspondingly, absolute numbers of cTECs expanded while mTEC numbers declined. Gene expression profiling of sorted *SCL/LMO1* cTECs revealed upregulation of the chemokines CXCL10 and CXCL12. Remarkably, CXCL12 produced by endothelial cells is a known factor controlling *in vivo* T-ALL maintenance. We moved on to study whether CXCL10 expression by TECs was T-ALL-dependent. Strikingly, we showed that CXCL10 upregulation in TEC cell lines could only be induced by direct co-culture with *SCL/LMO1* cells while wild-type control cells did not alter TEC CXCL10 expression. Moreover, increased CXCL10 chemokine concentrations were detected in *SCL/LMO1* thymic interstitial fluid. Next, the expression of the CXCL10 receptor CXCR3 was revealed on human T-ALL cell lines and on *SCL/LMO1* thymocytes. Finally, we demonstrated a CXCL10 dependent pro-survival effect within cultured *SCL/LMO1* thymocytes, which was associated with the activation of NOTCH1 signaling. In summary, the collected data support a novel T-ALL-promoting regulatory circuit in which emerging T-ALL lymphoblasts induce CXCL10 in expanding TECs which positively feeds back to T-ALL cells via the CXCL10 receptor CXCR3.

7 ZUSAMMENFASSUNG

Innerhalb des Thymus wird die Entwicklung von T-Zellen durch spezialisierte thymische Epithelzellen (TECs) gesteuert. Basierend auf ihrer Funktion und anatomischen Lage werden TECs in kortikale und medulläre Zellen (cTECs und mTECs) unterteilt. cTECs exprimieren den unverzichtbaren NOTCH-Liganden DLL4, der die T-Zell-Linienentscheidung kontrolliert, während mTECs eine zentrale Rolle bei der negativen Selektion von T-Zellen spielen. Erworbene NOTCH1-Mutationen spielen eine Schlüsselrolle bei der Entwicklung der akuten T-Zell lymphoblastischen Leukämie (T-ALL). Während der T-ALL Leukämogenese blockiert die aberrante Expression der Transkriptionsfaktoren SCL und LMO1 die T-Zelldifferenzierung und steigert die Selbsterneuerungsfähigkeit. Die Ligandenabhängigkeit der aktivierenden Wirkung von NOTCH1-Mutationen spricht für eine entscheidende Rolle von DLL4-exprimierende TECs innerhalb der T-ALL-Leukämogenese. In der vorliegenden Studie haben wir das *SCL/LMO1* T-ALL Mausmodell, murine TEC Zelllinien und menschliche T-ALL Zelllinien verwendet, um die Dynamik und Funktion der TECs im T-ALL Kontext zu untersuchen. Zuerst haben wir in Co-Kulturen gezeigt, dass TEC-Zelllinien ein *in vitro* T-ALL unterstützendes Potenzial besitzen, das mit der mesenchymalen Zelllinie OP9 vergleichbar ist. Als nächstes wiesen wir im *SCL/LMO1* T-ALL Mausmodell nach, dass präleukämische Thymozyten eine ausgeprägte Hochregulation der NOTCH1-Zielgene zeigten. Interessanterweise zeigte die Fluoreszenzmikroskopie eine relative Ausdehnung der kortikalen und eine relative Reduktion der medullären thymischen Bereiche in *SCL/LMO1* Thymi. Dementsprechend war auch ein Anstieg der absoluten thymischen cTEC Zellzahlen zu verzeichnen, während die mTEC-Zahlen zurückgingen. Die Genexpressionsanalysen von sortierten *SCL/LMO1* cTECs ergab eine signifikante Hochregulation der Chemokine CXCL10 und CXCL12. Bemerkenswert ist, dass CXCL12, das auch von Endothelzellen produziert wird, ein bekannter Faktor ist, der die *in vivo* T-ALL-Erhaltung steuert. Als nächstes untersuchten wir, ob die CXCL10-Expression durch TECs abhängig von der Interaktion mit T-ALL Zellen ist. Auffallend war, dass die CXCL10-Hochregulation in TEC-Zelllinien nur durch direkte Co-Kultur mit *SCL/LMO1*-Zellen induziert werden konnte, während Wildtyp-Kontrollzellen die TEC CXCL10-Expression nicht veränderten. Darüber hinaus wurden erhöhte CXCL10-Chemokinkonzentrationen in der interstitiellen *SCL/LMO1*-Thymusflüssigkeit nachgewiesen. Weiterhin wurde die Expression des CXCL10-Rezeptors CXCR3 auf humanen T-ALL-Zelllinien und auf *SCL/LMO1*-Thymozyten nachgewiesen. Schließlich

zeigten wir einen CXCL10-abhängigen Überlebenseffekt in kultivierten *SCL/LMO1*-Thymozyten, der mit der Aktivierung des NOTCH1-Signalweges verbunden war. Zusammenfassend sprechen die erhobenen Daten für einen neuartigen T-ALL-fördernden regulatorischen Kreislauf, in dem neu entstehende T-ALL-Lymphoblasten CXCL10 innerhalb von expandierenden TECs induzieren, das über den CXCL10-Rezeptor CXCR3 positiv auf T-ALL-Zellen zurückwirkt.

8 APPENDIX

8.1 PCR Protocol

Detection of the SCL

Conc.	Component	µl
	H2O	11.34
20 µM	Primer # SCL_hGH_fwd	0.2
20 µM	Primer # SCL_hGH_rew	0.2
20 µM	Primer #wt_SCL_fwd	0.2
20 µM	Primer # wt_SCL_few	0.2
25 mM	dNTPs	0.16
5X	Buffer	4
25mM	MgCl2	1.6
5 U/µl	Taq Polymerase	0.1
	Probe	2
	Total volume	20

Degrees	Time	Cycles
95	10 min	1X
95	15 sec	35X
55	15 sec	
72	40 sec	
72	3 min	1X
4	for ever	

Detection of the LMO1

Conc.	Component	µl
	H2O	10.74
20 µM	Primer #hLMO1_fwd	0.4
20 µM	Primer # hLMO1_rew	0.4
20 µM	Primer #wt_SCL_fwd	0.1
20 µM	Primer # wt_SCL_few	0.1
25 mM	dNTPs	0.16
5X	Buffer	4
25mM	MgCl2	2
5 U/µl	Taq Polymerase	0.1
	Probe	2
	Total volume	20

Degrees	Time	Cycles
95	10 min	1X
95	30 sec	35X
58	30 sec	
72	30 sec	
72	3 min	1X
4	for ever	

TaqMan Real-Time PCR-Protocol

Conc.	Component	µl
2x	MasterMix	10
20x	Assay	1
18ng	cDNA Probe	9
	Total volume	20

Degrees	Time	Cycles
95	20 sec	1X
95	1 sec	40X
60	20 sec	
4	for ever	

CHAPTER-9

BIBLIOGRAPHY

9 BIBLIOGRAPHY

1. Manley, N.R., Thymus organogenesis and molecular mechanisms of thymic epithelial cell differentiation. Semin Immunol, 2000. **12**(5): p. 421-8.
2. Le Douarin, N.M., F. Dieterlen-Lievre, and P.D. Oliver, Ontogeny of primary lymphoid organs and lymphoid stem cells. Am J Anat, 1984. **170**(3): p. 261-99.
3. Rossi, F.M., et al., Recruitment of adult thymic progenitors is regulated by P-selectin and its ligand PSGL-1. Nat Immunol, 2005. **6**(6): p. 626-34.
4. Wu, L., P.W. Kincade, and K. Shortman, The CD44 expressed on the earliest intrathymic precursor population functions as a thymus homing molecule but does not bind to hyaluronate. Immunol Lett, 1993. **38**(1): p. 69-75.
5. Godfrey, D.I., A. Zlotnik, and T. Suda, Phenotypic and functional characterization of c-kit expression during intrathymic T cell development. J Immunol, 1992. **149**(7): p. 2281-5.
6. Ceredig, R. and T. Rolink, A positive look at double-negative thymocytes. Nat Rev Immunol, 2002. **2**(11): p. 888-97.
7. Tan, J.B., et al., Requirement for Notch1 signals at sequential early stages of intrathymic T cell development. Nat Immunol, 2005. **6**(7): p. 671-9.
8. Massa, S., et al., Critical role for c-kit (CD117) in T cell lineage commitment and early thymocyte development in vitro. Eur J Immunol, 2006. **36**(3): p. 526-32.
9. Wang, H., L.J. Pierce, and G.J. Spangrude, Distinct roles of IL-7 and stem cell factor in the OP9-DL1 T-cell differentiation culture system. Exp Hematol, 2006. **34**(12): p. 1730-40.
10. Pelletier, A.J., et al., Presentation of chemokine SDF-1 alpha by fibronectin mediates directed migration of T cells. Blood, 2000. **96**(8): p. 2682-90.
11. Uehara, S., et al., Premature expression of chemokine receptor CCR9 impairs T cell development. J Immunol, 2006. **176**(1): p. 75-84.
12. Ciofani, M. and J.C. Zuniga-Pflucker, Notch promotes survival of pre-T cells at the beta-selection checkpoint by regulating cellular metabolism. Nat Immunol, 2005. **6**(9): p. 881-8.
13. Balciunaite, G., et al., The role of Notch and IL-7 signaling in early thymocyte proliferation and differentiation. Eur J Immunol, 2005. **35**(4): p. 1292-300.
14. Livak, F., et al., Characterization of TCR gene rearrangements during adult murine T cell development. J Immunol, 1999. **162**(5): p. 2575-80.
15. Misslitz, A., G. Bernhardt, and R. Forster, Trafficking on serpentines: molecular insight on how maturating T cells find their winding paths in the thymus. Immunol Rev, 2006. **209**: p. 115-28.
16. Yasutomo, K., et al., The duration of antigen receptor signalling determines CD4+ versus CD8+ T-cell lineage fate. Nature, 2000. **404**(6777): p. 506-10.

17. Robey, E. and B.J. Fowlkes, Selective events in T cell development. Annu Rev Immunol, 1994. **12**: p. 675-705.

18. Romano, R., et al., FOXN1: A Master Regulator Gene of Thymic Epithelial Development Program. Front Immunol, 2013. **4**: p. 187.

19. Boyd, R.L., et al., The thymic microenvironment. Immunol Today, 1993. **14**(9): p. 445-59.

20. Van Vliet, E., et al., Stromal cell types in the developing thymus of the normal and nude mouse embryo. Eur J Immunol, 1985. **15**(7): p. 675-81.

21. Savino, W., S.R. Dalmau, and V.C. Dealmeida, Role of extracellular matrix-mediated interactions in thymocyte migration. Dev Immunol, 2000. **7**(2-4): p. 279-91.

22. Small, M., et al., Identification of subpopulations of mouse thymic epithelial cells in culture. Immunology, 1989. **68**(3): p. 371-7.

23. Rouse, R.V., et al., Monoclonal antibodies reactive with subsets of mouse and human thymic epithelial cells. J Histochem Cytochem, 1988. **36**(12): p. 1511-7.

24. Akiyama, N., et al., Identification of embryonic precursor cells that differentiate into thymic epithelial cells expressing autoimmune regulator. J Exp Med, 2016. **213**(8): p. 1441-58.

25. Shortman, K., Cellular aspects of early T-cell development. Curr Opin Immunol, 1992. **4**(2): p. 140-6.

26. Jiang, W., et al., The receptor DEC-205 expressed by dendritic cells and thymic epithelial cells is involved in antigen processing. Nature, 1995. **375**(6527): p. 151-5.

27. Gray, D.H., A.P. Chidgey, and R.L. Boyd, Analysis of thymic stromal cell populations using flow cytometry. J Immunol Methods, 2002. **260**(1-2): p. 15-28.

28. Sitnik, K.M., et al., Mesenchymal cells regulate retinoic acid receptor-dependent cortical thymic epithelial cell homeostasis. J Immunol, 2012. **188**(10): p. 4801-9.

29. Moore, N.C., et al., Analysis of cytokine gene expression in subpopulations of freshly isolated thymocytes and thymic stromal cells using semiquantitative polymerase chain reaction. Eur J Immunol, 1993. **23**(4): p. 922-7.

30. Alves, N.L., et al., Characterization of the thymic IL-7 niche in vivo. Proc Natl Acad Sci U S A, 2009. **106**(5): p. 1512-7.

31. Wurbel, M.A., et al., The chemokine TECK is expressed by thymic and intestinal epithelial cells and attracts double- and single-positive thymocytes expressing the TECK receptor CCR9. Eur J Immunol, 2000. **30**(1): p. 262-71.

32. Murata, S., et al., Regulation of CD8+ T cell development by thymus-specific proteasomes. Science, 2007. **316**(5829): p. 1349-53.

33. Hozumi, K., et al., Delta-like 4 is indispensable in thymic environment specific for T cell development. J Exp Med, 2008. **205**(11): p. 2507-13.

34. Koch, U., et al., Delta-like 4 is the essential, nonredundant ligand for Notch1 during thymic T cell lineage commitment. J Exp Med, 2008. **205**(11): p. 2515-23.

35. Liu, C., et al., Coordination between CCR7- and CCR9-mediated chemokine signals in prevascular fetal thymus colonization. Blood, 2006. **108**(8): p. 2531-9.

36. Bleul, C.C. and T. Boehm, Chemokines define distinct microenvironments in the developing thymus. Eur J Immunol, 2000. **30**(12): p. 3371-9.

37. Itoi, M., N. Tsukamoto, and T. Amagai, Expression of Dll4 and CCL25 in Foxn1-negative epithelial cells in the post-natal thymus. Int Immunol, 2007. **19**(2): p. 127-32.

38. Zaballos, A., et al., Cutting edge: identification of the orphan chemokine receptor GPR-9-6 as CCR9, the receptor for the chemokine TECK. J Immunol, 1999. **162**(10): p. 5671-5.

39. Ciofani, M., et al., Obligatory role for cooperative signaling by pre-TCR and Notch during thymocyte differentiation. J Immunol, 2004. **172**(9): p. 5230-9.

40. Durum, S.K., et al., Interleukin 7 receptor control of T cell receptor gamma gene rearrangement: role of receptor-associated chains and locus accessibility. J Exp Med, 1998. **188**(12): p. 2233-41.

41. Singer, A., S. Adoro, and J.H. Park, Lineage fate and intense debate: myths, models and mechanisms of CD4- versus CD8-lineage choice. Nat Rev Immunol, 2008. **8**(10): p. 788-801.

42. Salmond, R.J., et al., T-cell receptor proximal signaling via the Src-family kinases, Lck and Fyn, influences T-cell activation, differentiation, and tolerance. Immunol Rev, 2009. **228**(1): p. 9-22.

43. Klein, L., et al., Positive and negative selection of the T cell repertoire: what thymocytes see (and don't see). Nat Rev Immunol, 2014. **14**(6): p. 377-91.

44. Ferrington, D.A. and D.S. Gregerson, Immunoproteasomes: structure, function, and antigen presentation. Prog Mol Biol Transl Sci, 2012. **109**: p. 75-112.

45. Farr, A.G. and S.K. Anderson, Epithelial heterogeneity in the murine thymus: fucose-specific lectins bind medullary epithelial cells. J Immunol, 1985. **134**(5): p. 2971-7.

46. Heino, M., et al., Autoimmune regulator is expressed in the cells regulating immune tolerance in thymus medulla. Biochem Biophys Res Commun, 1999. **257**(3): p. 821-5.

47. Petrie, H.T. and J.C. Zuniga-Pflucker, Zoned out: functional mapping of stromal signaling microenvironments in the thymus. Annu Rev Immunol, 2007. **25**: p. 649-79.

48. Misslitz, A., et al., Thymic T cell development and progenitor localization depend on CCR7. J Exp Med, 2004. **200**(4): p. 481-91.

49. Kwan, J. and N. Killeen, CCR7 directs the migration of thymocytes into the thymic medulla. J Immunol, 2004. **172**(7): p. 3999-4007.

50. Anderson, G., et al., MHC class II-positive epithelium and mesenchyme cells are both required for T-cell development in the thymus. Nature, 1993. **362**(6415): p. 70-3.

51. Dooley, J., M. Erickson, and A.G. Farr, Alterations of the medullary epithelial compartment in the Aire-deficient thymus: implications for programs of thymic epithelial differentiation. J Immunol, 2008. **181**(8): p. 5225-32.

52. Sawyers, C.L., C.T. Denny, and O.N. Witte, Leukemia and the disruption of normal hematopoiesis. Cell, 1991. **64**(2): p. 337-50.

53. Campo, E., et al., The 2008 WHO classification of lymphoid neoplasms and beyond: evolving concepts and practical applications. Blood, 2011. **117**(19): p. 5019-32.

54. Weinreich, M.A. and K.A. Hogquist, Thymic emigration: when and how T cells leave home. J Immunol, 2008. **181**(4): p. 2265-70.

55. Zlotoff, D.A. and A. Bhandoola, Hematopoietic progenitor migration to the adult thymus. Ann N Y Acad Sci, 2011. **1217**: p. 122-38.

56. Onciu, M., et al., Precursor T-cell acute lymphoblastic leukemia in adults: age-related immunophenotypic, cytogenetic, and molecular subsets. Am J Clin Pathol, 2002. **117**(2): p. 252-8.

57. Pui, C.H. and W.E. Evans, Treatment of acute lymphoblastic leukemia. N Engl J Med, 2006. **354**(2): p. 166-78.

58. McCormack, M.P., et al., The Lmo2 oncogene initiates leukemia in mice by inducing thymocyte self-renewal. Science, 2010. **327**(5967): p. 879-83.

59. Cauwelier, B., et al., Molecular cytogenetic study of 126 unselected T-ALL cases reveals high incidence of TCRbeta locus rearrangements and putative new T-cell oncogenes. Leukemia, 2006. **20**(7): p. 1238-44.

60. Aifantis, I., E. Raetz, and S. Buonamici, Molecular pathogenesis of T-cell leukaemia and lymphoma. Nat Rev Immunol, 2008. **8**(5): p. 380-90.

61. Paganin, M. and A. Ferrando, Molecular pathogenesis and targeted therapies for NOTCH1-induced T-cell acute lymphoblastic leukemia. Blood Rev, 2011. **25**(2): p. 83-90.

62. Clappier, E., et al., Cyclin D2 dysregulation by chromosomal translocations to TCR loci in T-cell acute lymphoblastic leukemias. Leukemia, 2006. **20**(1): p. 82-6.

63. Vogelstein, B., et al., Cancer genome landscapes. Science, 2013. **339**(6127): p. 1546-58.

64. Neely, M.D., et al., DMH1, a highly selective small molecule BMP inhibitor promotes neurogenesis of hiPSCs: comparison of PAX6 and SOX1 expression during neural induction. ACS Chem Neurosci, 2012. **3**(6): p. 482-91.

65. Weng, A.P., et al., Activating mutations of NOTCH1 in human T cell acute lymphoblastic leukemia. Science, 2004. **306**(5694): p. 269-71.

66. Tetzlaff, M.T., et al., Defective cardiovascular development and elevated cyclin E and Notch proteins in mice lacking the Fbw7 F-box protein. Proc Natl Acad Sci U S A, 2004. **101**(10): p. 3338-45.

67. Sulong, S., et al., A comprehensive analysis of the CDKN2A gene in childhood acute lymphoblastic leukemia reveals genomic deletion, copy number neutral loss of heterozygosity, and association with specific cytogenetic subgroups. Blood, 2009. **113**(1): p. 100-7.

68. Van Vlierberghe, P., et al., PHF6 mutations in T-cell acute lymphoblastic leukemia. Nat Genet, 2010. **42**(4): p. 338-42.

69. Berrih, S., W. Savino, and S. Cohen, Extracellular matrix of the human thymus: immunofluorescence studies on frozen sections and cultured epithelial cells. J Histochem Cytochem, 1985. **33**(7): p. 655-64.

70. Radtke, F., et al., Deficient T cell fate specification in mice with an induced inactivation of Notch1. Immunity, 1999. **10**(5): p. 547-58.

71. Ellisen, L.W., et al., TAN-1, the human homolog of the Drosophila notch gene, is broken by chromosomal translocations in T lymphoblastic neoplasms. Cell, 1991. **66**(4): p. 649-61.

72. Aster, J.C., Deregulated NOTCH signaling in acute T-cell lymphoblastic leukemia/lymphoma: new insights, questions, and opportunities. Int J Hematol, 2005. **82**(4): p. 295-301.

73. Allenspach, E.J., et al., Notch signaling in cancer. Cancer Biol Ther, 2002. **1**(5): p. 466-76.

74. Thompson, B.J., et al., The SCFFBW7 ubiquitin ligase complex as a tumor suppressor in T cell leukemia. J Exp Med, 2007. **204**(8): p. 1825-35.

75. Asnafi, V., et al., NOTCH1/FBXW7 mutation identifies a large subgroup with favorable outcome in adult T-cell acute lymphoblastic leukemia (T-ALL): a Group for Research on Adult Acute Lymphoblastic Leukemia (GRAALL) study. Blood, 2009. **113**(17): p. 3918-24.

76. Yan, X.Q., et al., A novel Notch ligand, Dll4, induces T-cell leukemia/lymphoma when overexpressed in mice by retroviral-mediated gene transfer. Blood, 2001. **98**(13): p. 3793-9.

77. Lowsky, R., et al., Defects of the mismatch repair gene MSH2 are implicated in the development of murine and human lymphoblastic lymphomas and are associated with the aberrant expression of rhombotin-2 (Lmo-2) and Tal-1 (SCL). Blood, 1997. **89**(7): p. 2276-82.

78. Robb, L. and C.G. Begley, The SCL/TAL1 gene: roles in normal and malignant haematopoiesis. Bioessays, 1997. **19**(7): p. 607-13.

79. Anantharaman, A., et al., Role of helix-loop-helix proteins during differentiation of erythroid cells. Mol Cell Biol, 2011. **31**(7): p. 1332-43.

80. Lecuyer, E. and T. Hoang, SCL: from the origin of hematopoiesis to stem cells and leukemia. Exp Hematol, 2004. **32**(1): p. 11-24.

81. Sanda, T., et al., Core transcriptional regulatory circuit controlled by the TAL1 complex in human T cell acute lymphoblastic leukemia. Cancer Cell, 2012. **22**(2): p. 209-21.

82. Gothert, J.R., et al., NOTCH1 pathway activation is an early hallmark of SCL T leukemogenesis. Blood, 2007. **110**(10): p. 3753-62.

83. Royer-Pokora, B., U. Loos, and W.D. Ludwig, TTG-2, a new gene encoding a cysteine-rich protein with the LIM motif, is overexpressed in acute T-cell leukaemia with the t(11;14)(p13;q11). Oncogene, 1991. **6**(10): p. 1887-93.

84. McGuire, E.A., et al., Thymic overexpression of Ttg-1 in transgenic mice results in T-cell acute lymphoblastic leukemia/lymphoma. Mol Cell Biol, 1992. **12**(9): p. 4186-96.

85. Chervinsky, D.S., et al., Disordered T-cell development and T-cell malignancies in SCL LMO1 double-transgenic mice: parallels with E2A-deficient mice. Mol Cell Biol, 1999. **19**(7): p. 5025-35.

86. Aplan, P.D., et al., An scl gene product lacking the transactivation domain induces bony abnormalities and cooperates with LMO1 to generate T-cell malignancies in transgenic mice. EMBO J, 1997. **16**(9): p. 2408-19.

87. Groom, J.R. and A.D. Luster, CXCR3 ligands: redundant, collaborative and antagonistic functions. Immunol Cell Biol, 2011. **89**(2): p. 207-15.

88. Salazar, N. and B.A. Zabel, Support of Tumor Endothelial Cells by Chemokine Receptors. Front Immunol, 2019. **10**: p. 147.

89. Torraca, V., et al., The CXCR3-CXCL11 signaling axis mediates macrophage recruitment and dissemination of mycobacterial infection. Dis Model Mech, 2015. **8**(3): p. 253-69.

90. Lasagni, L., et al., An alternatively spliced variant of CXCR3 mediates the inhibition of endothelial cell growth induced by IP-10, Mig, and I-TAC, and acts as functional receptor for platelet factor 4. J Exp Med, 2003. **197**(11): p. 1537-49.

91. Groom, J.R. and A.D. Luster, CXCR3 in T cell function. Exp Cell Res, 2011. **317**(5): p. 620-31.

92. Hoermannsperger, G., et al., Post-translational inhibition of IP-10 secretion in IEC by probiotic bacteria: impact on chronic inflammation. PLoS One, 2009. **4**(2): p. e4365.

93. Yeruva, S., G. Ramadori, and D. Raddatz, NF-kappaB-dependent synergistic regulation of CXCL10 gene expression by IL-1beta and IFN-gamma in human intestinal epithelial cell lines. Int J Colorectal Dis, 2008. **23**(3): p. 305-17.

94. Liu, M., S. Guo, and J.K. Stiles, The emerging role of CXCL10 in cancer (Review). Oncol Lett, 2011. **2**(4): p. 583-589.

95. Monteagudo, C., et al., CXCR3 chemokine receptor immunoreactivity in primary cutaneous malignant melanoma: correlation with clinicopathological prognostic factors. J Clin Pathol, 2007. **60**(6): p. 596-9.

96. Datta, D., et al., Ras-induced modulation of CXCL10 and its receptor splice variant CXCR3-B in MDA-MB-435 and MCF-7 cells: relevance for the development of human breast cancer. Cancer Res, 2006. **66**(19): p. 9509-18.

97. Moriai, S., et al., Production of interferon-{gamma}-inducible protein-10 and its role as an autocrine invasion factor in nasal natural killer/T-cell lymphoma cells. Clin Cancer Res, 2009. **15**(22): p. 6771-9.

98. Kawada, K., et al., Chemokine receptor CXCR3 promotes colon cancer metastasis to lymph nodes. Oncogene, 2007. **26**(32): p. 4679-88.

99. Maru, S.V., et al., Chemokine production and chemokine receptor expression by human glioma cells: role of CXCL10 in tumour cell proliferation. J Neuroimmunol, 2008. **199**(1-2): p. 35-45.

100. Nelson, A.J., C.H. Clegg, and A.G. Farr, In vitro positive selection and anergy induction of class II-restricted TCR transgenic thymocytes by a cortical thymic epithelial cell line. Int Immunol, 1998. **10**(9): p. 1335-46.

101. Farr, A.G., et al., Medullary epithelial cell lines from murine thymus constitutively secrete IL-1 and hematopoietic growth factors and express class II antigens in response to recombinant interferon-gamma. Cell Immunol, 1989. **119**(2): p. 427-44.

102. Nakano, T., H. Kodama, and T. Honjo, Generation of lymphohematopoietic cells from embryonic stem cells in culture. Science, 1994. **265**(5175): p. 1098-101.

103. Weiss, A., R.L. Wiskocil, and J.D. Stobo, The role of T3 surface molecules in the activation of human T cells: a two-stimulus requirement for IL 2 production reflects events occurring at a pre-translational level. J Immunol, 1984. **133**(1): p. 123-8.

104. Drexler, H.G., G. Gaedicke, and J. Minowada, Isoenzyme studies in human leukemia-lymphoma cell lines--1. Carboxylic esterase. Leuk Res, 1985. **9**(2): p. 209-29.

105. Morikawa, S., et al., Two E-rosette-forming lymphoid cell lines. Int J Cancer, 1978. **21**(2): p. 166-70.

106. Klein, L., et al., Shaping of the autoreactive T-cell repertoire by a splice variant of self protein expressed in thymic epithelial cells. Nat Med, 2000. **6**(1): p. 56-61.

107. Danzl, N.M., L.T. Donlin, and K. Alexandropoulos, Regulation of medullary thymic epithelial cell differentiation and function by the signaling protein Sin. J Exp Med, 2010. **207**(5): p. 999-1013.

108. Lin, Y.W., et al., Notch1 mutations are important for leukemic transformation in murine models of precursor-T leukemia/lymphoma. Blood, 2006. **107**(6): p. 2540-3.

109. Tremblay, M., et al., Modeling T-cell acute lymphoblastic leukemia induced by the SCL and LMO1 oncogenes. Genes Dev, 2010. **24**(11): p. 1093-105.

110. Xiong, J., M.A. Armato, and T.M. Yankee, Immature single-positive CD8+ thymocytes represent the transition from Notch-dependent to Notch-independent T-cell development. Int Immunol, 2011. **23**(1): p. 55-64.

111. Muller, S.M., et al., Neural crest origin of perivascular mesenchyme in the adult thymus. J Immunol, 2008. **180**(8): p. 5344-51.

112. Miettinen, P.J., et al., TGF-beta induced transdifferentiation of mammary epithelial cells to mesenchymal cells: involvement of type I receptors. J Cell Biol, 1994. **127**(6 Pt 2): p. 2021-36.

113. Calderon, L. and T. Boehm, Synergistic, context-dependent, and hierarchical functions of epithelial components in thymic microenvironments. Cell, 2012. **149**(1): p. 159-72.

114. Pitt, L.A., et al., CXCL12-Producing Vascular Endothelial Niches Control Acute T Cell Leukemia Maintenance. Cancer Cell, 2015. **27**(6): p. 755-68.

115. Gomez, A.M., et al., Chemokines and relapses in childhood acute lymphoblastic leukemia: A role in migration and in resistance to antileukemic drugs. Blood Cells Mol Dis, 2015. **55**(3): p. 220-7.

116. Triplett, T.A., et al., Endogenous dendritic cells from the tumor microenvironment support T-ALL growth via IGF1R activation. Proc Natl Acad Sci U S A, 2016. **113**(8): p. E1016-25.

117. Scupoli, M.T., et al., Thymic epithelial cells promote survival of human T-cell acute lymphoblastic leukemia blasts: the role of interleukin-7. Haematologica, 2003. **88**(11): p. 1229-37.

118. Chervinsky, D.S., et al., scid Thymocytes with TCRbeta gene rearrangements are targets for the oncogenic effect of SCL and LMO1 transgenes. Cancer Res, 2001. **61**(17): p. 6382-7.

119. Herblot, S., et al., SCL and LMO1 alter thymocyte differentiation: inhibition of E2A-HEB function and pre-T alpha chain expression. Nat Immunol, 2000. **1**(2): p. 138-44.

120. Ferrando, A.A., The role of NOTCH1 signaling in T-ALL. Hematology Am Soc Hematol Educ Program, 2009: p. 353-61.

121. Davey, G.M., C.L. Tucek-Szabo, and R.L. Boyd, Characterization of the AKR thymic microenvironment and its influence on thymocyte differentiation and lymphoma development. Leuk Res, 1996. **20**(10): p. 853-66.

122. Hauri-Hohl, M., et al., A regulatory role for TGF-beta signaling in the establishment and function of the thymic medulla. Nat Immunol, 2014. **15**(6): p. 554-61.

123. Kalluri, R. and M. Zeisberg, Fibroblasts in cancer. Nat Rev Cancer, 2006. **6**(5): p. 392-401.

124. Thiery, J.P., et al., Epithelial-mesenchymal transitions in development and disease. Cell, 2009. **139**(5): p. 871-90.

125. De Keersmaecker, K., P. Marynen, and J. Cools, Genetic insights in the pathogenesis of T-cell acute lymphoblastic leukemia. Haematologica, 2005. **90**(8): p. 1116-27.

126. De Francesco, E.M., M. Maggiolini, and A.M. Musti, Crosstalk between Notch, HIF-1alpha and GPER in Breast Cancer EMT. Int J Mol Sci, 2018. **19**(7).

127. Zhang, S.L. and A. Bhandoola, Trafficking to the thymus. Curr Top Microbiol Immunol, 2014. **373**: p. 87-111.

128. Aiuti, A., et al., Expression of CXCR4, the receptor for stromal cell-derived factor-1 on fetal and adult human lympho-hematopoietic progenitors. Eur J Immunol, 1999. **29**(6): p. 1823-31.

129. Deng, X., et al., Wnt5a and CCL25 promote adult T-cell acute lymphoblastic leukemia cell migration, invasion and metastasis. Oncotarget, 2017. **8**(24): p. 39033-39047.

130. de Vasconcellos, J.F., et al., Increased CCL2 and IL-8 in the bone marrow microenvironment in acute lymphoblastic leukemia. Pediatr Blood Cancer, 2011. **56**(4): p. 568-77.

131. Sarvaiya, P.J., et al., Chemokines in tumor progression and metastasis. Oncotarget, 2013. **4**(12): p. 2171-85.

132. Mukaida, N., S. Sasaki, and T. Baba, Chemokines in cancer development and progression and their potential as targeting molecules for cancer treatment. Mediators Inflamm, 2014. **2014**: p. 170381.

133. Ferrandino, F., et al., Intrathymic Notch3 and CXCR4 combinatorial interplay facilitates T-cell leukemia propagation. Oncogene, 2018. **37**(49): p. 6285-6298.

134. Chiaramonte, R., et al., Notch pathway promotes ovarian cancer growth and migration via CXCR4/SDF1alpha chemokine system. Int J Biochem Cell Biol, 2015. **66**: p. 134-40.

135. Hu, T.H., et al., SDF-1/CXCR4 promotes epithelial-mesenchymal transition and progression of colorectal cancer by activation of the Wnt/beta-catenin signaling pathway. Cancer Lett, 2014. **354**(2): p. 417-26.

136. Slettenaar, V.I. and J.L. Wilson, The chemokine network: a target in cancer biology? Adv Drug Deliv Rev, 2006. **58**(8): p. 962-74.

137. Bai, M., X. Chen, and Y.I. Ba, CXCL10/CXCR3 overexpression as a biomarker of poor prognosis in patients with stage II colorectal cancer. Mol Clin Oncol, 2016. **4**(1): p. 23-30.

138. Luster, A.D. and J.V. Ravetch, Biochemical characterization of a gamma interferon-inducible cytokine (IP-10). J Exp Med, 1987. **166**(4): p. 1084-97.

139. Romagnani, P., et al., Interferon-inducible protein 10, monokine induced by interferon gamma, and interferon-inducible T-cell alpha chemoattractant are produced by thymic epithelial cells and attract T-cell receptor (TCR) alphabeta+ CD8+ single-positive T cells, TCRgammadelta+ T cells, and natural killer-type cells in human thymus. Blood, 2001. **97**(3): p. 601-7.

140. Luster, A.D. and P. Leder, IP-10, a -C-X-C- chemokine, elicits a potent thymus-dependent antitumor response in vivo. J Exp Med, 1993. **178**(3): p. 1057-65.

141. Harlin, H., et al., Chemokine expression in melanoma metastases associated with CD8+ T-cell recruitment. Cancer Res, 2009. **69**(7): p. 3077-85.

142. Wennerberg, E., et al., CXCL10-induced migration of adoptively transferred human natural killer cells toward solid tumors causes regression of tumor growth in vivo. Cancer Immunol Immunother, 2015. **64**(2): p. 225-35.

143. Boorsma, D.M., et al., Chemokine IP-10 expression in cultured human keratinocytes. Arch Dermatol Res, 1998. **290**(6): p. 335-41.

144. Brightling, C.E., et al., The CXCL10/CXCR3 axis mediates human lung mast cell migration to asthmatic airway smooth muscle. Am J Respir Crit Care Med, 2005. **171**(10): p. 1103-8.

145. Aksoy, M.O., et al., CXCR3 surface expression in human airway epithelial cells: cell cycle dependence and effect on cell proliferation. Am J Physiol Lung Cell Mol Physiol, 2006. **290**(5): p. L909-18.

146. Outtz, H.H., et al., Notch1 deficiency results in decreased inflammation during wound healing and regulates vascular endothelial growth factor receptor-1 and inflammatory cytokine expression in macrophages. J Immunol, 2010. **185**(7): p. 4363-73.

147. Qin, Y., et al., Sox7 is involved in antibody-dependent endothelial cell activation and renal allograft injury via the Jagged1-Notch1 pathway. Exp Cell Res, 2019. **375**(2): p. 20-27.

148. Zhu, G., et al., CXCR3 as a molecular target in breast cancer metastasis: inhibition of tumor cell migration and promotion of host anti-tumor immunity. Oncotarget, 2015. **6**(41): p. 43408-19.

149. Cambien, B., et al., Organ-specific inhibition of metastatic colon carcinoma by CXCR3 antagonism. Br J Cancer, 2009. **100**(11): p. 1755-64.

150. Feldman, A.L., et al., Retroviral gene transfer of interferon-inducible protein 10 inhibits growth of human melanoma xenografts. Int J Cancer, 2002. **99**(1): p. 149-53.

151. Barash, U., et al., Heparanase enhances myeloma progression via CXCL10 downregulation. Leukemia, 2014. **28**(11): p. 2178-87.

152. Walser, T.C., et al., Antagonism of CXCR3 inhibits lung metastasis in a murine model of metastatic breast cancer. Cancer Res, 2006. **66**(15): p. 7701-7.

10 ACKNOWLEDGEMENT

I would like to thank many people who have supported me professionally and personally over the last three and a half years. The work I have done here has been a time of learning and growth in the scientific field. It would not have been possible alone, and that is why I am deeply grateful for all of them.

First of all, I would like to express my sincere gratitude and respect to my supervisor, **Dr. Joachim R. Göthert**, for the patient guidance, encouragement, and advice he has provided throughout my time as his student. Fortunately for me, I have a supervisor who took so much care of my work. His constructive idea and informative discussion have always encouraged me to work harder to achieve my goal.

I am thankful to **Prof. Dr. Ulrich Dührsen** for the warm acceptance in his research group. Special thanks goes to **Stefanie Kesper** and **Marco Luciani** for their help with mice work and support in the analysis. Many thanks to **Michael Möllmann** for his help in FACS analysis and cell sorting. I am also grateful to have a colleague like Karlotta Kahmann.

I would like to thank **Prof. Dr. Karl Lang** for allowing me to use the fluorescence microscope. Additionally, I thank to **Mrs. Delia Cosgrove**, who supported me in the BIOME Ph.D. program.

My PhD journey would not have been possible without the support of my family, who inspired me to follow my dreams. I would like to gratefully acknowledge my mother for her continued determination, affection, and love. And to my younger brother **Amit**, for his support.

I especially thank to a very special person, my partner, **Vishal** for his continued and unfailing love, support and understanding during this journey. You were always there when I thought it was impossible to go on, you helped me keep things in perspective.

I am immensely thankful for such an opportunity and for the amazing, inspiring experiences I had in Germany.

Thank you all,

Ashwini Patil

11 CURRICULUM VITAE

The biography is not included in the online version for reasons of data protection

12 ERKLÄRUNG

Hiermit erkläre ich, gem. § 6 Abs. (2) g) der Promotionsordnung der Fakultät für Biologie zur Erlangung der Dr. rer. nat., dass ich das Arbeitsgebiet, dem das Thema "**The CXCL10/CXCR3 axis cross-talk between emerging T cell acute lymphoblastic leukemia and thymic epithelial cells**" zuzuordnen ist, in Forschung und Lehre vertrete und den Antrag von **Ashwini M Patil** befürworte und die Betreuung auch im Falle eines Weggangs, wenn nicht wichtige Gründe dem entgegenstehen, weiterführen werde.

Essen, den __05.06.2019_____ _____

Unterschrift eines Mitglieds der Universität Duisburg-Essen

Erklärung:

Hiermit erkläre ich, gem. § 7 Abs. (2) d) + f) der Promotionsordnung der Fakultät für Biologie zur Erlangung des Dr. rer. nat., dass ich die vorliegende Dissertation selbständig verfasst und mich keiner anderen als der angegebenen Hilfsmittel bedient, bei der Abfassung der Dissertation nur die angegebenen Hilfsmittel benutzt und alle wörtlich oder inhaltlich übernommenen Stellen als solche gekennzeichnet habe.

Essen, den ____05.06.2019_____ _____

Unterschrift des/r Doktoranden/in

Erklärung:

Hiermit erkläre ich, gem. § 7 Abs. (2) e) + g) der Promotionsordnung der Fakultät für Biologie zur Erlangung des Dr. rer. nat., dass ich keine anderen Promotionen bzw. Promotionsversuche in der Vergangenheit durchgeführt habe und dass diese Arbeit von keiner anderen Fakultät/Fachbereich abgelehnt worden ist.

Essen, den 05.06.2019_____ _____

Unterschrift des Doktoranden